Functional effects of transplanted embryonic stem cell-derived neural aggregates overexpressing the neural cell adhesion molecule L1 in the MPTP model of Parkinson's disease and in a spinal cord injury model in *Mus musculus* (Linnaeus, 1758)

Dissertation

zur Erlangung des Doktorgrades des Departments Biologie der

Fakultät für Mathematik, Informatik und Naturwissenschaften an der

Universität Hamburg vorgelegt von Yifang Cui (Shanghai, P.R.China)

Hamburg, May, 2009

Genehmigt vom Department Biologie
der Fakultät für Mathematik, Informatik und Naturwissenschaften
an der Universität Hamburg
auf Antrag von Frau Professor Dr. M. SCHACHNER
Weiterer Gutachter der Dissertation:
Herr Professor Dr. K. WIESE
Tag der Disputation: 18. März 2009

Hamburg, den   03. März 2009
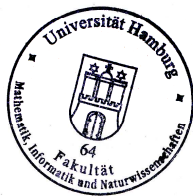
Professor Dr. Jörg Ganzhorn
Leiter des Departments Biologie

HARVARD MEDICAL SCHOOL
McLEAN HOSPITAL
DEPARTMENT OF NEUROLOGY AND
PROGRAM IN NEUROSCIENCE

CENTER FOR NEUROREGENERATION RESEARCH
NEUROREGENERATION LABORATORIES

Elizabeth D. Marlow

Neuroregeneration Laboratories

McLean Hospital

115 Mill Street

Belmont, MA 02478 USA

February 11, 2009

To Whom It May Concern

As an English native speaker I hereby confirm that Yifang Cui's thesis entitled
"Functional effects of transplanted embryonic stem cell-derved neural aggregates
overexpressing the neural cell adhesion molecule L1 in the MPTP model of Parkinson's
disease and in a spinal cord injury model in Mus musculus (L1, 1758)" is written with
correct grammar and in appropriate style.

Elizabeth Marlow

Elizabeth Marlow, BA

TABLE OF CONTENTS

IV Results   48

I Abstract

Adhesion molecules play important roles in the development and regeneration of the central and peripheral nervous system. The neural cell adhesion molecule L1 is a cell molecule belonging to the immunoglobulin superfamily. It can favor axonal growth in an inhibitory environment, promote neurite outgrowth, neuronal migration and survival.

Embryonic stem cells (ESC) derived from the inner cell mass of the blastocyst, have the ability to differentiate into cells of all three germ layers, including neural precursor cells. In this study, a murine embryonic stem cell line constitutively expressing L1 at all stages of differentiation was used to monitor the molecules effects on stem cell survival, differentiation, and ability to influence functional recovery in a murine model of Parkinson's disease and in a spinal cord injury model.

Parkinson's disease (PD) is the second most common neurodegenerative disorder after Alzheimer's disease with millions of people affected worldwide. In PD, the progressive degeneration of mesencephalic dopaminergic neurons of the nigrostriatal system results in a depletion of dopamine that creates severe motor dysfunction. One experimental approach is to enhance the number of dopaminergic neurons to restore the control of movement and motor activities. Although implantation of fetal dopaminergic neurons can reduce parkinsonism in patients, current methods are rudimentary, and a reliable donor cell source is lacking. Nowadays, stem cell replacement has emerged as a novel therapeutic strategy for Parkinson's disease.

Spinal cord injury is an insult to the spinal cord resulting in a change, either temporary or permanent, in its normal motor, sensory, or autonomic function. Causes include motor vehicle accidents, violence, falls, and recreational activities. Traumatic spinal cord injury immediately leads to irreversible primary tissue damage. Secondary damage follows afterwards. Current therapeutic approaches to spinal cord injury are inadequate. Therefore, increasing attention has been placed on the role of CNS stem cells in spinal cord repair, including embryonic stem cells.

This study applied a new ESC differentiation protocol. ES cell-derived

substrate-adherent neural aggregates (SENAs) that consist predominantly of neurons (>90%) and radial glial cells (>8%) were generated applying this procedure. Female C57BL/6J mice were intraperitoneally injected with mitochondrial toxin 1-methyl-4-phenyl-1,2,3,6-tetrahydropyridine (MPTP) to selectively deplete dopaminergic neurons. SENAs were unilaterally transplanted into the striatum or the substantia nigra four days after MPTP injection.

One month after transplantation, the mice grafted with L1 overexpressing SENAs showed a significant asymmetrical rotation bias to the grafted side after injection of apomorphine when compared to either mice grafted with control SENAs or sham-injected with PBS up to 10 weeks after transplantation. The behavioral change indicates that L1 overexpressing SENAs can improve locomotor function after MPTP-induced loss of doparminergic neurons.

Morphological analysis revealed that L1 overexpressing SENAs showed enhanced neuronal differentiation and increased survival of transplanted cells in the lesioned striatum when compared to control SENAs. Transplantation of L1 overexpressing, but not control, SENAs led to enhanced numbers of endogenous dopaminergic neurons in the host substantia nigra indicating a beneficial effect of L1 on endogenous cells. Moreover, engrafted L1 overexpressing SENAs enhanced striatal the dopamine level when compared to control SENAs but did not influence the level of GABA (Gamma-aminobutyric acid) in the striatum.

Furthermore, female C57BL/6J mice were traumatically lesioned by compression at the thoracic (T8-T10) level of the spinal cord. SENAs were transplanted into the spinal cord both rostral and caudal to the lesion site three days later.

Three weeks after transplantation, mice grafted with L1 overexpressing SENAs showed better locomotor function when compared with mice grafted with control SENAs or sham-injected with PBS. This effect was observed up to six weeks after transplantation. Morphological analysis revealed that L1 overexpressing SENAs showed enhanced neuronal differentiation, reduced glial differentiation. These cells also displayed increased viability in the inhibitory environment when compared to control SENAs. Moreover, engrafted L1 overexpressing SENAs rescued host motor

neurons and enhanced numbers of catecholaminergic (TH$^+$) nerve fibres distal to the lesion.

Thus, L1 overexpressing SENAs enhance functional recovery in an MPTP model of Parkinson's disease and in a comression lesion model of spinal cord injury.

II   Introduction

1   Stem cells

In mammals, the great majority of the somatic cells are derived from pluripotent precursors of the inner cell mass of the blastocyst which are termed embryonic stem (ES) cells when cultured. During the process of gastrulation, different groups of precursors differentiate from these ES cells into specific cell lineages that are found in the three germ layers: ectoderm, mesoderm, endoderm. These precursor cells subsequently generate organ and tissue-specific somatic stem cells that account for the progressive growth of the tissue mass during development (Faust and Magnuson; 1993). Somatic stem cells decrease in number with the tissue approaching maturity. Continuous cell replacement is important for creatures to maintain steady cell numbers during the adult life. This has been clearly demonstrated in the hemopoietic system, the epidermis and the intestinal epithelium. Recently, the subventricular zone lining the lateral ventricles and the subgranular zone of the dentate gyrus of the hippocampus have been recognized as germinative zones demonstrating the existence of neurogenesis and the presence of stem cells even in the adult mammalian central nervous system (CNS) (Gage; 2000).

A minimal definition of a stem cell is a cell that has the capacity both to self-renew and to generate several types of differentiated progeny (multipotency) by asymmetric cell division (Gage; 2000). This definition requires that at least one of the two progeny after a mitotic cell division remains a stem cell in order to maintain the stem cell population required for the continuous production of new cells over long periods of time. Stem cells display different levels of potency determined by their level of differentiation. Totipotency, a cell's ability to give rise to a full organism after implantation in the uterus of a living animal, has thus far only been shown for the zygote, the fertilized oocyte, which lacks the capacity for self-renewal. ES and embryonic germ (EG) cells are pluripotent cells that can give rise to every cell of the organism, except the trophoblasts of the placenta. It was recently discovered that oocytes can be derived from ES cells in vitro, offering a suggestion of totipotency

4

even in ES cells (Hubner, et al; 2003). Multipotent somatic stem cells like CNS and hemopoietic stem cells are usually defined by the organ of their origin; these cells were long assumed to be able to give rise to all, but exclusively, cells of that organ. This assumption has been challenged by the discovery that adult neural stem cells (ANSC) can give rise to hemopoietic cells (Bjornson, et al; 1999) and that bone marrow precursors can participate in the regeneration of organs of endodermal origin like the liver (Theise, et al; 2000) and are capable of converting into neural cell lineages (Mezey, et al; 2000). Thus, multipotent somatic stem cells have the capacity to give rise to many, though not all, cells originating from developmentally different germ layers. Stem cells are thus a potentially versatile tool for supporting or replacing endogenous regeneration.

1.1 Embryonic stem cells (ES cells)

ES cells are pluripotent cells derived from the inner cell mass (ICM) of developing blastocysts (Martin; 1981, Evans and Kaufman; 1981) that can be kept in an undifferentiated state under appropriate culture conditions for potentially indefinite periods of time (Suda, et al; 1987).

ES cell research dates back to the early 1970s, when embryonic carcinoma (EC) cells, the stem cells of germ line tumors called teratocarcinomas (Stevens; 1967), were established as cell lines (Gearhart and Mintz; 1974, Jacob, et al; 1973, Kahan and Ephrussi; 1970). Clonally isolated EC cells retained the capacity for differentiation and could produce derivatives of all three primary germ layers: ectoderm, mesoderm, endoderm. More importantly, EC cells demonstrated an ability to participate in embryonic development, when introduced into the ICM of early embryos to generate chimeric mice (Mintz and Illmensee; 1975). EC cells, however, showed chromosomal aberrations (Papaioannou, et al; 1975), lost their ability to differentiate (Bernstine, et al; 1973), or differentiated in vitro only under specialized conditions (Nicolas, et al; 1975) and with chemical inducers (McBurney, et al; 1982). Maintenance of the undifferentiated state relied on cultivation with feeder cells (Martin; 1981, Evans and Kaufman; 1981), and after transfer into early blastocysts,

EC cells only sporadically colonized the germ line (Mintz and Illmensee; 1975). These data suggested that the EC cells did not retain the pluripotent capacities of early embryonic cells and had undergone cellular changes during the transient tumorigenic state in vivo.

To avoid potential alterations connected with the growth of teratocarcinomas, a logical step was the direct in vitro culture of embryonic cells of the mouse. In 1981, two groups succeeded in cultivating pluripotent cell lines from mouse blastocysts. Evans and Kaufman employed a feeder layer of mouse embryonic fibroblasts (Evans and Kaufman; 1981), while Martin used EC cell-conditioned medium (Martin, 1981). These cell lines, termed ES cells, originated from the ICM or epiblast and could be maintained in vitro without any apparent loss of differentiation potential. The "pluripotency" of these cells was demonstrated in vivo by the introduction of ES cells into blastocysts. The resulting mouse chimeras demonstrated that ES cells could contribute to all cell lineages including the germ line (Bradley, et al; 1984). In vitro, mouse ES cells showed the capacity to reproduce the various somatic cell types (Doetschman, et al; 1985, Evans and Kaufman; 1981, Wobus, et al; 1984) and were found to develop into cells of the germ line (Geijsen, et al; 2003, Huebner, et al; 2003, Toyooka, et al; 2003). The establishment of human ES cell lines from in vitro fertilized embryos (Thomson, et al; 1998) and the demonstration of their developmental potential in vitro (Schuldiner, et al; 2001, Thomson, et al; 1998) have triggered widespread discussions concerning future applications of human ES cells in regenerative medicine.

2   Parkinson's Disease

Parkinson's disease (PD) is the most common serious movement disorder characterized by a progressive loss of dopaminergic neurons in the substantia nigra pars compacta with decreased levels of dopamine in the striatum leading to bradykinesia, rigidity, tremor, and postural instability in affected patients (Samii et al., 2004). Parkinson's disease was first described by the English physician James

Parkinson in 1817 in the famous monograph "An essay on the shaking palsy". In this report, he depicted a neurological illness characterized by resting tremor and progressive motor disability. The disease was subsequently termed Parkinson's disease, after its discoverer, by Jean-Martin Charcot.

The prevalence of Parkinson's disease in industrialized countries is estimated at 0.3% of the general population and about 1% of the population above the age of 60 (Rajput, 1992, de Rijk, et al; 2000). People of all ethnic origins can be affected, and men are slightly more susceptible to the disorder (Baldereschi, et al; 2000, Lai, et al; 2003). The initial symptoms of young-onset patients who have Parkinson's disease can arise between 21 and 40 years, and the first symptoms in juvenile-onset disease appear before the age of 20 years (Muthane, et al; 1994). The percentage of young patients among all Parkinson's disease patients is about 5-10% (Golbe, 1991).

The major features of Parkinson's disease are resting tremor, rigidity, bradykinesia and postural instability. Furthermore, symptoms unrelated to motor function appear in Parkinson's disease patients such as autonomic dysfunction, cognitive and psychiatric alterations, sensory symptoms, and sleep disturbances. Resting tremor, the shaking of limbs when they are not voluntarily being movied, is the first symptom in 70% of Parkinson's disease patients. Tremors are generally asymmetric, worsening with anxiety and during contralateral motor activity. Resting foot tremor is much less common than upper limb tremors (Samii et al., 2004). Rigidity is defined as an increased resistance to passive movement of the limbs or trunk that exists throughout the whole range joint movement. Tremor is not a prerequisite for rigidity but rigidity is typically more pronounced in more tremulous limbs. Rigidity can be enhanced by controlateral motor activity or mental task performance (Samii et al., 2004). Bradykinesia, slowness in the execution of movements, is a severe symptom of early Parkinson's disease. It first appears in fine motor movements such as writing or fist closing and opening, increasing in severity during the course of the disease. Postural instability is an impaired ability to keep the body in a stable or balanced position that also increases during the course of the disease.

Pathologically, Parkinson's disease is associated with the loss of dopaminergic

projections from substantia nigra pars compacta to the caudate nucleus and striatum. Lewy bodies and Lewy neurites are the pathological signs of the disease. Clinical signs of Parkinson's disease are evident when about 80% of the striatal dopamine and 50% of the nigral neurons are lost (Fearnley, et al; 1991). Lewy bodies are not only localized in the substantia nigra, but can also be found in cortex, amygdala, locus ceruleus, vagal nucleus, and the peripheral autonomic nervous system (Braak, et al; 2003, Wakabayashi, et al; 1997). Lewy bodies and neurites in these non-motor areas may be the cause of many non-motor symptoms of Parkinson's disease (Samii et al., 2004).

The cause of Parkinson's disease is probably a combination of several factors, including aging, genetic susceptibility, and environmental exposures (Steece-Collier, et al; 2002). Aging correlates with a decreased number of pigmented neurons in the substantia nigra pars compacta (McGeer, et al; 1977). It is reported that Lewy bodies can be found in up to 16% of the elderly asymptomatic people (Fearnley, et al; 1991). Also, PET and SPECT studies have showed that aging coincides with a subtle decrease of F-DOPA uptake (Cordes, et al; 1994) and a decline in striatal dopamine transporters (van Dyck, et al; 2002). Though these studies propose a link between aging and Parkinson's disease, this disorder is generally accepted not to be attributable solely to old age. As for the role of genetic susceptibility, the majority of patients do not have a family history. About 15% of patients have a first-degree relative with the disease, typically without a clear mode of inheritance (Payami, et al; 1994). To date, thirteen genetic loci associated with autosomal dominant or recessive parkinsonism have been identified; these genes are refered to as PARK genes. Twin studies were useful to clarify the role of genetic predisposition in Parkinson's disease. Results of such a study showed little concordance in twins regarding Parkinson's disease development after the age of 50, but complete concordance in monozygotic twins with a disease onset before this age (Tanner, et al; 1999). This finding points out that genetic disposition plays a role in early-onset Parkinson's disease. The discovery of PARK genes enhanced the interest in the genetic contribution to Parkinson's disease. PARK1 is the first identified gene linked to familiar Parkinson's disesase. It

8

encodes for the α synuclein (Polymeropoulos, et al; 1997). PARK2 is a gene encoding for the parkin protein which is associated with an autosomal recessive juvenile-onset form of Parkinsons's disease (Kitada, et al; 1998). The PARK5 gene encodes for the ubiquitin C-terminal hydrolase L1 that links to inherited Parkinson's disease (Leroy, et al; 1998).Though these single gene mutations only account for a minor fraction of Parkinson's disease cases (Gasser, 2001), the discovery of these genes and their products has broadened our understanding of the potential mechanisms of neurodegeneration in both familial and sporadic Parkinson's disease (McNaught, et al; 2001).

Environmental exposure is also a factor that could result in Parkinson's disease (Calne, et al; 1987).   In the early 1980s, Langston and his colleagues (Langston, et al; 1983) reported a series of patients who developed acute levodopa-responsive parkinsonism after exposure to MPTP, a toxic side product in the clandestine synthesis of a pethidine analogue. MPTP can easily cross the blood-brain barrier and is metabolized to MPP^+. MPP^+ is taken up by dopaminergic neurons through the dopamine transporter and acts as an inhibitor of mitochondrial complex I in the respiratory chain (Singer, et al; 1990). Other chemicals similar to MPTP have also been shown to cause parkinsonism have been described (Samii, et al; 1999). Furthermore, pesticide exposure, living in rural areas (in industrialised countries), and drinking well water have all been linked to Parkinson's disease (Priyadarshi, et al; 2001). While some environmental exposures increase the risk for Parkinson's disease, other factors like smoking (Morens, et al; 1995) decrease the risk of Parkinson's disease. Studies of the relation between caffeine and Parkinson's disease showed that the risk of this disease inversely correlated with the intake of caffeine from coffee and non-coffee sources (Ross, et al; 2000, Tan, et al; 2007). Infection has also been suggested to play a role in the pathogenesis of Parkinson's disease (Yamada, et al; 1996, Pradhan, et al; 1999, Tsui, et al; 1999).

Mitochondrial dysfunction, oxidative stress, excitotoxicity, apoptosis, and inflammation are potentially involved in the mechanism of neurodegeneration (Samii, et al; 1999) in Parkinson's disease. The discovery of mutations in the genes coding for

α-synuclein, parkin, and ubiquitin C-teminal hydrolase L1 in familial Parkinson's disease suggested that the ubiquitin-proteasome pathway is important in neurodegeneration (McNaught, et al; 2001). Ubiquitin molecules usually attach to damaged proteins as a signal for degradation. Ubiquitin-protein conjugates are degraded by the 26S proteasome, which is a multisubunit protease. Mutations in parkin and ubiquitin C-terminal hydrolase L1 are also likely to interfere with normal protein degradation (Samii, et al; 2004).

The currently most important treatment of Parkinson's disease is the application of either dopamine agonists or levodopa. As dopamine agonists rarely cause dyskinesias, a common adverse effect of long-term therapy with levodopa, monotherapy with dopamine agonists is generally being applied in younger patients as an initial therapy (Parkinson Study Group, 2000, Rascol, et al; 2000). In older patients, levodapa is the preferred drug. Common side-effects of dopamine agonists include nausea, hypotension, leg oedema, vivid dreams, hallucinations (Etminan, et al; 2003), somnolence (Etminan, et al; 2001), and sudden sleep attacks (Homann, et al; 2003). Levodopa remains the most important antiparkinson drug up to date (Rascol, et al; 2000). Side-effects of the drug are similar to dopamine agonists, except that somnolence, hallucinations, and leg oedema are less common with levodopa than with dopamine agonists. Unfortunately, long-term treatment with levodopa causes motor fluctuations between mobility and immobility (Nutt, 2001). The non-motor symptoms require different therapy based on the underlying symptom. For example, depression in Parkinson's disease is normally treated with a selective serotonin reuptake inhibitor (McDonald, et al; 2003).

Deep brain stimulation has recently been established as the best surgical treatment for Parkinson's disease. Before, thalamotomy (surgical lesioning of the thalamus), was applied to reduce contralateral tremor (Burchiel, 1995), pallidotomy (surgical lesioning of the Globus pallidus) was used to improve motor symptoms in Parkinson's disease (Guridi, et al; 1997). The risks of surgical treatment are brain haemorrhage, infarct, and seizures (Beric, et al; 2001, Umemura, et al; 2003). The key to success in functional neurosurgery is a careful selection of patients (Lozano, 2003, Deep-Brain

Stimulation for Parkinson's Disease Study Group, 2001).

The goal of transplantation is to replace neurons degenerated during the course of the disease and to enhance survival of endogenous neurons. Initial experimental transplantation of fetal mesencephalic tissue in Parkinson's disease patients showed successful graft survival determined by PET scanning and in autoptic tissue (Freed, et al; 1992, Kordower, et al; 1995). However, a subset of patients developed dyskinesia. Recently, Mendez et al. (2008) reported that fetal midbrain cells could survive and contain dopaminergic and serotonergic neurons without pathology in Parkinson's disease patients 14 years after intracerebral transplantation. Stem cells currently are a potential new therapy to replace the dying dopmainergic neurons or even to rescue these cells after differentiation into neuronal precursors.

3   1-Methyl-4-Phenylpyridinium (MPTP)

In the early 1980s the dopaminergic neurotoxin 1-methyl-4-phenyl-1,2,3,6-tetrahydropyridine (MPTP) was discovered accidentally. As a concomitant of the meperidine analogue 1-methyl-4-phenyl-propion-oxypiperidine (MPPP) used as "synthetic heroin", MPTP produced a parkinsonian syndrome in young drug abusers after its unintentional self-administration (Davis, et al; 1979, Langston, et al; 1983). Most of the biochemical, pathological and clinical features induced in these young addicts corresponded to the hallmarks of PD, with the exception of the presence of typical Lewy bodies (Langston, et al; 1983). A recently published follow-up study presented evidence that the severe and unremitting parkinsonism in these patients was probably caused by nerve cell degeneration induced by MPTP with characteristic features of neuroinflammation (Langston, et al; 1999). When injected in primates MPTP, causes nearly the same pathobiochemical alterations as observed in PD patients (Burns, et al; 1983, Cohen, et al; 1984, Jenner, et al; 1986). Therefore, MPTP was applied to develop animal models in order to elucidate the cellular mechanisms of the degenerative processes in PD (for review see Tipton and Singer; 1993, Przedborski

and Jackson-Lewis; 1998) and to test new therapeutic strategies (Heikkila, et al; 1984, Schmidt and Ferger; 2001, Teismann and Ferger; 2001). It was postulated that MPTP might also become a leading substance in research about environmental toxins that may initiate or promote PD. Epidemiological data suggest that environmental factors are able to promote PD in individuals over 50 years of age (Tanner, et al; 1999). Theoretically, the exposition to a low dose of a MPTP-like toxin may occur several years before the first symptoms become manifest. This may explain why only a few of the 300 individuals who may have been exposed to MPTP suffered from PD (Ballard, et al; 1985). However, there is currently no experimental evidence for MPTP-like toxins in the SNc in PD since neither MPTP nor related compounds could be found in the brain or CSF of PD patients (Ikeda, et al; 1992, Goodwin and Kite; 1998). Nevertheless, the MPTP-induced neurochemical, neuroanatomical and behavioral alterations are invaluable to study the pathological mechanism of PD in animal models.

4   Embryonic stem cell based strategies for the treatment of Parkinson＇s disease

Currently, no ES cell-based therapy studies are ongoing in humans. Only allogeneic donor-derived adult stem cells have been employed in human cell-grafting therapies, the best examples of which are bone marrow transplantations for the treatment of leukemia after myeloablative therapies. The availability of human ES cells (ESCs), however, represents an extraordinary opportunity for cell transplantation that may be applicable to a wide range of human ailments. ES cells display important properties for cell replacement therapies (Hochedlinger and Jaenisch; 2003) – 1) ESCs can be grown indefinitely in culture and 2) ESCs can be genetically manipulated, and loss of function genes (e.g., CTFR) can theoretically be repaired by the introduction of transgenes into ESCs. Because of these properties, a significant effort is required to direct their differentiation in vitro in order to prevent the formation of teratoma, an embryonal tumour derived form ESCs. Initial

transplatantion studies using ESC for cell replacement therapy in parkinsonian animals focused on grafting low numbers of cells with the hypothesis that neural induction occurs by default in the absence of other developmental signals (Tropepe, et al; 2003). Unfortunately, even transplantation of very low numbers of undifferentiated ESC facilitating neural differentiation (Bjorklund, et al; 2002) led to the development of teratoma in 20% of grafted animals. (Bjorklund, et al; 2002). Thus, it has become evident that it is necessary to restrict the potential fates of the stem cells and improve their differentiation prior to transplantation.

To date, two principal methods have focused on optimizing the differentiation of mouse ESCs (mESCs) in vitro to generate large numbers of dopaminergic neurons, the cell population degenerating in PD, thereby reducing the likelihood of mitotic cells in the graft and the development of tumors after transplantation (see minireview Hynes and Rosenthal; 2000). One method relies on a 5-stage protocol where mESC are initially cultured under serum conditions as embryoid bodies and then subsequently differentiated in a serum-free environment in the presence of Shh, FGF8 and the nonspecific mitogen FGF2, resulting in approximately 23% dopaminergic neurons (Lee, et al; 2000). Modifications of this protocol have examined the ability to increase dopaminergic yields by providing additional developmental signals. Kim et al (2002) used stable Nurr1 ESC lines (as well as Shh and FGF8) to increase dopaminergic differentiation in vitro and showed subsequent behavioral improvement in an animal model of PD without tumor formation.

The second differentiation protocol involves culturing ESC in serum-free conditions on bone-marrow-derived stromal cells that have been shown to be potent inducers of neuronal differentiation (this activity is referred to as stromal cell-derived inducing activity) (Sasai, 2002). Generated neurons are subsequently differentiated, resulting in a 16% yield of dopaminergic neurons (Kawasaki, et al; 2000) and even greater numbers when differentiated in the presence of Shh and FGF8 (Barberi, et al; 2003). Upon transplantation, these dopaminergic neurons ameliorated amphetamine-induced rotational behavior. The estimated survival of the dopaminergic neurons was approximately 22% (Kawasaki, et al; 2000), significantly better than the

5% survival rate seen in fetal-derived dopaminergic neurons. Similar differentiation protocols have recently been developed to generate dopaminergic neurons from human ESC (hESC); however, in vivo results were limited by poor (or no) survival of the grafts (Perrier, et al; 2004). This lack of survival of hESC-derived dopaminergic neurons (Winkler, et al; 2005, Freed, et al; 2001, Olanow, et al; 1996, Perrier, et al; 2004) indicates that current differentiation and transplantation protocols need to be further improved. However, a recent report has emphasized the need for glia-derived signals for proper differentiation and survival of hES-derived dopaminergic neurons in vivo (Roy, et al; 2006).

Recently, a third protocol for dopaminergic differentiation of mESC has been described (Ying, et al 2003). In this study, mESC were cultivated in the presence of FGF2, FGF8 and low concentrations of Shh with the transcription factor Lmx1a was over-expressed. Using this protocol, most of the mESC in the culture differentiated into dopaminergic neurons. However, the functional properties and safety of these cells in vivo as well as the applicability of this protocol to hESC remain to be determined.

An additional issue that limits the use of hESC in therapy is the risk of transplanting undifferentiated cells that may result in teratoma formation (Sonntag, et al; 2006) or the expansion of slow turnover neuroepithelial cells that may later present a risk (Roy, et al; 2006). With adequate differentiation it seems that this risk should be significantly reduced or eliminated (Brederlau, et al; 2006). Still, despite cell sorting or mitomycin treatments (Kawasaki, et al; 2000), a number of ESC studies still show such tumors. An alternative approach to improve safety in ESC transplantation has been to eliminate the expression of genes known to be involved in tumor formation, such as Cripto. Cripto, in addition to being overexpressed in various tumor types, has also been shown to be involved in promoting cardiomyocyte differentiation at the expense of neural differentiation (Shen; 2003). Interestingly, Cripto$^{-/-}$ ESC showed a significant increase in dopaminergic differentiation in vitro as a result of increased neural induction. Transplantation of low numbers of Cripto-deficient ESC resulted in numerous dopaminergic neurons as well as significant behavioral recovery in

parkinsonian rats (Parish, et al; 2005). More noteworthy, no teratomas were detected, whilst tumors were seen in 100% of control ESC grafts (Parish, et al; 2005). Thus, while teratomas remain one of the greatest tribulations for ESC therapies, finding 'switches' like Cripto that regulate or turn off excessive proliferation and tumorigenesis may prove to be a key tool in the future development of cell replacement therapy. An alternative method to enrich dopaminergic neurons and dopaminergic progenitors while avoiding the risk of tumors is the isolation of cells by flow cytometry prior to grafting, using fluorescence-activated cell sorting. These approaches so far involve genetic manipulation to introduce a marker such as the green fluorescent protein (GFP) or other selectable markers into the cell. This approach has been previously used to eliminate undifferentiated cells and select the desired cell type. To date, 2 transgenic lines have been used, Ngn2-GFP and Sox1-GFP (Thompson, et al; 2006, Chung, et al; 2006). In the future, as cell surface proteins are identified in differentiating cells, it may become possible to select the desired cell type without the need for genetic modification.

In conclusion, stem cells offer a great potential for the future of cell replacement therapy. In vitro, high numbers of dopaminergic cells can be generated from various sources that can induce functional recovery after transplantation in animal models of PD. However, a number of obstacles remain to be overcome. These include the need to (i) improve human culture conditions in order to obtain a similar number of dopaminergic cells to those seen in rodent cultures; (ii) improving survival and functional integration of cells after transplantation, and (iii) ensuring that the risk of teratoma formation and the presence of undesired cells are eliminated.

In addition to attempts to replace lost dopaminergic neurons using cell transplantation, it has been suggested that cell replacement therapy could also be achieved by inducing self-repair from endogenous adult stem cells in vivo. Within the adult nervous system two distinct stem cell niches have been well characterized: (i) the subventricular zone of the lateral ventricle and (ii) the subgranular zone of the dentate gyrus in the hippocampus. Within these 2 regions stem cells are continually proliferating and replacing neurons. For some years now, it has been proposed that

other stem cell niches may exist within the adult brain. Recently, a debate has evolved around the prospect of neurogenesis within the mammalian midbrain (Frielingsdorf, et al; 2004, Zhao, et al; 2003, Lie, et al; 2002). The overall conclusions of these studies have indicated that if neurogenesis occurs within these regions, it occurs at such an inefficient rate that it is unable to replace cells lost in the course of a degenerative disorder such as PD. A more recent study showed that endogenous neurogenesis could be enhanced in PD animals by administration of a dopaminergic receptor agonist (Van Kampen and Eckman, 2006). In general, a greater understanding of the mechanisms of neurogenesis in these regions of the brain could allow controlled induction or modulation of endogenous dopaminergic neurogenesis.

5 Spinal cord injury

Spinal cord injury is an insult to the spinal cord resulting in a change, either temporary or permanent, in its normal motor, sensory, or autonomic function. Causes include motor vehicle accidents (36–48%), violence (5–29%), falls (17–21%), and recreational activities (7–16%) (The National SCI Statistical Center, 1999).

Traumatic spinal cord injury immediately leads to potentially irreversible primary tissue damage (Allen, 1911) mediated by traction and compression by fractures with displaced bone fragments, disc material, or ligament injuries leading to damage of blood vessels and axons. Within minutes, microhaemorrhages appear in the central gray matter and increase in size over the next few hours (McDonald and Sadowsky, 2002). At the injury level, the spinal cord starts to swell and occupies the entire lumen of the spinal canal within minutes. When the pressure within the swollen spinal cord exceedes the venous blood pressure, secondary ischaemia occurs. The impaired autoregulation of blood flow is aggravated by the spinal neurogenic shock resulting in systematic hypotension, thus further increasing ischaemia. Ischaemia, the release of toxic chemicals from disrupted neural membranes, and electrolyte shifts trigger a secondary injury cascade leading to damage and apoptosis of neighbouring cells thus substantially compounds the initial mechanical damage (McDonald and Sadowsky,

2002).

After injury, the hypoperfusion first occurs in the grey matter (Tator and Koyanagi, 1997) and progresses to the surrounding white matter. This hypoperfusion slows or entirely blocks the conduction of action potentials along axons, resulting in spinal shock. Although this interpretation has been addressed for over two centuries, the pathophysiology of spinal shock is not yet clarified (Hall, 1841, Atkinson PP and Atkinson, 1996). Currently, several explantations of the mechanisms of secondary injury have been proposed. Toxic chemicals released from dying cells, axons and blood vessels can damage neighbouring cells. Glutamate, a neurotransmitter widespread in the spinal cord, plays an important role in excitotoxic damage. Under conditions of spinal cord injury, glutamate secretion increases leading to overexcitation of neighbouring neurons. The concentration of calcium ions is increased in these overexcited neurons and triggers a destructive cascade, including the generation of free radicals. Consequently, membranes and other cell components are attacked causing the degeneration of neurons. Excitotoxicity not only affects neurons, but also oligodendrocytes (Matute, et al; 1997, McDonald, et al; 1998). One of the glutamate receptors, the AMPA (α-amino-3-hydroxy-5-methyl-4-isoxazole propionic acid) receptor, plays a key role in oligodendrocyte injury. This observation could explain why axons suffer from demyelination and show decreased conduction of impulses after spinal cord trauma. Even in non-traumatic spinal cord injury, excitotoxicity can cause damage to the white matter by oligodendrocyte degeneration (Pitt, et al; 2000, Smith, et al; 2000).

6   Stem cell based strategies for the treatment of spinal cord injury

During the first decades of the 20th century, studies of the adult mammalian central nervous system (CNS) issued that regeneration after insult or injury was limited (Ramon Y Cajal, 1928). In the 1990s, scientists observed neurogenesis in the adult hippocampus and subventricular zone (Lois, et al; 1993, Eriksson, et al; 1998),

focussing attention on the therapeutic potential of both endogenous and exogenous CNS stem cells in the repair of the brain and spinal cord. The aim of developing stem cell based strategies for the treatment of spinal cord injury can be roughly classified into four categories: oligodendroglial replacement/functional remyelination, neuronal replacement/gray matter reconstitution, providing a permissive substrate for axonal regeneration, and neuroprotection (Enzmann, et al; 2006).

Demyelination contributes to dysfunction of the traumatically injured spinal cord in both humans and experimental animals (Blight, 2002, Bunge, et al; 1993, Cao, et al; 2005a, Gledhill, et al; 1973, Guest, et al; 2005, Waxman, 1989). Thus, remyelination of demyelinated, but otherwise intact axons is an important strategy to repair the injured spinal cord (Blight, 2002). Stem cells, which have the potential to differentiate into oligodendrocytes, are used for transplantation into the demyelinated/dysmyelinated spinal cord. However, undifferentiated embryonic stem cells cannot be used for transplantation without predifferentiation since undifferentiated stem cells often develop into heterotopias or tumors (Bjorklund, 2000; Reubinoff, et al; 2000, Thomson, et al; 1998). Both mouse (Brustle, et al; 1999, Liu, et al; 2000) and human (Nistor, et al; 2005) ES cell–derived glial precursors exhibit robust remyelination following transplantation into myelin-deficient mice. These precursor cells migrated broadly in the host CNS after transplantation into the dorsal column of myelin deficient rat or shiverer mouse spinal cord. Some of these cells completely differentiated into mature oligodendrocytes, ensheathed demyelinated axons and formed myelin (Brustle, et al; 1999, Liu, et al; 2000, Nistor, et al; 2005). Additionally, neural stem cells derived from rat striatum and midbrain can easily remyelinate axons in the myelin-deficient rat spinal cord after transplantation (Hammang, et al; 1997). Mouse neural stem cells can also remyelinate chemically demeylinated axons in the adult rat spinal cord (Liu, et al; 2000). Both human brain-derived neural stem cells (Akiyama, et al; 2001) and mouse subventricular zone neural stem cells (Pluchino, et al; 2003) extensively remyelinated axons demyelinated by ethidium bromide or by the induction of experimental autoimmune encephalomyelitic, respectively. *In vitro* differentiation of neural stem cells into

oligodendrocytes precursor cells (OPCs) before transplantation increased the capacity of differentiation into oligodendrocytes and the ability to remyelinate after grafting into the demyelinated/dysmyelinated spinal cord. Compared with undifferentiated neural stem cells, these differentiated OPCs led to significantly larger areas of myelination after transplantation into the spinal cord of the myelin-deficient rat (Zhang, et al; 1999) or demyelinated spinal cord (Smith, et al; 2000). Glial precursor cells can be derived not only from embryonic stem cells and neural stem cells, but can also be isolated from embryonic tissues, including the developing spinal cord (Mujtaba, et al; 1999, Rao et al; 1997), brain (Ben-Hur, et al; 1998), and optic nerve (Barres, et al; 1992). Neonatal brain-derived glial precursors differentiate into myelinating cells and remyelinate demyelinated axons after transplantation into the lesioned spinal cord (Keirstead, et al; 1999, Totoiu, et al; 2004). Keirstead ((Keirstead, et al; 1999) found that rat brain-derived precursor cells showed a Schwann cell differentiation after grafting into the lesioned spinal cord. Akiyama (Akiyama, et al; 2001) observed the same phenomenon useing human neural stem cells.

Thus, cells derived from different sources, including embryonic stem cells and neural stem cells can mediate remyelination in a variety of demyelinating and dysmyelinating models of spinal cord injury. This is probably due to the environment created in these models of dysmyelination or demyelination that seems to be favorable for oligodendrocyte differentiation and remyelination.

In models of traumatic spinal cord injury, the results were quite heterogeneous in comparison to the demyelinated/dysmyelinated model of spinal cord injury. McDonald et al. (1999) observed significant oligodendrocyte differentiation and locomotor improvement following grafting of ES cells into contused spinal cords. Keirstead et al. (2005) also observed myelination and partial hindlimb locomotor recovery after engrafing predifferentiated human ES cells into lesioned spinal cords, yielding more than 90% oligodendrocytes. Other groups observed a more limited or absent oligodendrocytic differentiation following engraftment of both embryonic and adult NSCs transplanted into traumatic SCI models (Cao, et al; 2001, Chow, et al; 2000, Cummings, et al; 2005, Hasegawa, et al; 2005, Iwanami, et al; 2005, Ogawa, et

al; 2002, Vroemen, et al; 2003). Glial-restricted A2B5$^+$/NG2$^+$ precursor cells isolated from the embryonic spinal cord either differentiated into astrocytes or remained undifferentiated after transplantation into the traumatically injured spinal cord (Cao, et al; 2005b, Han, et al; 2004, Hill, et al; 2004) with only small numbers of oligodendrocytes differentiating from engrafted precursor cells. Based on all these findings, the different microenvironment in the traumatically lesioned spinal cord compared to the demyelinated/dysmyelinated lesioned spinal cord, seems to restrict the differentiation of grafted stem cells into oligodendrocytes. Scientists are trying to identify inhibitors in the traumatically lesioned spinal cord, which prevent stem cells from differentiation into oligodendrocytes. Transplantation of sonic hedgehog together with OPCs into the contusion-injured spinal cord, which enhanced the survival of OPCs, resulting in functional recovery (both electrophysiological and behavioral) (Bambakidis et al; 2004). Hofstetter et al (2005) reported that neural stem cells that were genetically manipulated to express the neurogenic transcription factor Ngn2 showed decreased astrocytic differentiation and increased oligodendrocytic differentiation after engrafting into contusion-lesioned spinal cord.

After spinal cord injury, neuronal loss, especially of motor neurons in the cervical and lumbar enlargement, results in locomotor dysfunction. Thus, replacing or rescueing these motor neurons may be a desireable strategy to enhance functional recovery. Nevertheless, the majority of studies showed that embryonic stem cells and neural stem cells prefer glial differentiation after transplantation into the CNS (Ogawa, et al; 2002, Chow, et al; 2000, Cao, et al; 2001, Magnuson, et al; 2001, Benton, et al; 2005, Enzmann, et al; 2005, Vroemen, et al; 2003, Hofstetter, et al; 2005). These observations suggest that the microenvironment in the injured spinal cord favors glial differentiation of stem cells. Cao et al (2002b) reported that the environment in contused spinal cord limits neuronal differentiation. Thus, to replace lost neurons in the lesioned spinal cord optimized protocols for neuronal predifferentiation in vitro or methods to modify the host environment are required. Some studies showed that predifferentiation of NSCs into cholinergic motor neurons in vitro may be necessary for successful motor replacement after SCI (Gao, et al; 2005, Harper, et al; 2004, Kerr,

et al; 2003, Wu, et al; 2002) and thus protocols for differentiation of murine embryonic stem cells (Renoncourt, et al; 1998, Wichterle, et al; 2002) and human neural stem cells (Wu et al., 2002) into cholinergic neurons *in vitro* was optimized. After transplantion of ES- or NSCs-derived cholinergic neurons into the lesioned spinal cord, they could replace lost motor neurons and at lease partially restore motor function (Gao, et al; 2005, Harper, et al; 2004, Kerr, et al; 2003). Besides replacing lost motor neurons, another possibility to improve locomotor function after spinal cord injury is to facilitate the activation of spinal cord circuitry below the level of injury, resulting in the enhancement of segmental reflex arcs and the subsequent improvement of locomotor function (Pearson, 2001). Engrafted embryonic raphe cells into the lesioned spinal cord can reinnervate specific targets, presumably the central pattern generator in the lumbar part of the spinal cord (Cazalets, et al; 1995, Magnuson, et al; 1999) and can contribute to the restoration of neurotransmitter receptor densities and partial hindlimb weight support, as well as increase locomotor function (Ribotta, et al; 1998, Ribotta, et al; 2000).

Lineage-specific differentiation is not the only aim in stem cell-based therapeutic approaches in spinal cord injury. Constitutive expression and secretion of GDNF, NGF, and BDNF from stem cells can also improve functional recovery (Llado, et al; 2004, Lu, et al; 2003). Thus, in addition to their ability to replace lost neurons after SCI, stem cells seem capable of facilitating host repair mechanisms by secretion of growth factors and other mechanisms that await elucidation.

7   The neural cell adhesion molecule L1

Cellular interactions can temporally and spatially adjust the fate of cells in the nervous system. Neural recognition molecules are located at the cell surface and interact with molecules on neighboring cells or the extracellular matrix by homophilical interaction, one molecule binding to another of the same type, or heterophilical interaction, meaning molecules of different types interact with each other. The interaction can take place in cis- on the same cell or in trans- to connect

molecules on the surface of different cells. These interactions affect intercellular signal transduction procedures contributing to contact mediated attraction or repulsion. Neural recognition molecules have already been divided into different families Among these are molecules of the immunoglobulin (Ig) superfamily, integrins, receptor tyrosine kinases (including ephrin receptors), neuroligins, neurexins, neuropilins and plexins; it is likely that more of these associations will become evident in diverse functional contexts (Maness, et al; 2007).

Integrins are the most important cellular receptors mediating interactions with extracellular matrix molecules and also interact with cell adhesion molecules of the Ig superfamily during development and in the adult nervous system.

Antibodies were the first molecules consisting of several Ig-like domains. This observation led to the description of the Ig superfamily of cell adhesion molecules (Edelmann; 1969). The neural cell adhesion molecule NCAM was the first neural cell adhesion molecule fully characterized (Hoffmann et al., 1982) showing evolutionary relationship to antibodies. In contrast to the dimeric antigen recognizing molecules, neural cell adhesion molecules of the Ig superfamily do not inevitably form dimers, offering the potential for additional interactions by pairing of domains between molecules (Becker et al., 1989). The common structure of the Ig superfamily is the Ig-like domain consisting of 70-110 amino acids that form two β-sheath structures, which create a hydrophobic nucleus, and comprising two conserved cystein residues separated by 55–75 amino acids that stabilize the structure with disulfide bonds (Williams, et al; 1989). Fibronectin type III (FNIII) domains are also a common structure found in several neural cell adhesion molecules of the Ig superfamily in various copy numbers (Main, et al; 1992). This domain consists of roughly 90 amino acids composed of two opposing β-sheath structures. In contrast to the Ig-like domains, the structure of the FNIII domain is not stabilized by disulfide bonds and shows a different topology (Brümmenorf and Rathjen; 1993). FNIII domains can interact with extracellular matrix molecules (Ruoslahti and Pierschbacher; 1987) and effect neurite outgrowth (Appel, et al; 1993). The L1, NCAM and DCC-family, three closely related families of neural cell adhesion molecules within the Ig superfamily,

contain both Ig-like and FNIII domains.

The molecules of the L1 family are characterized by the extracellular L1-cassette, consisting of six Ig-like domains followed by at least four FNIII repeats (Holm, et al; 1996). The L1-cassette is either linked to the membrane by a glycosylphosphatidylinositol (GPI)-anchor or contains a single transmembrane domain followed by a short cytoplasmic domain defining two subgroups of the L1 family with the expression of additional isoforms of the transmebrane molecules by alternative splicing (Brümmendorf and Rathjen; 1993). The members of the L1 family are highly glycosylated (up to 20% of the apparent molecular weight) and express the HNK-1 epitope (Schachner; 1989). Most molecules are expressed in the central and peripheral nervous system and, not being restricted to neurons, are expressed by subgroups of glial cells with coexpression of several members of the L1 family defining a cell type specific, temporospatial expression pattern (Moscoso and Sanes; 1995).

L1 is a transmambrane glycoprotein that homophilically and/or heterophilically interacts with other molecules. The molecular weight of L1 is about 200 kDa. L1 consists of six Ig-like domains, followed by five FNIII domains, a transmembrane region, and a cytoplasmatic domain (Moos, et al; 1988). In the CNS, L1 becomes detectable on unmyelinated axons of postmitotic neurons when they start growing towards their targets, is expressed throughout adulthood, and is absent from cell bodies and dendrites (Persohn and Schachner; 1987, Bartsch, et al; 1989). In the peripheral nervous system, L1 is not only expressed on neurons, but also on Schwann cells before myelination and under conditions of regeneration (Martini and Schachner; 1988). Moreover, L1 is expressed in cells of the hemopoietic lineage, in proliferating epithelial cells of the intestinal crypts and also in several peripheral tumor cells (Thor, et al; 1987). Alternative splicing generates a neuronal isoform of L1 containing a sequence (RSLE) inserted in the cytoplasmic domain that enables an interaction of L1 with the AP2-clathrin adaptor protein involved inendocytosis (Kamiguchi, et al; 1998).

L1 is involved in neuronal migration, neurite outgrowth, and myelination

(Brummendorf, et al; 1998) as well as axon guidance, fasciculation, and regeneration (Castellani, et al; 2000, Zhang, et al; 2000). Furthermore, it enhances cell survival (Chen, et al; 1999), neuronal differentiation of neural stem cells (Dihné, et al; 2003), and synaptic plasticity (Luthi, et al; 1996, Saghatelyan, et al; 2004). L1 engages in homophilic and heterophilic cell interactions. Heterophilic binding partners are the RGD-binding integrins and TAG-1/axonin-1, F3/F11/contactin, NCAM, CD9, CD24, and phosphacan (Silletti, et al; 2000). These interactions are likely to depend on the presentation of the L1 molecule either in a membrane-bound form or as a proteolytic fragment, which has been described in various forms (Nayeem, et al; 1999).

Different mutations in the extracellular or intracellular domain of L1 cause severe human neuropathological disorders (Kenwrick, et al; 1999). This discovery highlights the critical role of L1 in neural development. Up to date, almost 100 different mutations of L1 gene have been categorized into three syndromes: hydrocephalus as a result of stenosis of the Aqueduct of Sylvius (HSAS), mental retardation, aphasia, shuffling gait, and adducted thumbs (MASA), and X-linked spastic paraplegia (XLSP). Anatomical deformations found in the CNS of L1 mutationed patients are enhanced ventricles or hydrocephalus, hypoplasia or aplasia of the corticospinal tract, corpus callosum, or septum pellucidum, and fusion of the thalami or colliculi. In the L1 deficient mouse, similar malformations of the CNS were described (Dahme, et al; 1997, Cohen, et al; 1997).

Due to the positive effects of L1 on neuronal differentiation and survival L1 was applied to enhance survival and differentiation of neural cells in vitro and in vivo and to enhance functional regeneration in mouse models of neurodegenerative disease and spinal cord trauma. L1 rescued fetal dopaminergic neurons when cultured in vitro as well (Hulley, et al; 1998). Substrate-bound L1 promoted neuronal attachment and neurite outgrowth in the presence of astrocytes and fibroblasts (Webb, et al; 2001). Ectopic expression of L1 in astrocytes in transgenic mice not only led to better learning and memory and higher flexibility in relearning (Mohajeri, et al; 1996), but also to precocious development of the corticospinal tract (Ourednik, et al; 2001). Application of the extracellular domain of L1 to adult rats after spinal cord injury

promoted locomotor recovery (Roonprapunt, et al; 2003). Embryonic stem cells overexpressing L1 increased neuronal differentiation of grafted cells and enhanced locomotor function after transplantation in a mouse model of Huntington's disease (Bernreuther, et al; 2006). Chen et al (2005) reported an increased regrowth of corticalspinal tract axons into the lesion site after intraspinal transplantation of L1 overexpressing embryonic stem cells into the lesion site in a murine spinal cord injury paradigm. Moreover, adeno-associated virus-mediated L1 expression enhaned locomotor function mice with compression –lesioned spinal cords (Chen, et al; 2007).

8 <u>S</u>ubstrate-adherent <u>e</u>mbryonic stem cell-derived <u>n</u>eural <u>a</u>ggregates (SENAs).

Dihné and Bernreuther (Dihné, et al; 2006) developed an optimized protocol for pre-differentiation of murine ES cells and isolation of ES cell-derived neural aggregates for transplantation, which gives rise to substrate-adherent embryonic stem cell-derived neural aggregates (SENAs). SENAs resulted in a high yield and improved survival of fully differentiated neurons in vitro and after transplantation in vivo. Furthermore, there was reduced tumor formation in a syngeneic transplantation paradigm in which pre-differentiated ES cell-derived neural aggregates from C57BL/6J mice were injected into the quinolinic acid-lesioned striatum of adult C57BL/6J recipient mice.

9 The aim of this study

Recent advances in embryonic stem cell-based therapeutic approaches in Parkinson's disease and spinal cord injury emphasize the necessity to enhance graft survival and to prevent tumoru formation by grafted cells. The SENA differentiation protocol has been shown to efficiently reduce tumor formation and enhance the survival and neuronal differentiation of grafted cells in a mouse model of Huntington's disease. Furthermore, the neural cell adhesion molecule L1 has been shown to enhance functional recovery in a mouse model of Huntington's disease.

25

Thus, the aim of this study was to combine the favorable properties of the SENA differentiation protocol and the overexpression of the neural cell adhesion molecule L1 in grafted cells and to monitor the potentially further enhanced regenerative protocol of L1 overexpressing embryonic stem cells differentiated by the SENA protocol in a mouse model of Parkinson's disease and a mouse model of traumatic spinal cord injury.

III   Materials and Methods

1   Materials

1.1   Chemicals

If not indicated otherwise, all chemicals were obtained from the following companies in p.a. quality: Macherey-Nagel (Düren, Germany), Merck (Darmstadt, Germany), Serva (Heidelberg, Germany) and Sigma (Deisenhofen, Germany). DNA Purification kits were purchased from Invitrogen, Amersham Pharmacia Biotech (Freiburg, Germany), Macherey & Nagel and Qiagen (Hilden, Germany). The Dopamine Research RIA kit and GABA Research ELSA KIT were ordered from Labor Diagnostika Nord GmbH & Co. KG (Germany). Cell culture material was ordered from Nunc (Roskilde, Denmark) or Invitrogen.

1.2   Solutions and Buffers

(in alphabetical order)

Antibody buffer	0.3	% (w/v)	bovine serum albumine (BSA)
(Immunocytochemistry)			in PBS pH 7.4
	0.02	% (w/v)	Triton X-100
Anesthetics	20	% (w/v)	Ketanest (Parke-Davis/Pfizer, Karlsruhe, Germany)
	8	% (w/v)	Rompun (Bayer, Leverkusen, Germany)
	72	% (w/v)	0.9% NaCl
Blocking buffer	3	% (w/v)	BSA in PBS pH 7.4
(Immunocytochemistry)	0. 2	% (w/v)	Triton X-100
Blocking buffer	1-4	% (w/v)	instant milk powder in TBS
(Western Blot) or	1	% (v/v)	block solution (boehringer) in

			TBS
Blotting buffer	25	mM Tris	
(Western Blot)	192	mM Glycin	
DNA-sample buffer (5x)	20	% (w/v)	glycerol in TAE buffer
(DNA-gels)	0,025	% (w/v)	orange G
dNTP-stock solutions	20	mM each	DATP, dCTP, dGTP, dTTP
			(PCR)
Ethidiumbromide-	10	µg/ml	ethidiumbromide in 1xTAE
staining solution *(DNA-gels)*			
HBSS$^-$	5.33	mM	KCl
	0.44	mM	KH_2PO_4
	4.00	mM	$NaHCO_3$
	138.0	mM	NaCl
	0.3	mM	Na_2HPO_4
	5.6	mM	D-glucose
Phosphate buffered saline	150	mM	NaCl
(PBS)	20	mM	Na_3PO_4 pH 7.4

Protease-inhibitors solution   COMPLETE™ pills. Resuspending 1 tablet in 2 ml

results in a 25x stock solution

RIPA-buffer	50	mM	Tris-HCl, pH 7.4
(cell lysis)	1	% (w/v)	Triton X-100
	150	mM	NaCl
	1	mM	EGTA

	1	mM	Na$_3$VO$_4$
Running Gel 10% (8%)	3.92	ml (4.89 ml)	deionized water
(protein gels)	5.26	ml (5.26 ml)	1 M Tris pH 8.8
	0.14	ml (0.14 ml)	10% SDS
	4.70	ml (3.73 ml)	30% Acrylamide – Bis 29:1
	70.0	µl (70 µl)	10% APS
	7.00	µl (7 µl)	TEMED
Sample buffer (5x)	0.312	M	Tris-HCl pH 6.8
(protein-gels)	10	% (w/v)	SDS
	5	% (w/v)	β-Mercaptoethanol
	50	% (v/v)	Glycerol
	0.13	% (w/v)	Bromphenol blue
SDS running buffer (10x)	0.25	M	Tris-HCl, pH 8.3
(protein-gels)	1.92	M	glycine
	1	M	SDS
Stacking Gel 5%	3.77	ml	deionized water
(protein gels)	0.32	ml	
	1	M	Tris pH 6.8
	0.05	ml	10% SDS
	0.83	ml	30% Acrylamide – Bis 29:1
	25.0	µl	10% APS
	7.00	µl	TEMED
Stripping buffer	0.5	M	NaCl
(Western blots)	0.5	M	acetic acid
TAE (50x)	2	M	Tris-Acetat, pH 8.0

(DNA-gels)	100	mM	EDTA
TE (10x)	0,1	M	Tris-HCl, pH 7.5
	10	mM	EDTA
Tris Buffered Saline (TBS)	10	mM	Tris-HCl, pH 8.0
	150	mM	NaCl

1.3 Cell lines

L1$^+$ ES cells	Embryonic stem cell line established from transgenic C57 black/6J mice expressing GFP under the influenceof the chick β-actin promoter (Okabe, et al; 1997), and transfected with full length mouse L1 under the control of the isoform 1 of the 3-phosphoglycerokinase (PGK) (Bernreuther et al., 2006)
Control ES cells	Embryonic stem cell line established from transgenic C57 black/6J mice expressing GFP under the influenceof the chick β-actin promoter transfected with a control plasmid (empty vector) (Okabe, et al; 1997, Bernreuther, et al; 2006)

1.4 Cell culture Media

Media was purchased from Invitrogen and supplemented as described

ES-medium	Dulbecco's MEM (DMEM, 4.5 g/l D-glucose, 25mM HEPES, 0.58 g/l L-glutamine, no sodium pyruvate) supplemented with		
	15 %	(v/v)	fetal calf serum (FCS, ES qualified) (Perbio, Erembodegem, Belgium)
	2	mM	L-glutamine
	1	×	MEM non-essential amino acids
	1	mM	sodium pyruvate

	1	×	nucleoside mix (containing 3mM of each adenosine, cytidine, guanosine, uridine and thymidine in PBS
	0.1	mM	2-mercaptoethanol
	1,000	U/ml	murine leukemia inhibitory factor (ESGRO^{TM} LIF) (Chemicon, Temecula, CA, USA)
	50	U/ml	penicillin
	50	µg/ml	streptomycin
ES-medium ∅ LIF	ES-medium without ESGRO^{TM} LIF		
ES selection-medium	ES-medium supplemented with		
	250	µg/ml	G418 (Geneticin) (Invitrogen)
ITSFn-medium with	DMEM/Ham's F12 (DMEM/F12) (1:1) supplemented		
	5	µg/ml	insulin
	50	µg/ml	transferrin
	30	nM	sodium selenite
	5	µg/ml	fibronectin
	2	mM	L-glutamine
	50	U/ml	penicillin
	50	µg/ml	streptomycin
MEF-medium	DMEM (4.5 g/l D-glucose, with Glutamax™ I, no pyruvate) (Invitrogen) supplemented with		
	9	%	FCS
	1	×	MEM non-essential amino acids

31

50	U/ml	penicillin
50	µg/ml	streptomycin

mN3   DMEM/F12 supplemented with

1	×	B27-supplement (Invitrogen)
2	mM	L-glutamine
50	U/ml	penicillin
50	µg/ml	streptomycin

mN3-bFGF   mN3 supplemented with

20	ng/ml	basic fibroblast growth factor
		(bFGF)
		(PreproTech, Rocky Hill, NY, U
		USA)

NSC-medium   DMEM/F12 supplemented with

1	×	B27-supplement
0,6	%	D-glucose
2	mM	L-glutamine
3	mM	sodium bicarbonate
5	mM	HEPES
50	U/ml	penicillin
50	µg/ml	streptomycin
10	ng/ml	bFGF
10	ng/ml	epidermal growth factor (EGF)
		(PreproTech, Rocky Hill, NY,
		USA)

1.5 Antibodies
1.5.1 *Primary antibodies*

anti-β-III-tubulin   mouse monoclonal antibody Tuj1 (Sigma)

IH: 1:400

anti-BrdU   mouse monoclonal antibody (Sigma)

IH: 1:200

anti-caspase-3   rabbit polyclonal antibody (R&D Systems, Minneapolis,

MN, USA)

IH: 1:2000

anti-ChAT   goat polyclonal antibody (Millipore)

IH: 1:100

anti-CNPase   mouse monoclonal antibody (Sigma)

IH: 1:1000

anti-GAD-6   mouse monoclonal antibody (Developmental Studies

Hybridoma Bank, Iowa City, IA, USA)

IH: 1:10

anti-FN   rabbit polyclonal antibody (Sigma)

IH: 1:100

anti-GAD-65/67   rabbit polyclonal antibody (Sigma)

IH: 1:500

anti-GFAP   rabbit polyclonal antibody (Dako)

IH: 1:1000

anti-Iba 1   rabbit polyclonal antibody (Wako Chemicals, Richmond, VA)

IH: 1:1500

anti-L1   mouse monoclonal antibody (Appel, et al; 1993)

IH: 1:100

anti-L1   rabbit polyclonal antibody (Rathjen and Schachner, 1984

IH: 1:100

IB: 1:10.000

anti-NeuN   mouse monoclonal antibody (Chemicon)

IH: 1:1000

anti-NF-200   rabbit polyclonal antibody (Sigma)

IH: 1:200

anti-TH   rabbit polyclonal antibody (Millipore)

IH: 1:800

1.5.2 *Secondary antibodies*

For indirect immunofluorescence and Western blot analysis, Cy2™, Cy3™, and Cy5™ conjugated antibodies (diluted 1:200-1:300) and horseradish peroxidase-conjugated antibodies (diluted 1:10,000) to rabbit, rat, human or mouse IgG were used, respectively (Jackson Immuno Research via Dianova, Hamburg, Germany).

2   Methods

2.1   Western-blot analysis
2.1.1 *Electrophoretic transfer*
(Towbin, et al; 1979)

Proteins were transferred from the SDS-gel to a Nitrocellulose membrane (Protran Nitrocellulose BA 85, 0,45 mm, Schleicher & Schüll, Dacssel, Germany) using a MINI TRANSBLOT-apparatus (BioRad). After equilibration of the SDS-PAGE in blot buffer for 5 min, the blotting sandwich was assembled as described in the manufacturer's protocol. Proteins were transferred electrophoretically at 4°C in blot buffer at constant voltage (70 V for 120 min or 35 V overnight). The prestained marker BenchMark™(Invitrogen) was used as a molecular weight marker and to monitor electrophoretic transfer.

2.1.2 *Immunological detection of proteins on nitrocellulose membranes*
(Ausrubel, 1996)

After electrophoretic transfer, the membranes were removed from the sandwiches, washed once in TBS and incubated in blocking buffer for 1 h at room temperature. Afterwards, the primary antibody was added in the appropriate dilution either for 2 h at RT or overnight at 4°C. The primary antibody was removed by washing the membrane 5×5 min with TBS. The appropriate secondary antibody was applied for 2 h at RT. The membrane was washed again 5×5 min with TBS and immunoreactive bands were visualized using the enhanced chemiluminescence detection system.

2.1.3 *Immunological detection using enhanced chemiluminescence*
The antibody bound to the membrane was detected using the enhanced chemiluminescence detection system (Pierce, Rockford, IL, USA). The membrane was soaked for 1 min in detection solution (1:1 mixture of solutions I and II). The solution was removed and the blot was placed between two cellophane foils. The membrane was exposed to X-ray film (Biomax-MR, Eastman Kodak, Rochester, NY, USA) for several time periods, starting with a 2 min exposure time.

2.1.4 *Determination of protein concentration (BCA)*
(Ausrubel, 1996)

The protein concentration of cell lysates was determined using the BCA kit (Pierce). Solutions A and B were mixed in a ratio of 1:50 to give the BCA solution. 20 µl of the cell lysate were mixed with 200 µl BCA solution in microtiter plates and incubated for 30 min at 37°C. A BSA standard curve was co-incubated ranging from 100 µg/ml to 2 mg/ml. The extinction of the samples was determined at 568 nm in a microtiter plate reader.

2.2 Immunohistochemistry

2.2.1 *Immunocytochemistry of living cells*

Coverslips with attached cells were washed with HBSS⁻ and placed on Parafilm in a humid chamber. 100 µl of HBSS⁻ containing the primary antibody in the appropriate dilution was added onto the coverslips and incubated at RT for 20 min. Afterwards, the coverslips were put into 12-well dishes and washed twice with HBSS⁻. Coverslips were subsequently placed on Parafilm™ in the humid chamber again, covered with 100 µl of HBSS⁻ containing the fluorescent dye-coupled secondary antibody in a 1:200 dilution, and incubated at 37°C for 20 min in the dark. Finally, the coverslips were washed twice with HBSS⁻, fixed and mounted on glass slides with Aqua Poly-Mount medium (Polysciences, Warrington, PA, USA).

2.2.2 *Immunohistochemistry of fixed cells and tissues*

Cultured cells were washed in PBS, pH 7.3 and fixed for 15 minutes in 4% paraformaldehyde before incubation with 0.1% BSA in PBS for 40 min. Primary antibodies were applied for 1 hour at room temperature. After washing in PBS, appropriate secondary antibodies were applied for 40 minutes at room temperature.

For preparation of tissue sections, animals were perfused with PBS followed by 4% paraformaldehyde in PBS. Brains were post-fixed overnight in the same fixative and then cryoprotected with 20% sucrose for 2 days at 4°C. Brains were frozen in liquid nitrogen, and 25 µm serial cryosections were mounted on SuperfrostPlus slides

(Menzel, Braunschweig, Germany) and allowed to dry overnight at room temperature. After incubation in 0.1% BSA in PBS for 40 min, primary antibodies were applied for 24 hours at 4°C.

For detection of primary antibodies, appropriate secondary antibodies, coupled to Cy2, Cy3, or Cy5 (all from Dianova, Hamburg, Germany) were used. Some cell cultures and tissue sections were counterstained for 10 min with 50 μg/ml DAPI (Sigma) to visualize cell nuclei. To immunostain with the monoclonal mouse antibody to bromodeoxyuridine (BrdU), DNA was denatured with 70% ethanol for 5 min at room temperature followed by 2.4 M HCl for 10 min at 37°C. Monoclonal mouse antibody to BrdU was administered overnight at 4°C. For neurofilament 200 staining, tissue sections were incubated in 10 mM sodium citrate, pH 9.0, at 80°C for 30 min prior to PBS/BSA incubation. Specimens were examined with a fluorescence (Axioplan 2; Carl Zeiss Microimaging, Thornwood, NY, USA) or confocal laser-scanning (LSM510; Carl Zeiss Microimaging) microscope.

2.3 Culture, manipulation, differentiation and transplantation of embryonic stem cells

2.3.1 *Gelatinizing of cell culture dishes*

Cell culture dishes were treated for 1 - 2 h with an autoclaved 0.1% (w/v) gelatin solution (type A from porcine skin, approximately 300 Bloom). After removal of this coating solution, dishes were air-dried and stored before usage at 4°C ù for up to 2 weeks

.

2.3.2 *Cultivating feeder cells*

ES cells were grown on a single cell layer of mitotically inactivated, neomycin-resistant embryonic fibroblasts. Such embryonic fibroblasts were derived from E13.5 - E14.5 embryos of neo-transgenic mice (FV-Neo, kindly provided by Dr. Irm Hermanns-Borgmeyer, ZMNH, Hamburg). Confluent cultures of neomycin-resistant fibroblasts were mitotically inactivated before use as a feeder layer for ES cells. Therefore, fibroblasts were kept 2.5 - 3 h in 10 g/l Mitomycin C in

fibroblast medium. After washing 3× with PBS, cells were trypsinized (0.05% trypsin-EDTA, Invitrogen) and stored as aliquots in liquid nitrogen. 16 - 24 h before culturing ES cells on a feeder layer, these mitotically inactivated fibroblasts were seeded with a density of 5×10^4 cells per cm^2 on gelatinized cell culture dishes. Cells were cultured in MEF-medium at 37°C, 7.5% CO_2.

2.3.3 *ES cell culture*

$L1^+$ and control ES cells were cultured in ES cell medium (37°C, 7.5% CO_2). Cells were maintained on a feeder layer of mitotically inactivated mouse embryonic fibroblasts at all times. The ES cells grew in spheres showing sharp boundaries and were subcultivated before individual spheres contacted each other. Medium was changed daily. For subcultivating, cells were washed with PBS once and trypsinized with trypsin-EDTA (0.25 % (w/v) trypsin, 1mM EDTA) for 3 min at 37°C. Cells were dissociated in an appropriate amount of ES cell medium and seeded in intial to final density ratios of 1:2 to 1:5. For cryopreservation an equal volume ES-cell medium was added to the trypsin-digests, followed by addition of two volumes freeze medium (80% ES-qualified FCS, 20% (v/v) DMSO). Cells were slowly cooled down to – 80°C and kept on liquid nitrogen for long-term storage.

2.3.4 *Generation and isolation of substrate-adherent embryonic stem cell-derived neural aggregates*

The lineage selection protocol according to Okabe et al. (1996) and Lee et al. (2000) was slightly modified. Briefly, this protocol comprises a five stage differentiation process:

Stage 1   Expansion of undifferentiated ES cells in ES-medium in gelatine-coated dishes without feeder cells

Stage 2   Generation of free-floating embryoid bodies in suspension culture in ES-medium $\varnothing$ LIF (4d)

Stage 3   Selection of neural precursor cells in ITSFn-medium

Stage 4   Expansion of neural precursor cells in mN3-bFGF

Stage 5   Induction of differentiation by growth factor removal

ES cell lines used in this study were a GFP expressing embryonic stem cell line transfected to overexpress the neural cell adhesion molecule L1 at all stages of differentiation and a corresponding GFP expressing ES cell line transfected with a control plasmid generated in our laboratory. Maintenance of undifferentiated ES cells, embryoid body formation and selection of neural precursor cells was carried out as described (Okabe et al., 1996; Lee et al., 2000) with minor modifications. Undifferentiated (stage 1) ES cells were expanded on a monolayer of mitomycin-treated murine embryonic fibroblasts on gelatine-coated cell culture dishes in the presence of 1,000 U/ml leukemia inhibitory factor (LIF) ES-medium. For passaging, ES cells were detached and dissociated into a single-cell suspension by 0.25% trypsin / 0.04% EDTA in HBSS-. Formation of embryoid bodies (stage 2) was induced by plating dissociated cells onto nonadherent bacterial culture dishes at a density of 2.5×10^4 cells / cm^2 in the absence of LIF (ES $\varnothing$ LIF). Four days later, selection of neural precursors was initiated with ITSFn-medium for 8 days (stage 3).

To generate substrate-adherent embryonic stem cell-derived neural aggregates (SENAs), pre-differentiated ES cell-derived neural precursors (stage 4), seeded at 100,000 cells/ml medium onto poly-L-ornithine coated cell culture dishes or coverslips, were maintained for 18 days in mN3-bFGF under the influence of bFGF, which was exchanged every second day. Since neural precursors are conventionally expanded in the presence of bFGF for only 4 - 7 days before differentiation is induced by bFGF withdrawal while SENAs are generated under the prolonged influence of bFGF for 4-6 weeks, this period was termed "prolonged stage 4" (ps4). During this period, aggregates of approximately 10.000 cells (SENAs) formed within the monolayer of neural precursor cells. Thereafter, bFGF was withdrawn for 7 days to induce terminal differentiation of SENAs (stage 5). During ps4 (1^+ till 28^+; the number of days after plating of neural precursors in the presence of bFGF will be referred to as n^+) and during the subsequent differentiation period in stage 5 without

FGF-2 ($28^+/7^-$; number of days after stage 4 or ps4 without bFGF will be referred to as n^-), SENAs developed intermixed with neural precursors growing in a monolayer. These monolayer cells shared features similar to those of "conventional" stage 4 or stage 5 ES cell cultures. To obtain highly enriched SENA preparations, cultures were treated with 0.3 μg/ml collagenase XI (Sigma) at 37°C for 10 minutes in order to gently detach entire SENAs and monolayer precursors from the substrate. Collagenase was preferred to trypsin or accutase because it did not result in dissociation of SENAs. Detached cells were carefully pipetted up and down 10-times with a fire-polished Pasteur pipette to separate monolayer precursors from SENAs that remained intact during this procedure. SENAs were harvested by sedimentation at 1×g for 2 minutes and resuspended in HBSS- in order to pick SENAs individually using a 10 μl pipette tip.

2.3.5 Transplantation

2.3.5.1 Transplantion of SENAs into MPTP- lesioned mice

Four days prior to transplantation, 2-month-old female C57BL/6J mice were lesioned by intraperatoneal injection of 1-methyl 4-phenyl 1,2,3,6-tetrahydropyridine (MPTP) (15 mg/kg, 2 hours apart, 4 times). On the day of transplantation, SENAs were harvested at $28^+/7^-$ and resuspended in HBSS$^-$ with about 10 SENAs per μl. Cell number per SENAs was estimated by dissociation with trypsin, showing that, on average, one SENA consisted of about 10,000 cells. One μl of $L1^+$ SENAs, either control SENAs or vehicle (PBS) only was grafted into the striatum unilaterally using the coordinates in relation to bregma: 0.1mm posterior, 2.5 mm mediolatral, and 3.0 mm dorsal. Grafts were analyzed 4 and 12 weeks after transplantation. All animal experiments were approved by the University and State of Hamburg Animal Care Committees.

2.3.5.2 Transplantation of SENAs into the lesioned spinal cord

Three days before transplantation, the spinal cord of 2-month-old female C57BL/6J mice was lesioned. Laminectomy was performed at the T7–T9 level with

mouse laminectomy forceps (Fine Science Tools, Heidelberg, Germany). A mouse spinal cord compression device was used to elicit a compression injury (Curtis, et al; 1993). Compression force (degree of closure of the forceps) and duration were controlled by an electromagnetic device. The spinal cord was maximally compressed (100%, according to the operational definition of Curtis, et al; 1993) for 1 second by a time-controlled current flow through the electromagnetic device. On the day of transplantation, SENAs were harvested at $28^+/7^-$ and resuspended in $HBSS^-$ with 10 SENAs per μl. Cell numbers per SENAs was estimated by dissociation with trypsin, showing that, on average, one SENA consisted of about 10,000 cells. One μl of $L1^+$ SENAs, either control SENAs or vehicle (PBS) only was injected 0.5 mm both rostral and caudal to the lesion site using a glass micropipette (tip diameter 100 μm) 1 mm deep into the spinal cord. Grafts were analyzed 6 weeks after transplantation. All animal experiments were approved by the University and State of Hamburg Animal Care Committees.

2.3.6 *Morphologic analysis*

2.3.6.1 *Analysis of differentiation, cell death and proliferation*

To determine total cell numbers in vitro, cells were counterstained with DAPI and the ratio of cell type-specific (e.g. β-III tubulin and TH) marker-positive cells to all $DAPI^+$ cells was calculated. To determine total numbers of donor cells in vivo, $EGFP^+$ cells were counted and the ratio of cell type-specific or functional marker-positive cells of all $EGFP^+$ cells was calculated. At least three independent experiments in duplicates and at least 1000 cells per marker and experiment were analysed. Percentages of double-labeled cells were determined and mean values ± standard error of the mean (s.e.m.) were calculated. Student´s t-test was used for statistical evaluation unless otherwise indicated. All experiments were performed in a double-blinded manner.

2.3.6.2 *Analysis of graft volume and density*

Unbiased estimates of the total number of grafted cells and graft volume per

animal were calculated 1 and 3 months after transplantation according to the optical dissector and Cavalieri methods (Unbiased Stereology, Howard and Reed, Bios Scientific Publishers, 1998), respectively. An Axioskop microscope (Carl Zeiss) equipped with a motorized stage and a Neurolucida software-controlled computer system was used for quantitative analysis (MicroBrightField Europe, Magdeburg, Germany). Graft volume and cell density of the graft were determined measuring every tenth section of the graft. Transplanted cells were identified by their EGFP signal. Graft areas were outlined on digitized images to calculate volumes based on section thickness and frequency. Using random sampling in the graft core and in the periphery of the graft, cell counts were performed according to the optical dissector principle at a magnification of ×40. Nuclei of DAPI$^+$ and EGFP$^+$ grafted cells were counted according to their position in each disector. All counts were performed in a double-blinded manner.

2.3.6.3 *Analysis of scar volume*

In the spinal cord lesion paradigm, mice were sacrificed six weeks after transplantation and spinal cords were cut in sagittal sections on a cryostat. Serial sections spaced 250 µm apart were stained with anti-GFAP and anti-FN antibodies to estimate the scar volume using the Cavalieri principle.

2.3.6.4 *Analysis of cell migration*

The shortest distance between at least 400 individual cells and the graft edge of recipient animals was determined on digitized images.

2.3.6.5 *Analysis of differentiation of SENAs in vivo*

To determine the differentiation of SENAs after transplantation in vivo, the ratio of double-labelled marker-positive and GFP$^+$ cells of all GFP$^+$ cells was assessed by confocal laser scanning microscopy in serial sections, and mean values ± standard error of the mean (SEM) were calculated. At least 1,000 cells per marker and experiment were analyzed in a double-blinded manner.

2.3.6.6 *Neurite outgrowth assay*

To determine the maturation of neurons differentiated from grafted SENAs, the longest neurite length per cell was measured by Neurolucida™ software. Sections were stained with anti-NeuN antibody. In each experiment, at least 50 cells per section were analyzed.

2.3.6.7 *Quantitative analysis of TH$^+$ neurons in the Substantia nigra, pars compacta*

In the MPTP lesion paradigm, TH$^+$ neurons were counted in the right and left Substantia nigra, pars compacta (SNpc) of every tenth section throughout the entire extent of the SNpc. An Axioskop microscope (Carl Zeiss) equipped with a motorized stage and a Neurolucida software-controlled computer system was used for quantitative analysis (MicroBrightField Europe, Magdeburg, Germany). The border of SNpc and ventral tegmental area was delineated at lower magnification observing TH immunostaining. Using random sampling in the SNpc, cell counts were performed according to the optical dissector principle at a magnification of ×40. All counts were performed in a double-blinded manner.

2.3.6.8 *Motoneuron soma size and quantification of perisomatic puncta*

Estimations of soma areas and perisomatic puncta were performed as described (Irintchev et al., 2005). Longitudinal spinal cord sections stained for ChAT were examined under a fluorescence microscope to select sections that contained motoneuron cell bodies at least 500 µm distal from the lesion scar. Stacks of images of 1 µm thickness were obtained on a LSM 510 confocal microscope (Zeiss) using a 40x oil immersion objective lens and digital resolution of 1024 x 1024 pixel. Four adjacent stacks (frame size 115 x 115 µm) were obtained consecutively in a rostro-caudal direction in order to sample motoneurons located both close and remote to the lesion scar were sampled. One image per cell at the level of the largest cell body cross-sectional area was used to measure soma area, perimeter and number of perisomatic puncta. Motoneurons were identified by immunolabeling in sections

stained for ChAT, and by the size of the cell bodies (unstained profiles surrounded by immunoreactive puncta) and by bis-benzimide counterstained nuclei. Areas and perimeters were measured using the Image Tool 2.0 software program (University of Texas, San Antonio, TX, USA; free software available at http://ddsdx.uthscsa.edu/dig/). Linear density was calculated as the number of perisomatic puncta per unit length.

2.3.6.9 *Monoaminergic reinnervation of spinal cord distal to the lesioned site*

To assess monoaminergic reinnervation of the spinal cord caudal to the injury, TH^+ axons projecting beyond an arbitrarily selected border 250 µm caudally to the lesion site were counted in spaced serial parasagittal sections 6 weeks after the injury.

2.3.6.10 *Analysis of glial and microglial reactions to the grafts*

To determine the reaction of the host tissue to grafted cells, immunostaining with anti-GFAP (astrocytes) and anti-Iba 1 (microglia) was perfomed and confocal images were taken around the edge of transplanted cells. At least 20 images were made from one mouse. The software Image J (http://rsbweb.nih.gov/ij/index.html) was used to measure fluorescence intensities from all 3 groups. For statistical evaluation, fluorescent intensities from $L1^+$ and control groups were normalized to the PBS group, and Turkey's One-way ANOVA was subsequently performed for analysis.

2.3.7 *Analysis of striatal levels of dopamine and GABA*
2.3.7.1 *Analysis of striatal levels of dopamine*

The commercial radioimmunoassay kit (Dopamine Research RIA, Labor Diagnostika Nord Gmbh & Co. KG, Germany) was used to measure dopamine level in striatum. One month fter transplantation, mice were sacrificed and striata were dissected out of the brain and stored at -80°C until analysis. On the day of analysis, striata were homogenized in 0.01 N HCl with 1mM EDTA and 4mM sodium metabisulfite. Protein concentrations were measured using BCA protein assay (Pierce). Samples were processed according to the manufacturer's instructions while ensuring

proper standards and controls.

2.3.7.2 *Analysis of striatal levels of GABA*

The commercial ELISA kit (GABA Research ELISA, Labor Diagnostika Nord Gmbh & Co. KG, Germany) was used to measure the GABA level in the striatum. One month after transplantation, mice were sacrificed and striata were dissected out of the brain and stored at -80°C until analysis. On the day of analysis, striata were homogenized in 0.01 N HCl with 1mM EDTA and 4mM sodium metabisulfite. Protein concentrations were measured using BCA protein assay (Pierce). Samples were processed according to the manufacturer's instructions while ensuring proper standards and controls.

2.3.8 *Evaluation of behavior*

2.3.8.1 *Evaluation of behavior of MPTP lesioned mice*

Apomorphine-induced rotations were analysed one day before and 1, 3, 4, 6, 8, 10, and 12 weeks after transplantation, to evaluate the effects of transplantation on symmetry of motor function. All mice received systemic MPTP-injections as described above. Mice were then randomly assigned to three groups that received either a unilateral striatal transplantation of L1 overexpressing SENAs, control SENAs, or a PBS injection only (sham-injected group). Mice were tested for rotation in response to intraperitoneal injection of 1 mg/kg apomorphine in PBS. All behavioural tests were performed at the beginning of the animals´ dark phase. Rotations were measured in an open field box for 30 minutes at 50 lux. Ethovision software (Noldus, Wageningen, The Netherlands) was used for processing data. Relative meander, which is net ipsilateral turning angle divided by distance, was calculated. Tukey's One-way ANOVA was used for statistical evaluation.

2.3.8.2 *Evaluation of behavior of spinal cord-lesioned mice*

The recovery of ground locomotion was evaluated using the Basso, Beattie, Bresnahan (BBB) rating scale (Basso, et al; 1995), modified for mice (Joshi and

Fehlings, 2002), and a novel single-frame motion analysis (Apostolova, et al; 2006). This method includes evaluation of four parameters in three different tests: beam walking (foot-stepping angle and rump-height index), voluntary movements without bodyweight support (extension–flexion ratio). All mice received a spinal cord compression lesion as described above. Mice were then randomly assigned to three groups that received an intraspinal injcion of L1 overexpressing SENAs, control SENAs, or a PBS injection only (sham-injected group). Assessments were performed before and at 1, 3, and 6 weeks after the injury. Values for the left and right extremities were averaged. Recovery indices were used as a measure of functional recovery for each individual animal level as previously described (Apostolova et al., 2006). The recovery index (RI) is an individual animal estimate for any given parameter described above and is calculated in percent as: $RI = [(X_{7+n} - X_7) / (X_0 - X_7)] \times 100$, where X_0, X_7 and X_{7+n} are values prior to operation, 7 days after injury, and a time-point n days after the spinal cord injury, respectively. In simpler terms, this measure estimates gain of function $(X_{7+y} - X_7)$ as a fraction of the functional loss $(X_0 - X_7)$ induced by the operation. It may attain 0 or negative values if no improvement or further impairment occur during the observation time-period. The index cannot be calculated only if the operation causes no change in the value $(X_0 - X_7 = 0)$ which is precluded by selection of reliable parameters. The recovery index is a meaningful and comprehensive parameter allowing better comparisons within one investigation and between results of different laboratories. Calculation of recovery indices is absolutely necessary if a parameter is prone to variability as a result of individual animal variability in body constitution and behavioral traits. An example is the rump-height index defined above. The index values are influenced not only by functional impairment but also by the animal's size and the beam thickness.

2.3.9 *H-reflex recordings*

The sciatic nerve was stimulated using bipolar electrical pulses of 0.2-ms duration to elicit reflex responses. The stimulus intensity was gradually increased until both M- and H-waves with latencies of approximately 2 and 5 ms, respectively, were visible.

After the threshold measurement, the stimulus intensity was further increased until maximal and stable H-responses were elicited. Thereafter, stimulation continued at the defined suprathreshold level at frequencies of 0.1, 0.3, 0.5, 1, 2, 10, 20 Hz. Six consecutive responses were recorded at each frequency. The amplitudes of M- and H-waves were measured as peak-to-peak values, averaged (excluding the first response at each frequency) and used to calculate H/M ratios. The latencies of the responses were measured as time elapsed between the trigger and peak of each waveform.

2.3.10   *Statistical evaluation*

All experiments were performed in a blinded manner and Student's t-test was used for statistical evaluation, if not indicated otherwise.

IV   Results

1. Transplantation of SENAs into the MPTP mouse model of Parkinson's disease

1.1 Characterization of L1 overexpressing SENAs in vitro

In this study, we used embryonic stem cells expressing green fluorescent protein (GFP) under the chicken beta-actin promoter and the neural cell adhesion molecule L1 under the promoter of 3-phosphoglycerokinase at all stages of differentiation as previously described (Bernreuther, et al; 2006). L1 overexpressing embryonic stem cells and GFP expressing control cells were differentiated according to the five stage protocol (Lee, et al; 2000) modified as described (Dihné, et al; 2006) in order to give rise to neural aggregates containing a high percentage of neurons (SENAs). Proliferation of neural precursor cells under the influence of FGF2 was briefly, prolonged in stage 4 giving rise to neural aggregates consisting mainly of neurons and radial glial cells. Throughout differentiation (stage 4 and 5), L1 overexpressing cells showed enhanced levels of L1 in vitro determined by Western blot analysis when compared to control cells (Fig. 1A).

To determine whether L1 influences neuronal differentiation of SENAs in vitro, indirect immunofluorescent staining was carried out at day 7 of stage 5 ($28^+/7^-$). SENAs contained a high percentage of β-III-tubulin$^+$ neurons among all GFP$^+$ cells (Fig. 1B) that did not differ between the L1 overexpressing and control group (L1: $92.59 \pm 1.293\%$, control: $89.17 \pm 1.15\%$). A tendency towards enhanced numbers of TH$^+$ neurons in L1 overexpressing versus control SENAs (L1: $4.514 \pm 0.478\%$, control: $3.300 \pm 0.340\%$) was observed, thouth the variation was not statistically significant (Fig. 2C).

Thus, L1 overexpressing SENAs showed enhanced levels of L1 that did not improve overall neuronal differentiation but contributed to a tendency towards increased dopaminergic differentiation.
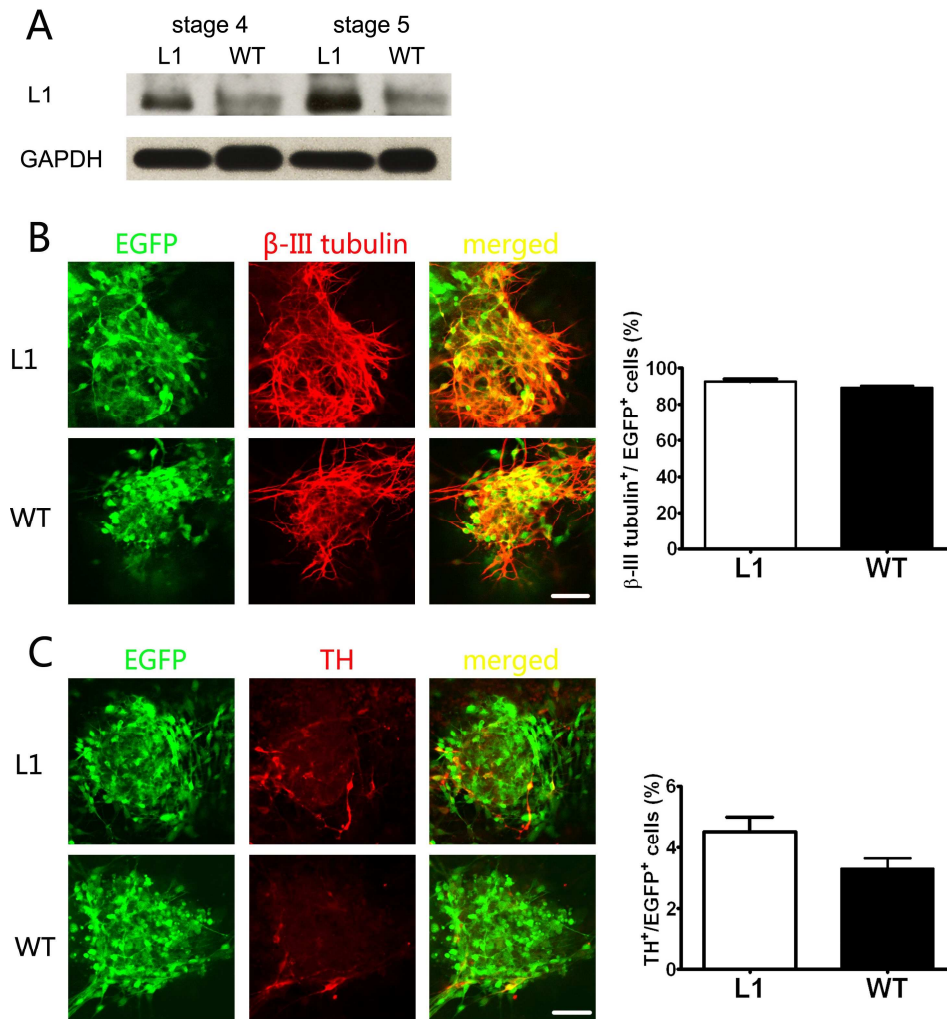
48

Figure 1. L1 overexpression does not affect neuronal differentiation of substrate-adherent embryonic stem cell-derived neural aggregates (SENAs) *in vitro*.

(A) Immunoblot analysis of L1 expression in SENAs generated from transfected (L1[+]) and mock-transfected (WT) embryonic stem cells expressing enhanced green fluorescent protein (EGFP) at all stages of differentiation that were differentiated by the protocol described by Dihné et al. 2006 at day 28 of prolonged stage 4 and at day 7 of stage 5. Note that L1 expression is enhanced in L1[+] versus WT SENAs throughout differentiation. Immunoblot analysis of glyceraldehyde 3-phosphate dehydrogenase (GAPDH) is shown as a loading control. (B) Generation of neurons from L1[+] and WT SENAs was determined at day 7 of stage 5 by immunostaining and fluorescence light microscopy for β-III tubulin (red). EGFP^{+} cells (green), β-III tubulin[+]/EGFP^{+} cells (yellow). Percentages of β-III tubulin^{+} cells of all EGFP^{+} cells are shown at day 7 of stage 5 (mean ± s.e.m.). No difference in neuronal differentiation was observed between L1[+] and WT SENAs with a percentage of 90% neurons in both groups. Scale bar, 100 μm. (C). The proportion of TH^{+} cells was determined at day 7 of stage 5 by immunohistochemistry and fluorescence light microscopy. TH[+] (red), EGFP^{+} cells (green), TH[+]/GFP^{+} cells (yellow). Scale bar, 100 μm. Percentages of TH^{+} cells of all EGFP^{+} cells are shown at day 7 of stage 5 (mean ± s.e.m.) Student's t-test was performed for statistical analysis. The enhanced number of TH^{+} cells in L1[+] SENAs was not statistically significant.

1.2 L1 overexpression in SENAs enhances graft size, number of surviving cells in the graft, and migration from the graft edge after transplantation into the MPTP-lesioned mouse brain

Intraperitoneal injection of MPTP into wild type adult C57BL/6J mice resulted in a reproducible reduction in the number of surviving TH$^+$ cells in the substantia nigra (Fig. 2) when compared to animals sham-injected with PBS 7 days after injection (MPTP: 5380 ± 516; PBS: 10610 ± 360). To determine the effects of L1 overexpression on survival of transplanted SENAs and the migration of cells from the graft into the host tissue, GFP$^+$ SENAs differentiated to day 7 of stage 5 were injected either unilaterally into the striatum (Fig. 3A) or adjacent to the substantia nigra (Fig. 3B) four days after intraperitoneal injection of MPTP. Four weeks after grafting L1 overexpressing SENAs showed increased graft size (Fig. 3C, D) and enhanced numbers of surviving cells (Fig. 3C, E) when compared to control SENAs after transplantation into both the striatum (graft size - L1: 0.24 ± 0.03 mm3, control: 0.11 ± 0.01 mm3; cell number - L1: 9332 ± 744, control: 4650 ± 657) and adjacent to the substantia nigra (graft size - L1: 0.21 ± 0.03 mm3, control: 0.1 ± 0.01 mm3; cell number: L1: 7114 ± 452, control: 4092 ± 86). This effect was confirmed three months after transplantation of SENAs into the striatum (Fig. 4A). Furthermore, migration of grafted cells from the graft edge of transplanted L1 overexpressing SENAs versus control SENAs into the host striatum (Fig. 3F, G) and into the host substantia nigra (Fig. 3G) was increased 4 weeks after grafting (striatum - L1: 126 ± 10 μm, control: 52 ± 2 μm).

Thus, graft size, cell number, and migration into the host tissue was enhanced in L1 overexpressing versus control SENAs after transplantation into the striatum or adjacent to the substantia nigra of MPTP-lesioned mice.
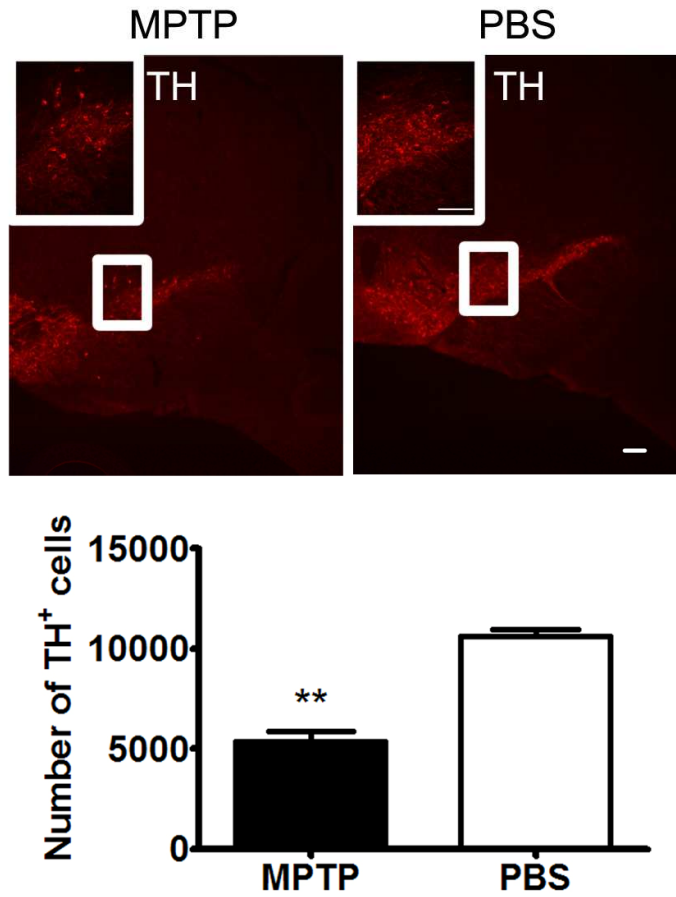
Figure 2. Intraperitoneal injection of MPTP reduces the number of TH^+ neurons in the murine substantia nigra. Immunohistochemical analysis of TH^+ neurons (red) in the murine substantia nigra 1 week after MPTP lesion or sham-injection of PBS. Absolute numbers of endogenous TH^+ neurons are shown (mean ± s.e.m.). Student's t-test was performed for statistical analysis (** $p < 0.01$).
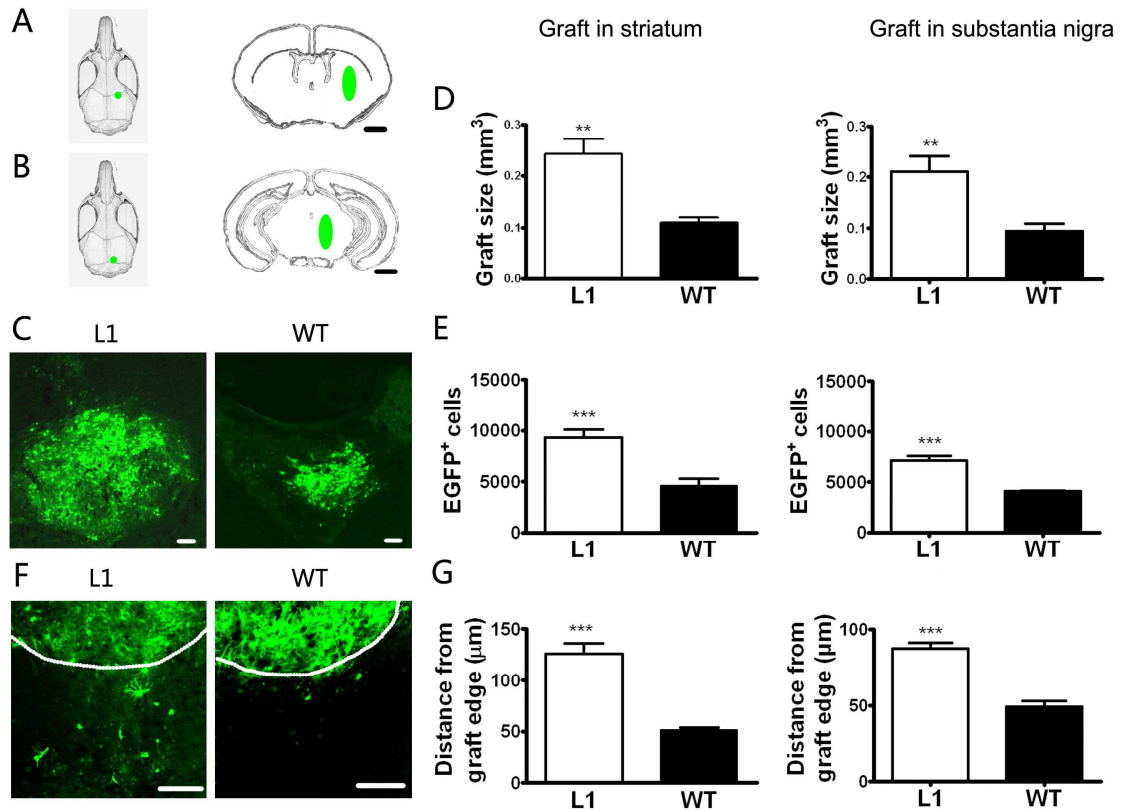
Figure 3. L1 overexpression in SENAs enhances graft size, number of surviving cells in the graft, and migrationfrom the graft edge. SENAs differentiated to day 7 of stage 5 were transplanted into the mouse striatum (**A**) or the substantia nigra (**B**) Four days after MPTP lesion. (**C**) Laser scanning microscopy of an L1[+] and a control (WT) SENA graft four weeks after transplantation into the host striatum. Grafts were detected by green fluorescence of transplanted cells. Scale bar, 100 μm. (**D**) Graft volume 4 weeks after transplantation of L1[+] (n=6) and WT (n=6) SENAs into the striatum or substantia nigra (mean ± s.e.m.). Student's t-test was performed for statistical analysis (** $p < 0.01$). (**E**) Number of EGFP^{+} cells 4 weeks after transplantation of L1[+] (n=6) and WT (n=6) SENAs into the striatum or substantia nigra (mean ± s.e.m.). Student's t-test was performed for statistical analysis (** $p < 0.01$, *** $p < 0.001$) (**F**) Laser scanning microscopy of the periphery of L1[+] and WT SENA grafts 4 weeks after transplantation. White lines indicate graft edges. Note the enhanced number of EGFP^{+} cells migrated from the L1[+] graft. Scale bar, 100 μm (**G**). Migration distance from the edge of L1[+] (n=6) and WT (n=6) SENA grafts four weeks after transplantation is shown. (mean ± s.e.m.). Student's t test was performed for statistical analysis (** $p < 0.01$; *** $p < 0.001$).
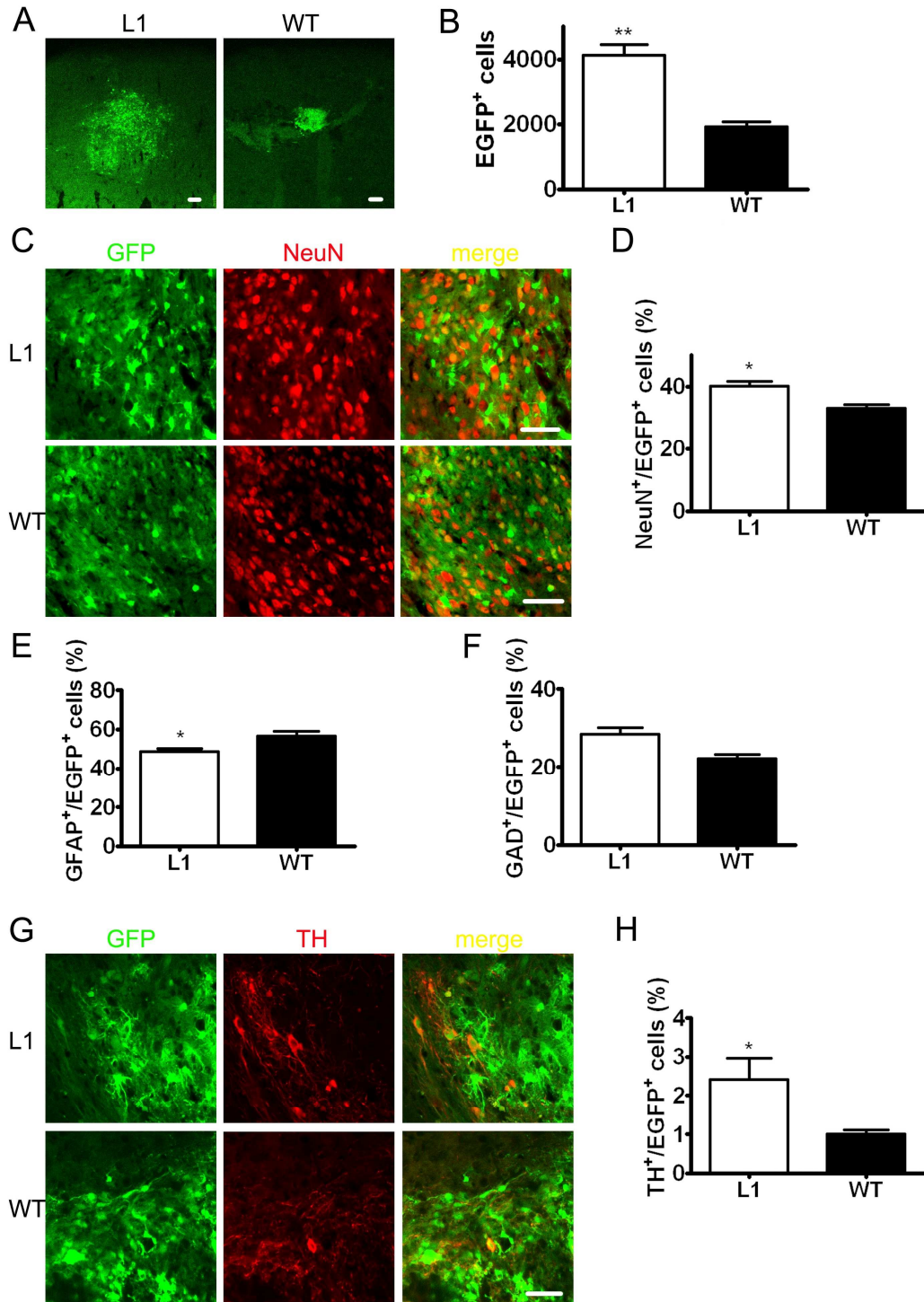
Figure 4. L1 overexpressing SENAs show increased number of cells, increased neuronal differentiation, decreased astrocytic differentiation, and increased number of TH$^+$ cells three months after transplantation into MPTP lesioned mouse striatum when compared to control (WT) SENA grafts. (**A**) Confocal images of an L1$^+$ and a WT graft (green) three months after transplantation into the host striatum. Scale bar, 100 μm. (**B**) Number of EGFP$^+$ cells three months after transplantation of L1$^+$ (n=6) and WT (n=6) SENAs into the striatum (mean ± s.e.m.). Student's t-test was performed for statistical analysis (** p < 0.01) (**C**) Confocal images of L1$^+$ and WT SENA grafts (green) immunostained for the neuronal marker neuronal nuclear antigen (NeuN, red) three months after transplantation into the striatum. Scale bar, 50μm. (**D**) Percentages of NeuN$^+$ cells of all EGFP$^+$ cells three months after transplantation of L1$^+$ (n=6) and WT (n=6) SENAs into the striatum (mean ± s.e.m.) are shown. Student's t-test was performed for statistical analysis (** p < 0.05). (**E**) Percentages of GFAP$^+$ cells of all EGFP$^+$ cells three months after transplantation of L1$^+$ (n=6) and WT (n=6) SENAs into the striatum (mean ± s.e.m.) are shown. Student's t-test was performed for statistical analysis (* $p < 0.05$). (**F**) Percentages of GAD$^+$ cells of all EGFP$^+$ cells three months after transplantation of L1$^+$ (n=6) and WT (n=6) SENAs into the striatum (mean ± s.e.m.) are shown. (**G**) Confocal images of L1$^+$ and WT SENAs (green) immunostained with an antibody against tyrosin hydroxylase (TH, red) three months after transplantation into the striatum. Scale bar, 50 µm. (**H**) Percentages of TH$^+$ cells of all EGFP$^+$ cells 12 months after transplantation of L1$^+$ (n=6) and WT (n=6) SENAs into the striatum or substantia nigra (mean ± s.e.m.) are shown. Student's t-test was performed for statistical analysis (* $p < 0.05$).

1.3 L1 overexpressing SENAs show enhanced numbers of TH$^+$ cells after transplantation into the MPTP-lesioned mouse brain

Percentages of NeuN$^+$ neurons among all GFP$^+$ cells (Fig. 5A, Fig. 4B) were slightly enhanced in L1 overexpressing SENAs when compared to control SENAs four weeks and three months after transplantation into the striatum (four weeks - L1: 46 ± 2%, control: 39 ± 1%; 3 months - L1: 40 ± 2%, control: 33 ± 1) and four weeks after transplantation adjacent to the substantia nigra (L1: 42 ± 1%, control: 37 ± 1). GFAP$^+$ astrocytes were less abundant in L1 overexpressing SENAs (Fig. 5B, Fig. 4B) four weeks and three months after transplantation into the striatum (four weeks – L1: 41 ± 2%, control: 53 ± 2; three months - L1: 49 ± 2, control: 57 ± 2). The percentage of oligodendrocytes was negligible in both groups and amounted to less than 1% of all GFP$^+$ cells (not shown).

The percentages of GABAergic neurons as identified by immunohistochemical labelling with GAD antibodies (Fig. 6A) did not differ between the groups at all investigated time points after transplantation (Fig. 6A, Fig. 4F). In contrast, the

percentage of dopaminergic neurons of all grafted GFP$^+$ cells as determined by immunohistochemical labelling with TH antibodies was enhanced in L1 overexpressing SENAs versus control SENAs four weeks and three months after transplantation into the striatum (Fig. 6B, Fig. 4G, H; four weeks: L1: 5.5 ± 0.5%, control: 3.5 ± 0.4%; three months: L1: 2.4 ± 0.6, control: 1 ± 0.1%) and four weeks after transplantation adjacent to the substantia nigra (Fig. 6B; L1: 5.3 ± 0.6%, control: 3.6 ± 0.2%).

Thus, L1 overexpressing SENAs favour neuronal versus astrocytic differentiation and show an enhanced percentage of graft-derived dopaminergic neurons after transplantation into the MPTP-lesioned mouse brain.

1.4 L1 overexpressing SENAs rescue endogenous nigral dopaminergic neurons after transplantation adjacent to the substantia nigra but not after transplantation into the striatum of MPTP-lesioned mice

To monitor the effects of L1 overexpressing SENAs on the survival of endogenous dopaminergic neurons in the substantia nigra, the percentage of TH$^+$ cells in the substantia nigra was determined ipsilateral and contralateral to the grafted side four weeks after transplantation of L1 overexpressing or control SENAs into either the striatum or adjacent to the substantia nigra; the same was true after sham-injection of PBS (Fig. 7). While no differences in the percentage of TH$^+$ cells were observed between the ipsilateral and contralateral side after transplantation of SENAs into the striatum, L1 overexpressing but not control SENAs enhanced the numbers of endogenous TH$^+$ cells in the substantia nigra ipsilateral to the grafted side when compared to the contralateral side.
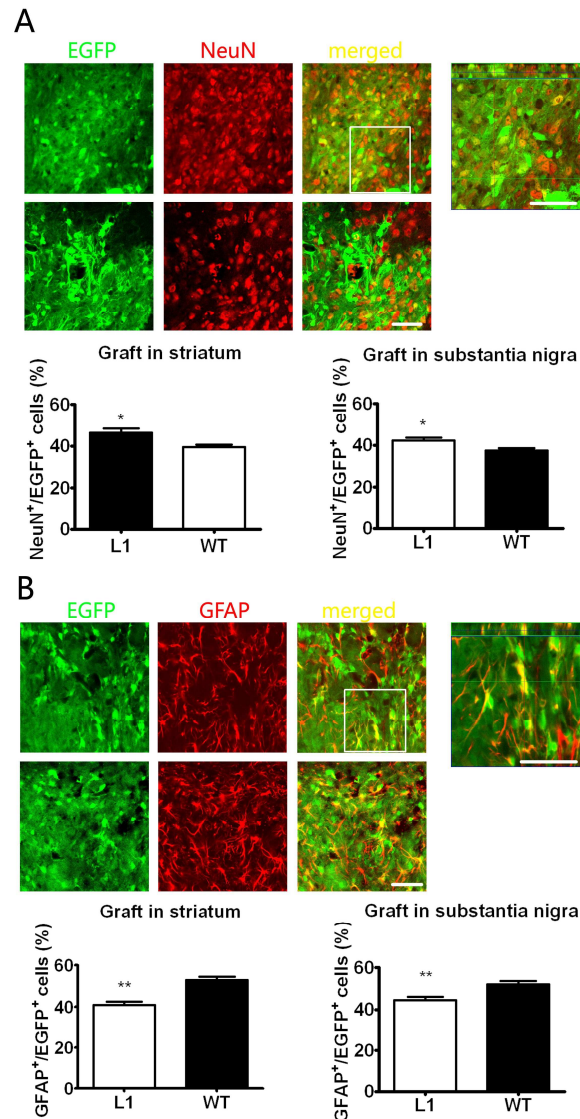
Figure 5. L1 overexpressing SENAs show increased neuronal differentiation and decreased astrocytic differentiation after transplantation into the mouse striatum or substantia nigra after MPTP lesion. **(A)** Confocal images of L1$^+$ and control (WT) SENA grafts (green) immunostained for the neuronal marker neuronal nuclear antigen (NeuN, red) four weeks after transplantation into the striatum. Scale bar, 50µm. In the upper right, a Z-stack of 15 images of 1µm thickness of the area outlined by a square in the merged image of the L1$^+$ graft is shown with orthogonal views of the xz- and yz-planes showing EGFP$^+$/NeuN$^+$ neurons. Scale bar, 50 µm. Percentages of NeuN$^+$ cells of all EGFP$^+$ cells four weeks after transplantation of L1$^+$ (n=6) and WT (n=6) SENAs into the striatum or substantia nigra (mean ± s.e.m.) are shown. Student's t-test was performed for statistical analysis (** p < 0.01). **(B)** Confocal images of L1$^+$ and WT SENAs (green) immunostained with an antibody against glial fibrillary acidic protein (GFAP, red) four weeks after transplantation. Scale bar, 50 µm. In the upper right, a Z-stack of 15 images of 1µm thickness of the area outlined by a square in the merged image of the L1$^+$ graft is shown with orthogonal views of the xz- and yz-planes showing EGFP$^+$/GFAP$^+$ astrocytes. Scale bar, 50 µm. Percentages of GFAP$^+$ cells of all EGFP$^+$ cells four weeks after transplantation of L1$^+$ (n=6) and WT (n=6) SENAs into the striatum or substantia nigra (mean ± s.e.m.) are shown. Student's t-test was performed for statistical analysis (* p < 0.05).
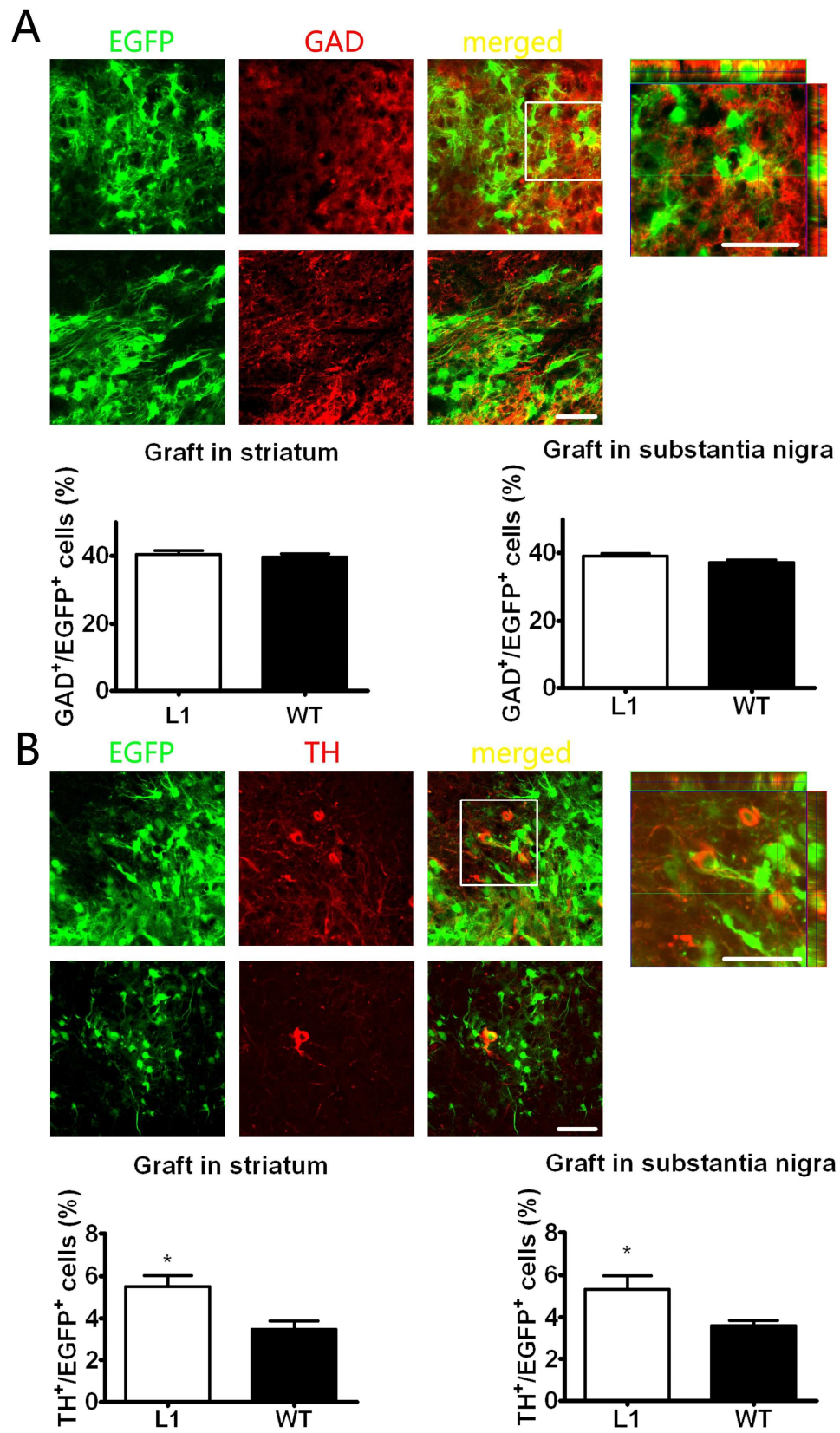
Figure 6. L1 overexpressing SENAs show increased differentiation into TH^{+} neurons with unchanged GABAergic differentiation after transplantation into either MPTP lesioned mouse striatum or substantia nigra. **(A)** Confocal images of L1[+] and control (WT) SENA grafts (green) immunostained for glutamate decarboxylase (GAD, red), a marker for GABAergic neurons, four weeks after transplantation into the striatum. Scale bar, 50μm. In the upper right, a Z-stack of 15 images of 1μm thickness of the area outlined by a square in the merged image of the L1[+] graft is shown with orthogonal views of the xz- and yz-planes showing EGFP[+]/GAD^{+} neurons. Scale bar, 50 μm. Percentages of GAD^{+} cells of all EGFP^{+} cells four weeks after transplantation of L1[+] (n=6) and WT (n=6) SENAs into the striatum or substantia nigra (mean ± s.e.m.) are shown. **(B)** Confocal images of L1[+] and WT SENAs (green) immunostained with an antibody against tyrosin hydroxylase (TH, red) four weeks after transplantation. Scale bar, 50 μm. In the upper right, a Z-stack of 15 images of 1μm thickness of the area outlined by a square in the merged image of the L1[+] graft is shown with orthogonal views of the xz- and yz-planes showing EGFP[+]/TH[+] astrocytes. Scale bar, 50 μm. Percentages of TH^{+} cells of all EGFP^{+} cells four weeks after transplantation of L1[+] (n=6) and WT (n=6) SENAs into the striatum or substantia nigra (mean ± s.e.m.) are shown. Student's t-test was performed for statistical analysis (* $p < 0.05$; ** $p < 0.01$)
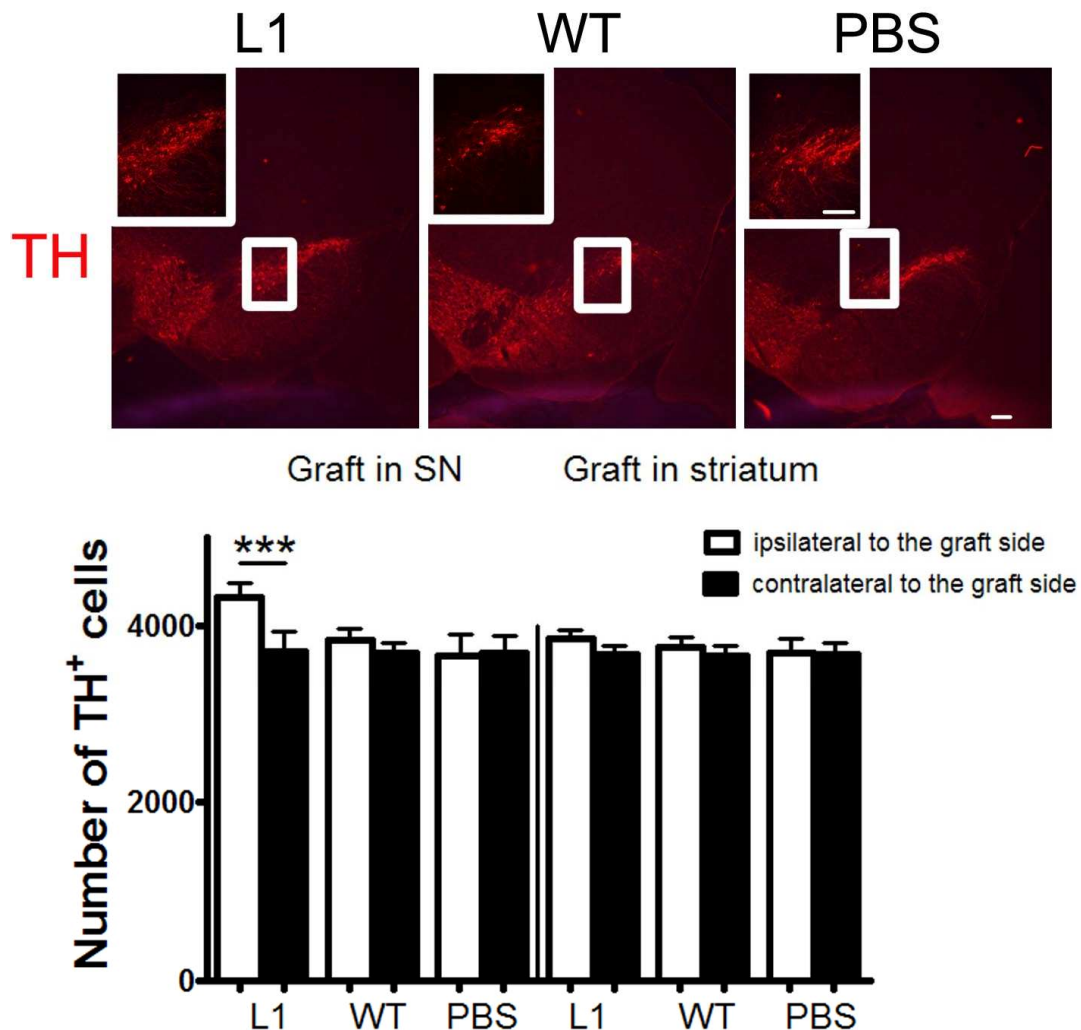
Figure 7. Transplantation of L1 overexpressing SENAs into the substantia nigra but not into the striatum rescues host dopaminergic neurons after MPTP lesioning. Immunohostochemical analysis of endogenous TH$^+$ neurons (red) four weeks after transplantation of L1$^+$ (n=7) and control (WT) (N=7) SENA grafts into the substantia nigra or striatum of MPTP-lesioned mice. Scale bar, 100 µm. Absolute numbers of endogenous TH$^+$ neurons ipsilateral and contralateral to the grafted side are shown (mean ± s.e.m.). Note the increased number of endogenous TH$^+$ neurons ipsilateral to the grafted side in mice transplanted wit L1$^+$ SENAs. Student's t-test was performed for statistical analysis (*** $p < 0.001$).

1.5 L1 overexpressing SENAs but not control SENAs enhance apomorphine-induced rotation behavior and striatal dopamine level after transplantation into the striatum of MPTP-lesioned mice

To test the effect of L1 overexpressing SENAs on motor behaviour, we analysed apomorphine-induced rotation in MPTP-lesioned mice with unilateral grafts of L1$^+$ SENAs, WT SENAs, or sham-injected with PBS. (Fig. 8A) As expected, the animals showed no rotational behavior after lesioning one day before transplantation because systemic MPTP application induces symmetric cell death of the dopaminergic neurons in the substantia nigra. Animals transplanted with control SENAs showed a tendency towards an ipsilateral rotation bias in apomorphine-induced rotation behaviour one to four weeks after transplantation when compared to the PBS group that was not statistically significant at any time point. In contrast, transplantation of L1 overexpressing SENAs led to a stable ipsilateral rotation bias in apomorphine-induced rotation behaviour three to ten weeks after transplantation when compared to the group transplanted with control SENAs and sham-injected control animals. Thus, L1 overexpressing SENAs but not control SENAs influenced rotation behaviour in MPTP-lesioned mice.

As reported, apomorphine-induced rotations correlate to the underlying degree of nigrostriatal loss and dopaminergic depletion (Hudson JL, et al; 1993). In order to reconfirm the correlation, we analysed the striatal dopamine level 1 month after striatal transplantation (Fig. 8B). L1 overexpressing but not control SENAs enhanced the level of dopamine in the striatum ipsilateral to the grafted side when compared to the contralateral side(Fig. 8B) but did not influence striatal GABA levels (Fig. 8C)
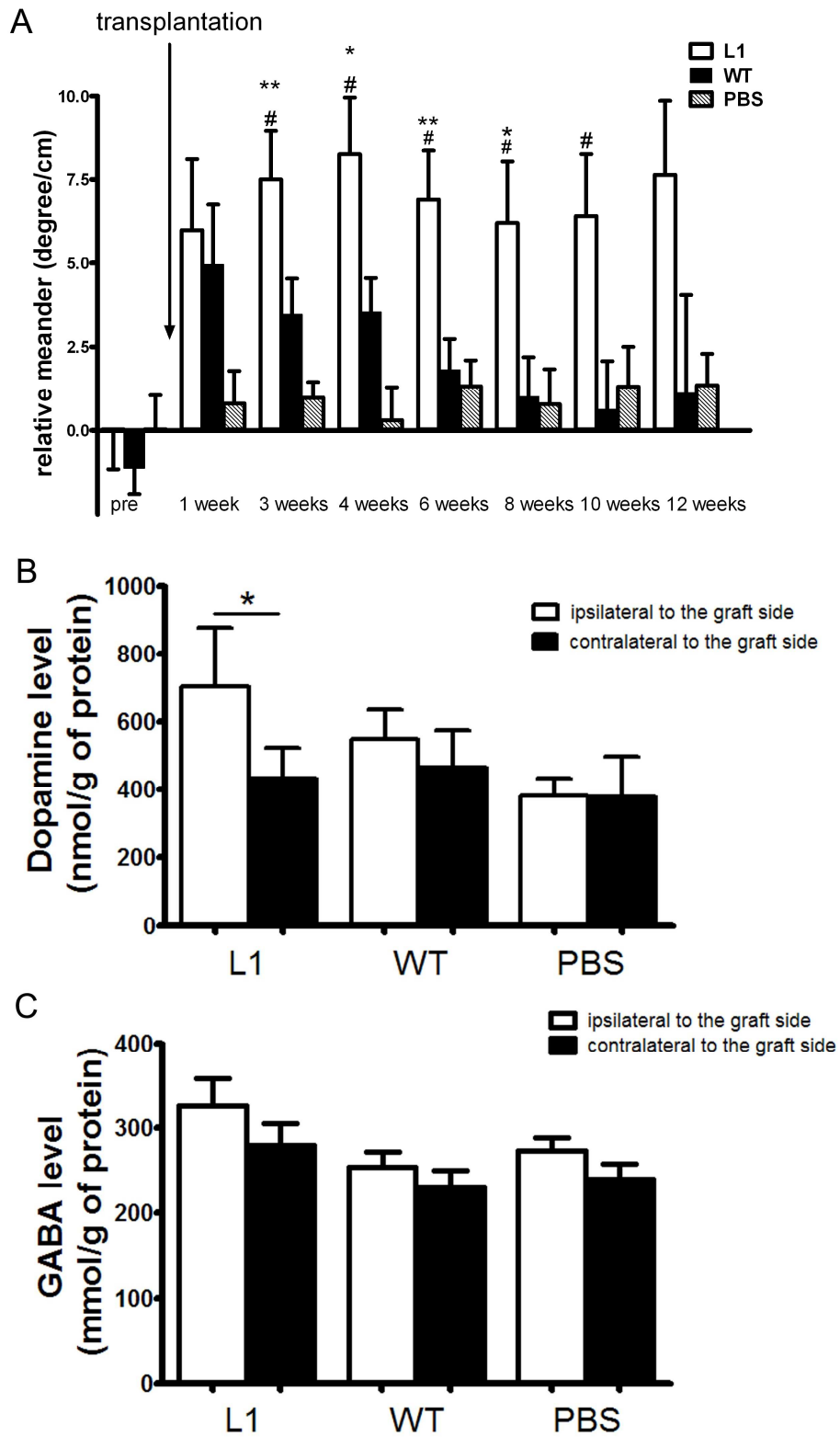
Figure 8. (A) Behavioral analysis of apomorphine-induced rotation in MPTP-lesioned mice with unilateral grafts of L1$^+$ SENAs (n=10), control (WT) SENAs (n=10), or sham-injected with PBS (PBS, n=9). Relative meander was calculated as turning angle divided by the distance moved (mean ± s.e.m.). Tukey's one-way ANOVA was performed for statistical analysis. (*,** $p < 0.05$ and 0.01, compared with PBS group, # $p < 0.05$, compared with WT group). **(B)** Striatal dopamine expression level one month after striatal transplantation with L1$^+$ SENAs (n=7), WT SENAs (n=5), or sham-injected with PBS (PBS, n=5), (mean ± s.e.m.). Student's t-test was performed for statistical analysis (* $p < 0.05$). **(C)** Striatal GABA expression level one month after unilateral striatal transplantation with L1$^+$ SENAs (n=7), WT SENAs (n=5), or sham-injected with PBS (PBS, n=5), (mean ± s.e.m.). Student's t-test was performed for statistical analysis.

1.6 L1 overexpressing SENAs but not control SENAs decrease microglial activation but not reactive astrogliosis in the host tssue after transplantation into the striatum of MPTP-lesioned mice

The immune reation of the host to grafted cells is an important obstacle in transplantation paradigms. In order to investigate whether grafted L1$^+$ and control SENAs trigger an immune response after transplantation, we analysed the expression of GFAP, a marker for astrocytes, and Iba-1, a marker for microglia cells, in the vicinity of grafted cells. Analysis revealed no significant differences in the glial reaction monitore by GFAP expression of host cells between L1 overexpressing and control SENAs 1 month after transplantation (Fig. 9A, B). In contrast, the microglial reaction monitored by Iba-1 expression, was reduced in animals transplanted with L1 overexpressing SENAs when compared to control SENAs and PBS (Fig. 9C, D)
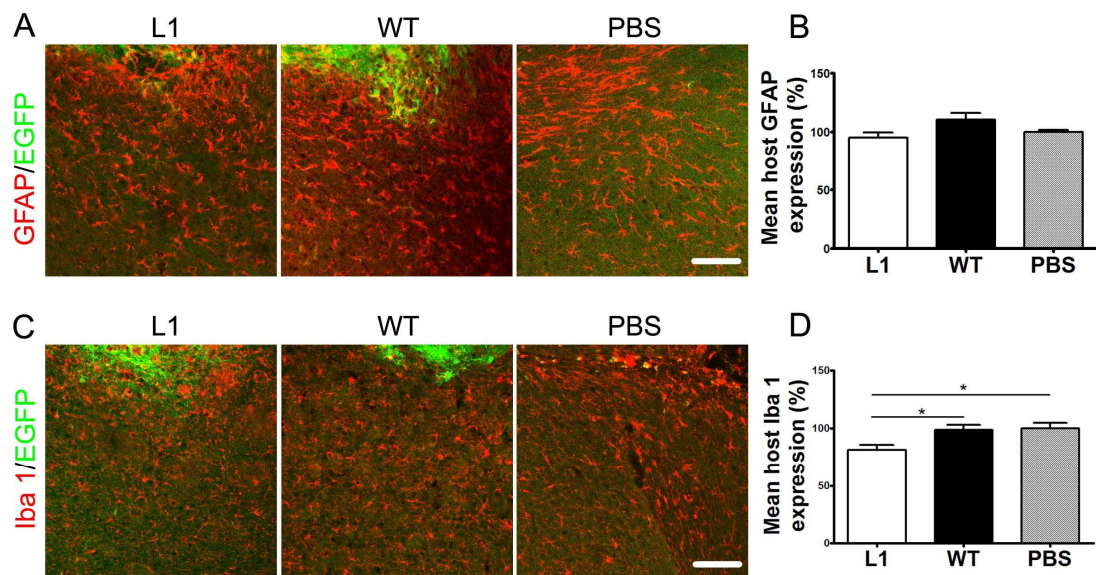
Figure 9. The host tissues show a decreased microgial reaction to L1 overexpressing SENAs when compared to control SENAs and PBS, but no difference in the astroglial reaction. **(A)** Confocal images of host striatal tissues grafted with L1[+] SENAs, control (WT) SENAs (green) or PBS immunostained with an antibody against GFAP (red). Scale bar, 100 µm. **(B)** Mean value of GFAP expression in the host tissues of mice transplanted with L1[+] SENAs (n=5), control SENAs (n=5), normalized or sham-injected with PBS (n=5) are displayed. The expression level in sham-injcted mice is adjusted to 100%. Turkey's one-way ANOVA was performed for statistical analysis. (** $p < 0.01$) **(C)** Confocal images of host striatal tissues grafted by L1[+] SENAs, WT SENAs or PBS (green) immunostained with an antibody against Iba 1 (red). Scale bar, 100 µm. **(B)** Mean value of GFAP expression in the host tissues of mice transplanted with L1[+] SENAs (n=5), control SENAs (n=5), normalized or sham-injected with PBS (n=5) are displayed. The expression level in sham-injcted mice is adjusted to 100%. Tukey's one-way ANOVA was performed for statistical analysis (**, *** $p < 0.01$ and 0.001).

2. Transplantation of SENAs into the compression-lesioned murine spinal cord

2.1 L1 overexpression in SEAs reduces the glial scar after transplantation into the compression-lesioned spinal cord

In order to evaluate the potential positive effects of SENAs overexpressing the neural cell adhesion molecule L1 in the inhibitory environment of the compression-lesioned spinal cord, GFP[+] SENAs overexpressing L1 and control GFP[+] SENAs differentiated to day 7 of stage 5 ($28^{+}/7^{-}$) were transplanted rostral and caudal to the center of the lesion site 3 days after compression-lesioning of the spinal cord of

C57BL/6J mice. These data were compared to mice sham-injected with PBS (Fig. 10A). Six weeks after transplantation, SENAs were detectable at the injection sites (Fig. 10B). Since the volume of the glial scar correlates with locomotor function in the spinal cord injury mouse model (Apostolova, et al; 2006), the scar volume in each mouse was estimated applying the Cavalieri principle. Mice grafted with L1 overexoressing SENAs showed a significantly reduced scar volume when compared to sham-injected animals, but only a slight, though not significant, reduced scar volume in comparison with mice grafted with control SENAs (Fig. 10C) (scar volume: L1: 0.689 ± 0.018 mm^3, WT: 0.793 ± 0.040 mm^3, PBS: 0.921 ± 0.056 mm^3).
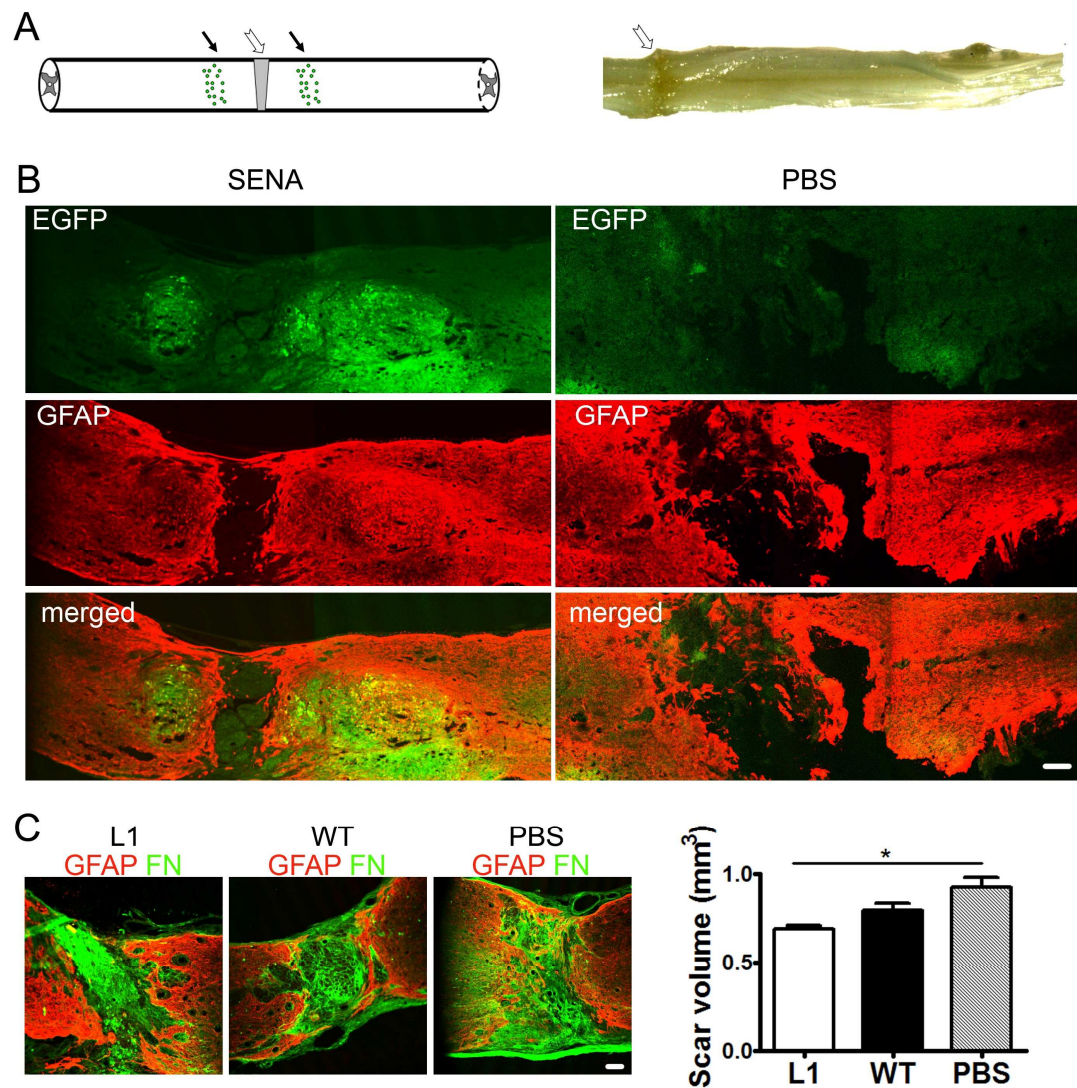
Figure 10. L1 overexpression in SENAs reduces scar volume after transplantation into the compression lesioned spinal cord of adult mice. (**A**) Spinal cords were compressed at the T7-T9 level (indicated by hollow arrows), SENAs were grafted 0.5 mm rostral and caudal to the lesion site (indicated by arrows). (**B**) Localization of SENAs (GFP$^+$) (green) in the lesioned spinal cords 6 weeks after transplantation. PBS was injected into lesioned spinal cords as control. The lesion site is deineated by glial fibrillary acidic protein (GFAP) expressing astrocytes (red). Scale bar, 100 μm. (**C**) Double immunofluorescence of a parasagittal section for GFAP (red) and fibronectin (FN; green) at the lesion site six weeks after transplantation. Mean scar volumes ± s.e.m. in mice transplanted with L1 overexpressing SENAS, control (WT) SENAS, or sham-injected with PBS are displayed. (L1$^+$, n=7; WT, n=7, PBS, n=5). Note the decreased scar volume in mice grafted with L1 overexpressing SENAs. Tukey's one-way ANOVA was performed for statistical analysis. (* $p < 0.05$). Scale bar, 100 μm.

2.2 L1 overexpression in SENAs enhances graft size, number of surviving cells in the graft, and migration from the graft edge after transplantation into the lesioned spinal cord

To determine the effects of L1 overexpression on survival of transplanted SENAs and migration of cells from the graft into the host tissue, the number of surviving grafted cells and migration distance of transplanted cells from the graft edge were analysed. Six weeks after grafting, L1 overexpressing SENAs showed an increased graft size (Fig. 11A, B) and enhanced numbers of surviving cells (Fig. 11A, C) when compared to control SENAs caudal to the lesion site (number of grafted cells caudal to the lesion, L1: 5597 ± 207, WT: 4657 ± 294; graft size caudal to the lesion, L1: 0.242 ± 0.007 mm^3, WT: 0.207 ± 0.012 mm^3). Rostral to the lesion site, L1 overexpressing SENAs showed only slightly increased numbers of surviving cells (Fig. 11A, C) and a slightly increased graft size (Fig. 11A, B) six weeks after transplantation (number of grafted cells rostral to the lesion, L1: 6090 ± 281, WT: 5450 ± 195; graft size rostral to the lesion, L1: 0.264 ± 0.019 mm^3, WT: 0.248 ± 0.017 mm^3). Furthermore, migration of grafted cells from the graft edge was enhanced in the grafts both rostrally and caudally to the lesion site in L1 overexpressing SENAs versus control SENAs (Fig. 11D, E) 6 weeks after grafting (rostral, L1: 106.3 ± 1.6 μm, WT: 66.2 ± 1.5 μm; caudal, L1: 99.2 ± 3.5 μm, WT: 65.22 ± 1.2 μm).

Thus, graft size, cell number, and migration into the host tissue was enhanced in

L1 overexpressing versus control SENAs after transplantation caudal to the lesion site. Rostral to the lesion site, migration ability is enhanced in L1 overexpressing vesus control SENAs as well, while graft size and cell number were only slightly altered by L1 overexpression six weeks after transplantation.
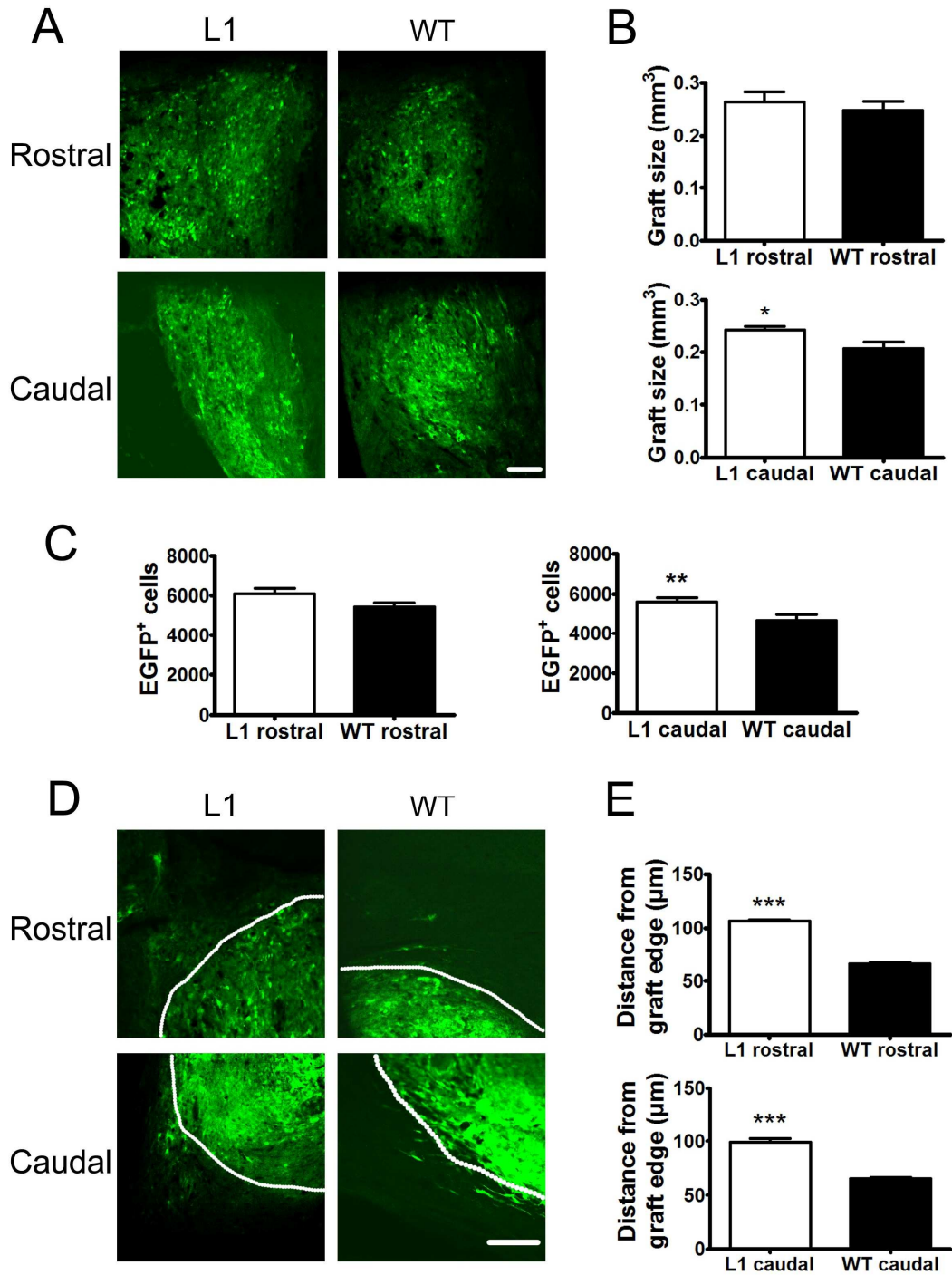
Figure 11. L1 overexpressing SENAs show enhanced graft size and number of surviving cells as well as enhanced migration from the graft edge. (**A**) Laser scanning microscopy of an L1 overexpressing and a control (WT) SENA graft six weeks after transplantation into the spinal cord rostral and caudal to the lesion site. Grafts were detected by green fluorescence of transplanted cells. Scale bar, 100 μm. Graft volume (**B**) and number of GFP$^+$ cells (**C**) six weeks after transplantation of L1$^+$ (n=7) and WT (n=7) rostral and caudal to the lesion site. Shown are mean ± s.e.m. Student's t test was performed for statistical analysis (*, ** $p < 0.05$ and 0.01). (**D**) Laser scanning microscopy of the periphery of L1 overexpressing and WT SENA grafts six weeks after transplantation. White line indicates graft edges. Scale bar, 100 μm. (**E**) Migration distance from the edge of L1 overexpressing (n=7) and WT (n=7) SENA grafts six weeks after transplantation is shown. (mean ± s.e.m.). Student's t test was performed for statistical analysis (*** $p < 0.001$).

2.3 L1 overexpressing SENAs increase neuronal differentiation, decrease astrocytic differentiation, and enhance neurite outgrowth of differentiated neurons

The percentages of NeuN$^+$ neurons among all GFP$^+$ cells (Fig. 12A) were enhanced in L1 overexpressing SENAs when compared to control SENAs six weeks after transplantation into the compression-lesioned spinal cord (L1: 50.9 ± 2.7%, control: 40.1 ± 1.9%) while GFAP$^+$ astrocytes were less abundant in L1 overexpressing SENAs (Fig. 12B) six weeks after transplantation (L1: 39.1 ± 1.4%, control: 43.5 ± 1.4%). The percentage of oligodendrocytes was negligible in both groups and amounted to less than 1% of all GFP$^+$ cells (not shown).

Furthermore, the length of graft-derived NeuN$^+$ neurons was determined. Neurites of neurons differentiated from engrafted L1 overexpressing SENAs were longer than the neurons differentiated from control SENAs (Fig. 12C; L1: 90.0 ± 2.5μm; control: 59.8 ± 1.7μm).

Thus, L1 ovexpressing SENAs favored neuronal differentiation, reduced astrocytic differentiation, and showed enhanced neurite length of neurons differentiated from grafts.
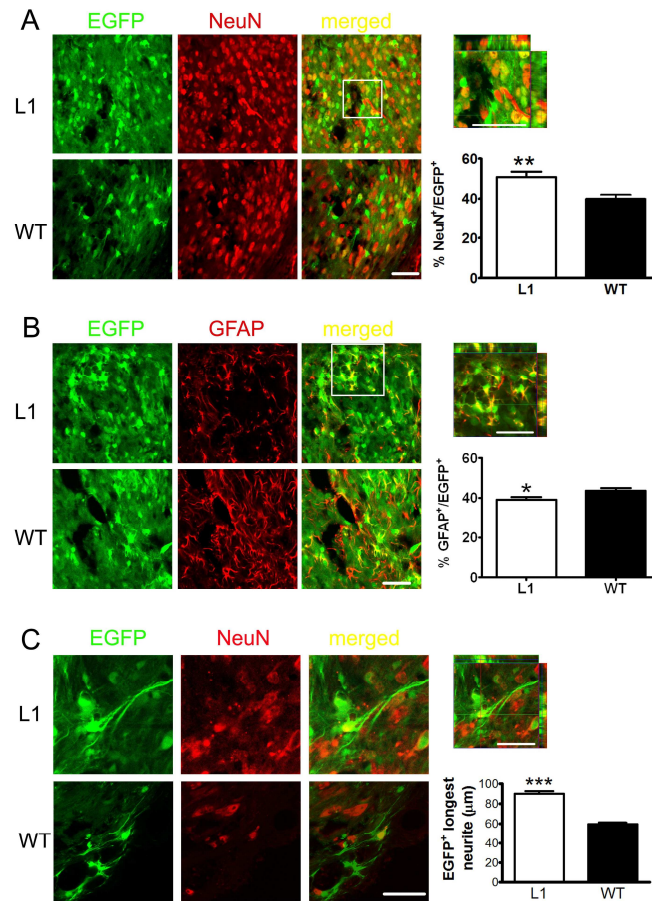
Figure 12. L1 overexpressing SENAs show increased neuronal differentiation and neurite length and decreased astrocytic differentiation after transplantation into lesioned spinal cord. **(A)** Confocal images of L1$^+$ and control (WT) SENA grafts (green) immunostained for the neuronal marker neuronal nuclear antigen (NeuN, red) six weeks after transplantation into the striatum. Scale bar, 50µm. In the upper right, a Z-stack of 15 images of 1µm thickness of the area outlined by a square in the merged image of the L1$^+$ graft is shown with orthogonal views of the xz- and yz-planes showing EGFP$^+$/NeuN$^+$ neurons. Scale bar, 50 µm. Percentages of NeuN$^+$ cells of all GFP$^+$ cells six weeks after transplantation of L1$^+$ (n=6) and WT (n=6) SENAs into the lesioned spinal cord (mean ± s.e.m.) are shown. Student's t-test was performed for statistical analysis (** p < 0.01). **(B)** Confocal images of L1$^+$ and WT SENAs (green) immunostained with an antibody against glial fibrillary acidic protein (GFAP, red) six weeks after transplantation. Scale bar, 50 µm. In the upper right, a Z-stack of 15 images of 1µm thickness of the area outlined by a square in the merged image of the L1$^+$ graft is shown with orthogonal views of the xz- and yz-planes showing GFP$^+$/GFAP$^+$ astrocytes. Scale bar, 50 µm. Percentages of GFAP$^+$ cells of all GFP$^+$ cells six weeks after transplantation of L1$^+$ (n=6) and WT (n=6) SENAs into the lesioned spinal cord (mean ± s.e.m.) are shown. Student's t-test was performed for statistical analysis (* p < 0.05). **(C)** Laser scanning images of neurites from grafted L1$^+$ and WT SENAs (green) immunostained with the neuronal marker NeuN (red) six weeks after transplantation. Scale bar, 50 µm. In the upper right, a Z-stack of 10 images of 1µm thickness the L1$^+$ graft is shown with orthogonal views of the xz- and yz-planes showing GFP$^+$/NeuN$^+$ neurons. Scale bar, 50 µm. The length of the longest neurite from the grafted SENAs was analysed (L1$^+$, n=7; WT, n=7). Mean values ± s.e.m. are shown. Student's t-test was performed for statistical analysis (*** p < 0.001).

2.4 L1 overexpressing SENAs rescue endogenous motoneurons was indicated by increased soma size and increased number of synaptic inputs caudal to the lesion site after transplantation into lesioned spinal cord

To analyse whether L1 overexpressing SENAs could influence the recovery of host cells after spinal cord injury, mean areas of cell bodies of motoneurons and densities of synaptic terminals around the cell bodies of motoneurons caudal to the lesion site were measured six weeks after transplantation. The linear density (number per unit length) of large perisomatic ChAT[+] boutons (Fig. 13A), known to form C-type synapses on motoneurons associated with muscarinic receptors type 2 (Davidoff and Irintchev, 1986; Hellström, et al; 2003), was increased in mice grafted with L1 overexpressing SENAs compared to mice grafted with control SENAs or sham-injected with PBS (Fig. 13C). Mice grafted with control SENAs also showed an enhanced linear density of ChAT[+] boutons caudal to the lesion site compared to sham-injected mice (Fig. 13C) (L1: 40.4 ± 0.8/mm, WT: 35.6 ± 2.0/mm, PBS: 26.0 ± 1.6/mm). The soma size of motoneurons was also enhanced in animals that had been transplanted with L1 overexpressing SENAs six weeks after transplantation into lesioned spinal cord when compared to control SENAs and sham-injected animals (Fig. 13B) (L1: 817 ± 65µm², WT: 581 ± 18µm², PBS: 556 ± 24µm²).

Thus, the results concerning perisomatic ChAT[+] boutons and soma size of motoneurons indicate that L1 can help to rescue motoneurons after spinal cord injury.
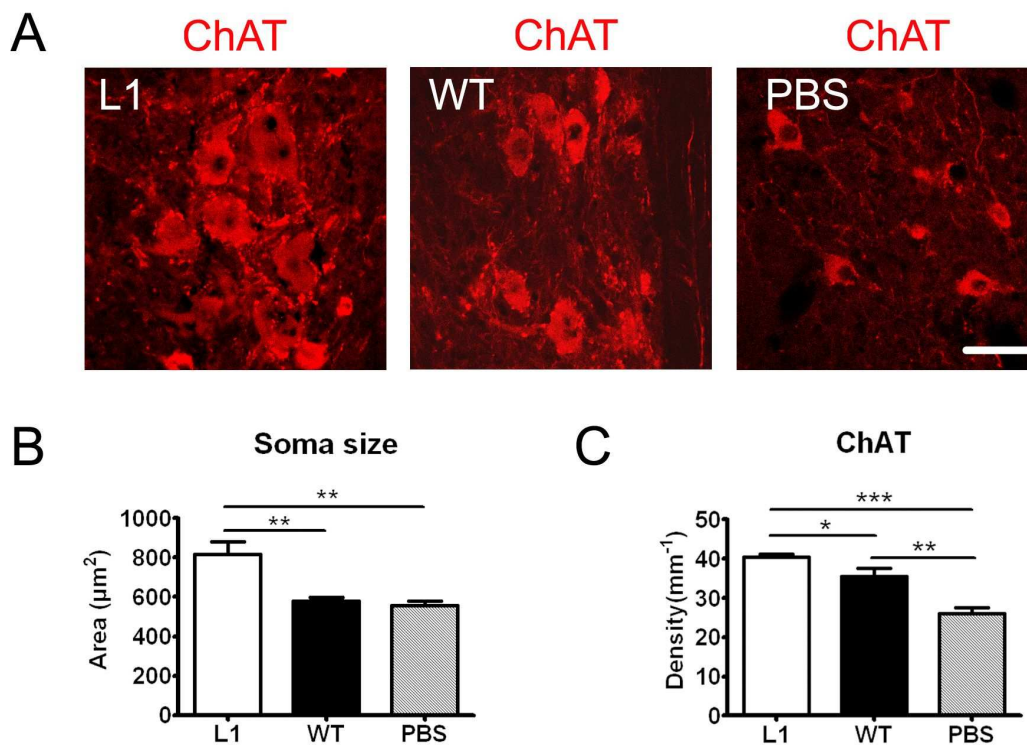
Figure 13. L1 overexpressing SENAs increase the soma size of host ChAT[+] motoneurons and the linear densities of ChAT[+] boutons six weeks after transplantation into the lesioned spinal cord. (**A**) Confocal images of host motoneurons, which were immunostained with an antibody against choline acetyltransferase (ChAT, red), caudal to the lesion site six weeks after transplantation. Scale bar, 50 µm. The soma size of host ChAT[+] motoneurons (**B**) and linear density of ChAT[+] punctae (**C**) caudally to the lesioned site are shown (mean ± s.e.m.). (L1[+], n=6; control (WT), n=6; PBS, n=5) Tukey's one-way ANOVA was performed for statistical analysis (*, **, *** $p < 0.05$, 0.01, 0.001).

2.5 L1 overexpressing SENAs enhance catecholaminergic reinnervation of the distal spinal cord six weeks after transplantation into the compression-lesioned spinal cord

Reinnervation of the compression-lesioned spinal cord caudal to the lesion site by tyrosin hydroxylase-positive (TH[+]) axons correlates with locomotor functional recovery (Jakovcevski et al; 2007). The number of TH[+] axons projecting beyond an arbitrarily selected border 250µm caudal to the lesion site in spaced serial parasagittal sections six weeks after transplantation was counted (Fig. 14A, B). Mice engrafted with L1 overexpressing SENAs had more TH[+] axons (L1: 7.3 ± 0.4) distal to the lesion site when compared to mice grafted with control SENAs (WT: 3.8 ± 0.5) or

sham-injected with PBS (PBS: 1.8 ± 0.3). Control SENAs also enhanced the number of TH$^+$ axons distal to the lesion site when compared to sham-injected mice (Fig. 14C).
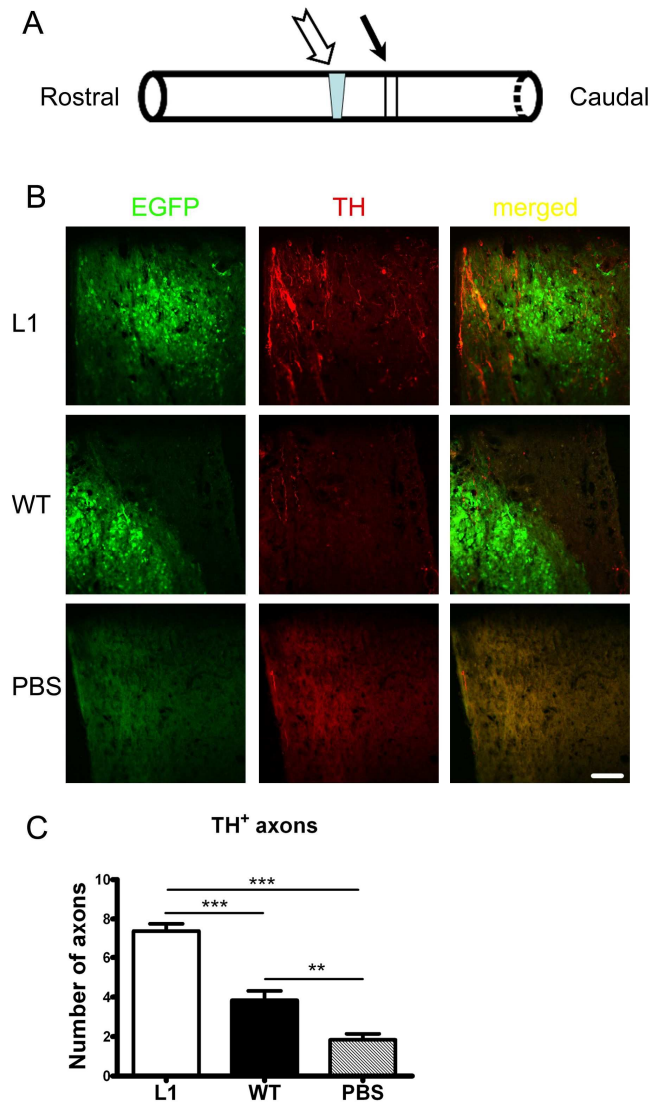
Figure 14. L1 overexpressing SENAs enhance the number of host TH$^+$ axons caudal to the lesion site 6 weeks after transplantation. (**A**) TH$^+$ fibers crossing an arbitrary border 250 µm (indicated by arrows) caudal to the lesion site (indicated by hollow arrows) were observed six weeks after transplantation. (**B**) Laser scanning images of TH$^+$ (red) axons 250 µm caudal to the lesion site in spinal cords grafted with L1$^+$ SENAs (n=6), control (WT) SENAs (n=6) or PBS (n=6). (**C**) The number of TH$^+$ axons 250 µm caudal to the lesion site is shown. (mean ± s.e.m.) Tukey's one-way ANOVA was performed for statistical analysis (**, *** $p < 0.01, 0.001$).

2.6 L1 overexpressing SENAs, but not control SENAs, improve locomotor function after transplantation into the lesioned spinal cord

Spinal cord compression injury caused severe disabilities in all three experimental

groups of mice as estimated by the BBB score one week after injury (Fig. 15A). Three and six weeks after injury, mice grafted with L1 overexpressing SENAs showed an increased BBB score when compared with mice grafted with control SENAs indicating an enhanced locomotor function. Furthermore, L1 overexpressing SENAs showed increased BBB scores when compared with sham-injected mice six weeks after transplantation (Fig. 15A). Besides the BBB score, we analysed the plantar stepping ability of the animals by measuring the foot-stepping angle (Apostolova, et al; 2006). This parameter revealed, in agreement with the BBB scores, enhanced functional recovery in mice grafted with L1 overexpressing SENAs when compared with mice transplanted with control SENAs and PBS three and six weeks after injury (Fig. 15B).

As the foot-stepping angle is a measure of involuntary movement rather than more complex motor functions the rump-height index, a parameter to estimate the ability to support body weight during ground locomotion, was analysed (Fig. 15C). This parameter also indicated enhanced recovery in mice grafted with L1 overexpressing SENAs compared to mice grafted with PBS, but only a slight improvement compared to mice grafted with control SENAs six weeks after transplantation. Moreover, the extension-flextion ratio, a parameter to judge voluntary movements without body weight support, revealed no significant differences among the experimental groups of mice, though L1 overexpressing SENAs did minutely improved motor function measured by this parameter compared to the control SENAs and sham-injected groups (Fig. 15D). From the values of the parameters at different time points shown in Fig. 15A–D, group mean values were determined (Fig. 15E) and overall recovery index for each animal were calculated (Fig. 15F) indicating an overall best outcome in mice grafted with L1 overexpressing SENAs compared to mice grafted with control SENAs or sham-injected with PBS. (Recovery Index = $[(X_{7+n} - X_7) / (X_0 - X_7)]$ x 100, where X_0, X_7 and X_{7+n} are values prior to operation, 7 days after injury, and a time-point n days after the spinal cord injury, respectively.)
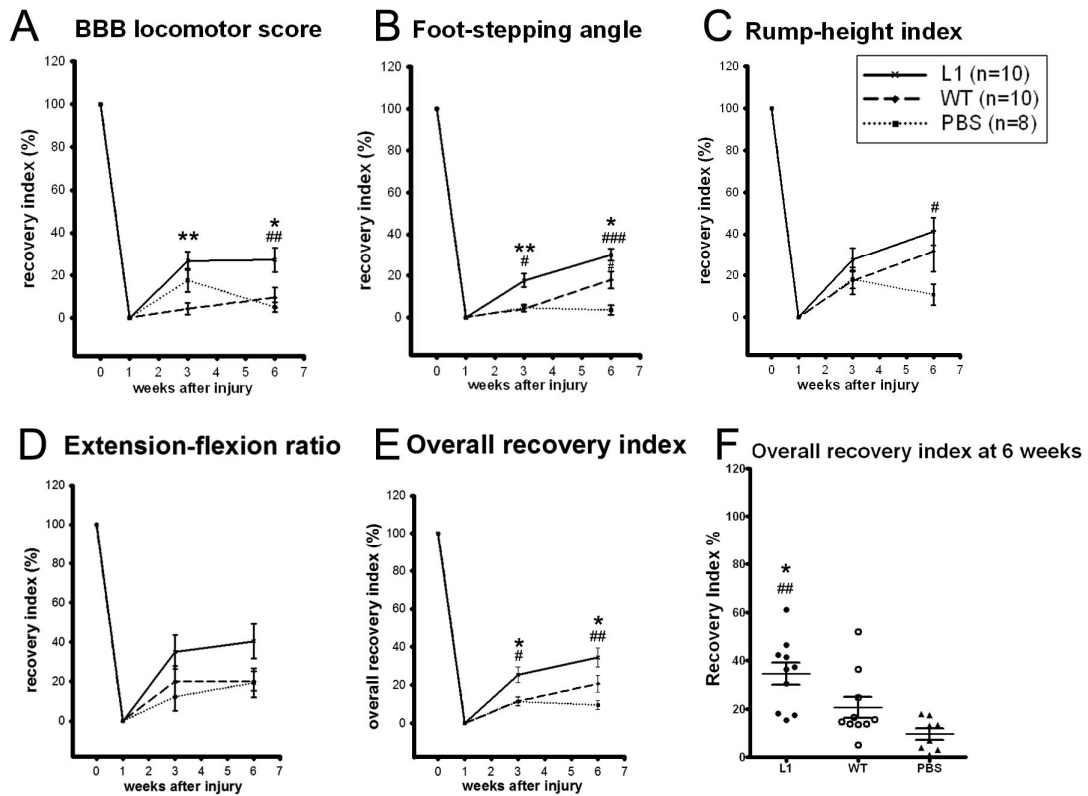
Figure 15. Time course and degree of functional recovery after spinal cord compression injury in mice grafted with $L1^+$ SENAs (n=10), control (WT) SENAs (n=10), or sham-injected with PBS (n=8). Shown are mean values ± s.e.m. of recovery indexes calculated from the BBB scores (**A**), the foot stepping angles (**B**), the rump-height indices (**C**), the extension-flexion ratio (**D**), and an overall recovery index. (**E**) one to six weeks after injury. Individual values of overall recovery indices at 6 weeks are shown in panel **F**. The numbers of mice studied per group are given in panel **C**. Statistical analysis was performed by Tukey's One-way ANOVA (*, ** $p < 0.05$, 0.01 when compared between L1 and WT group at a given time point; #, ## $p < 0.05$, 0.01 when compared to the PBS group at a given time point).

2.7 L1 overexpressing SENAs alter the H/M ratio in electrical stimulation of the sciatic nerve after transplantation into the lesioned murine spinal cord

We analyzed the reflex responses in C57BL/6J mice six weeks after the compression injury of the spinal cord. Electrical stimulation of the sciatic nerve produced typical EMG responses at baseline stimulation frequencies (0.1 Hz – 20 Hz) consisting of a short-latency M- (muscle) wave and a long-latency H-wave elicited by stimulation of motor axons and afferent type Ia fibers, respectively. Based on these results, the H/M ratio was calculated (Fig. 16). L1 overexpressing SENAs showed an increased H/M ratio at low stimulation frequencies ranging from 0.1 Hz to 0.5 Hz

when compared to control SENAs six weeks after transplantation and an increased H/M ratio at frequencies ranging from 0.2 Hz to 0.5 Hz when compared to sham-injected mice.
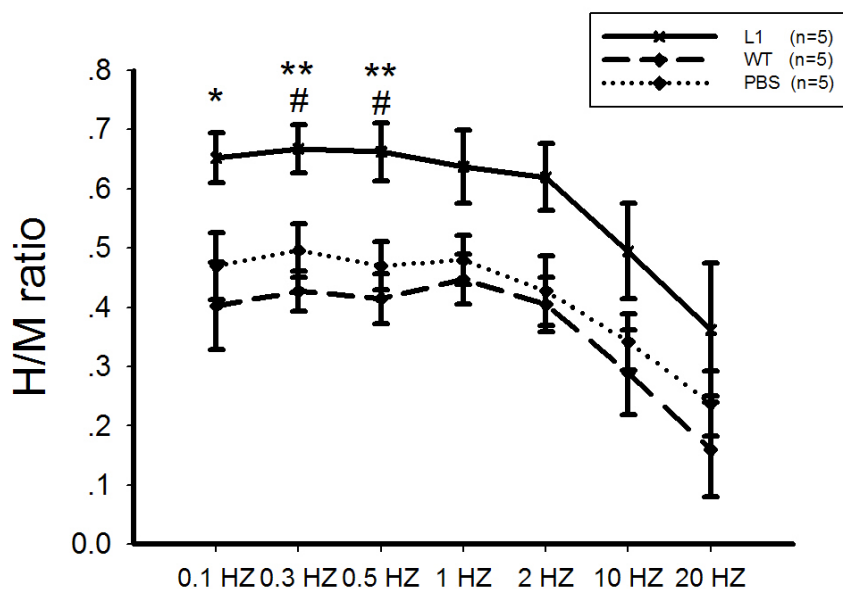
Figure 16. The H/M ration at different frequencies six weeks after spinal cord injury in mice grafted with L1$^+$ SENAs, control (WT) SENAs, or sham-injected with PBS. The alterations of M- and H-responses were measured in the plantar muscle during repetitive stimulation of the sciatic nerve with electric pulses at frequencies ranging between 0.1 and 20 Hz. Note the significantly increased H/M ratio in L1$^+$ SENAs at low stimulation frequencies. Shown are mean values ($\pm$ s.e.m.) of H/M ratios at different stimulation frequencies at six weeks after spinal cord injury. (*, ** $p < 0.05$ and 0.01, when compared to WT group, # $p < 0.05$, when compares to PBS. One-way ANOVA for repeated measurements with Tukey's *post hoc* test; $n = 5$ mice per group).

2.8 L1 overexpressing SENAs but not control SENAs decrease microglial activation but do not influence reactive astrogliosis of the host tissue after transplantation into the lesioned spinal cord

The immune reaction of the host to grafted cells is a major concern in stem cell transplantation. In order to measure the immune reaction of the host, the expression of glial and microglial marker proteins was analysed in the vicinity of the graft. No difference was observed in the astroglial reaction determined by analysis of the expression of the glial fibrillary acidic protein (GFAP) between the experimental

groups six weeks after transplantation (Fig. 17A-D). In contrast, L1 overexpressing SENAs reduced the microgial reaction of the host tissues as determined by analysis of the expression of the microglial marker protein Iba-1 when compared to control SENAs rostral to the lesion site (Fig. 17E, F) and compared to the PBS group caudal to the lesion site (Fig. 17G, H).
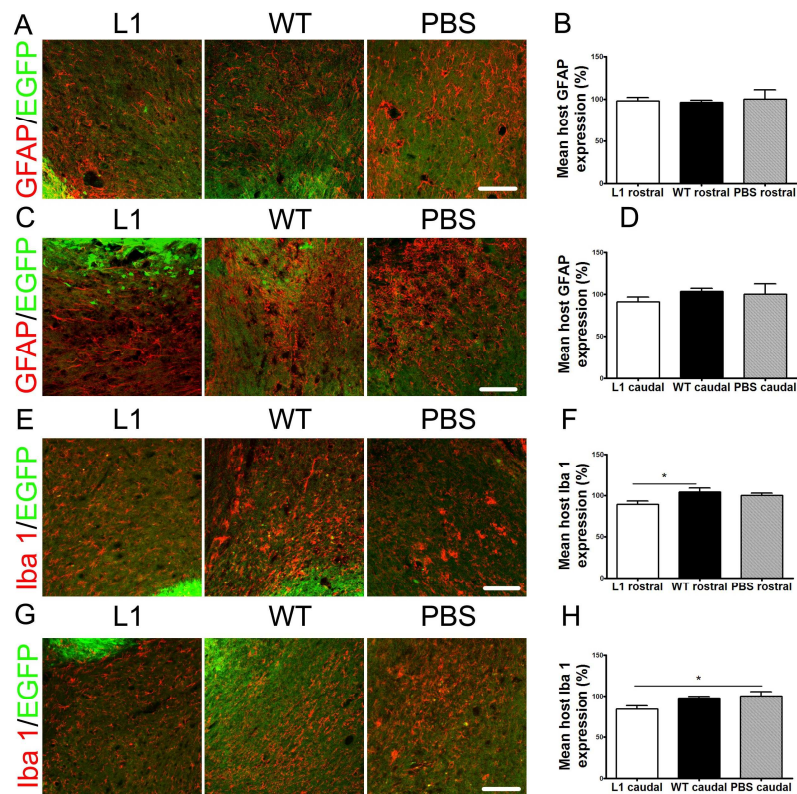
Figure 17. Host tissues show decreased microgial reaction to L1 overexpressing SENAs when compared to control (WT) SENAs and sham-injected animals, but no difference in the astroglial reaction. Confocal images of host spinal cord grafted by L1$^+$ SENAs, WT SENAs (green) or sham-injectd with PBS immunostained with an antibody against GFAP (red) rostral **(A)** and caudal **(C)** to the lesion site. Scale bar, 100 µm. **(B) (D)** Mean fluorescence intensity of GFAP staining in the host tissues rostral **(B)** and caudal **(D)** to the lesion site in mice grafted with L1$^+$ SENAs (n=5) or WT SENAs (n=5) was compared to the fluorescence intensity in sham-injected animals (n=5) which was adjusted to 100%. Tukey's one-way ANOVA was performed for statistical analysis. **(E) (G)** Confocal images of host striatal tissues grafted with L1$^+$ SENAs, WT SENAs (green) or sham-injected with PBS immunostained with an antibody against Iba 1 (red) rostral **(E)** and caudal **(G)** to the lesion site. Scale bar, 100 µm. **(F) (H)** Mean fluorescence intensity of Iba-1 in the host tissue of mice grafted with L1$^+$ SENAs (n=5) and WT SENAs (n=5) was compared to the fluorescence intensity in sham-injected animals (n=5) which was adjusted to 100%. Tukey's one-way ANOVA was performed for statistical analysis. (* $p < 0.05$).

V   Discussion

1. Transplantation of SENAs into the MPTP-lesioned mice model

In this study it was shown that the neural cell adhesion molecule L1 beneficially influences survival of grafted SENAs, migration of cells from grafted SENAs, and the differentiation of embryonic stem cells into neurons, particularly TH^{+} neurons in SENAs, most prominently in vivo after syngeneic transplantation into the MPTP-lesioned mouse brain. This study also demonstrates that L1 overexpressing SENAs rescued endogenous nigral dopaminergic neurons. Previous studies showed that L1 increased neuronal differentiation of embryonic and neural stem cells and enhanced migration of transplanted neural precursor cells in the quinolinic acid-lesion paradigm of Huntington's disease (Dihné, et al; 2003, Bernreuther, et al; 2006). Furthermore, neural differentiation of embryonic stem cells into SENAs enhanced neuronal differentiation and migration of transplanted cells in the quinolinic acid-lesion model (Dihné, et al; 2006). Not surprisingly, L1 did not show an effect on neuronal differentiation of SENAs in vitro in our study as control SENAs already consisted of 90% β-tubulin III^{+} neurons. In vivo, L1 overexpressing SENAs contained a higher proportion of neurons after transplantation than control SENAs and showed enhanced migration of transplanted cells into the host tissue. Furthermore, L1 overexpressing SENAs showed an enhanced fraction of TH^{+} neurons after transplantation when compared to control SENAs; this is most likely due in part to the overall enhanced neuronal differentiation. On the other hand, L1 has been described as a survival factor for fetal dopaminergic neurons in vitro (Hulley, et al; 1998) and thus, the enhanced fraction of TH^{+} neurons could be caused by a paracrin or autocrin effect of L1 expressed by grafted cells on transplanted dopaminergic neurons. This is further supported by our finding that L1 overexpressing SENAs but not control SENAs rescue endogenous TH^{+} neurons in the substantia nigra pars compacta indicating that control SENAs do not secrete survival factors for dopaminergic neurons. Previous studies showed that both the addition of sonic hedgehog (SHH), FGF8, and ascorbic acid and the overexpression of the transcription factor Nurr1 led

to increased percentages of TH^{+} neurons derived from murine embryonic stem cells in vitro ranging from 30% to 90% (Kawasaki, et al; 2000, Lee, et al; 2000, Kim, et al; 2002, 2006, Nishimura, et al; 2003). In this study, dopaminergic differentiation was not enhanced by addition of these factors because the aim was to examine the effects of L1 overexpression combined with the SENA differentiation protocol on neuronal differentiation, survival, and migration. Thus the fraction of TH^{+} neurons that was observed in vitro was lower than in the studies mentioned above. Nevertheless, L1 enhanced the percentage of TH^{+} cells after grafting of SENAs in the MPTP model of PD and increased overall survival of grafted cells. This is an important finding in view of the fact that several studies describe poor survival of especially human neural and embryonic stem cell-derived TH^{+} neurons after transplantation in rat models of PD (Ostenfeld, et al; 2000, Schulz, et al; 2004, Zeng, et al; 2004, Park, et al; 2005, Brederlau, et al; 2006, Martinat, et al; 2006). This study shows that L1 may prove useful in enhancing the survival of transplanted dopaminergic neurons after transplantation in vivo. Furthermore, this study showed that L1 overexpressing but not control SENAs increased the number of surviving endogenous dopaminergic neurons in the ipsilateral substantia nigra pars compacta after unilateral transplantation adjacent to the substantia nigra in MPTP-lesioned animals. This result indicatesthat L1 overexpressing SENAs have the potential to positively influence the progressive loss of dopaminergic neurons in the substantia nigra, a major feature of PD. This seems to be an L1-specific local effect as transplantation does not influence cell survival in the contralateral substantia nigra and transplantation of L1 overexpressing SENAs into the striatum does not show any effect on the survival of endogenous dopaminergic neurons. This agrees with the finding of Hulley et al. (1998) who described L1 as a survival factor for fetal dopaminergic neurons in vitro. Alternatively, the increased number of surviving endogenous dopaminergic neurons ipsilateral to L1 overexpressing grafts may be caused by the increased fraction of graft-derived TH^{+} cells potentially secreting trophic factors rescuing host nigral neurons. Few transplantation studies describe the rescue of endogenous dopaminergic neurons in animal models of PD. Ourednik et al. (2002) and Moses et al. (2007)

described a neuroprotective effect of grafted neural precursor cells on host cells in the murine MPTP model. The authors proposed spontaneous expression of neuroprotective agents by the neural precursor cells as the underlying cause. In this study, a similar effect after transplantation of embryonic stem cell-derived SENAs was not observed. Most probably, this is due to the decreased numbers of neural precursor cells in the SENA grafts that consist almost exclusively of neurons and astrocytes leading to decreased expression of neuroprotective factors when compared to neural precursor cells. Other studies described a protection of nigral TH$^+$ cells by astrocytes transduced to overexpress glial cell line-derived neurotrophic factor or fibrobalsts expressing brain-derived neurotrophic factor (Lucidi-Phillipi, et al; 1995, Ericson, et al; 2005). Redmont et al. (2007) showed a neuroprotective effect of human neural stem cells in a primate model of Parkinson's disease. Other groups showed enhanced rescue of endogenous dopaminergic neurons after transplantation of mesenchymal stem cells that was attributed to either the expression of trophic factors or immunomodulatory mechanisms (Keshet, et al; 2007, Park, et al; 2008). Thus, this study shows for the first time that transplanted neural cells overexpressing a cell adhesion molecule rescue endogenous dopaminergic neurons in an animal model of Parkinson's disease.

L1 overexpressing SENAs but not control SENAs or sham-injected PBS led to a stable ipsilateral bias in apomorphine-induced rotation behaviour after intrastriatal transplantation into the MPTP-lesioned brain indicating improved motor behaviour. Most stem cell transplantation studies involve unilateral lesioning of the rat striatum applying 6-hydroxy-dopamine or MPTP. In these experiments, decrease of apomorphine- or amphetamine-induced rotation behaviour was used to measure functional recovery (Kim, et al; 2002, Dezawa, et al; 2004, Park, et al; 2005, Sanchez-Pernaute, et al; 2005, Fu, et al; 2006). In this study, cells were syngeneically transplanted into mice that had received intraperitoneal injections of MPTP and thus showed a symmetric loss of dopaminergic neurons in the substantia nigra mimicking disease progression in PD. Consequently, no rotation bias was observed in apomorphine-induced rotation before transplantation. In contrast, transplantation of

L1 overexpressing SENAs led to an ipsilateral rotation bias after stimulation with apomorphine that was not observed in the control SENA and PBS group. One can interpret this as a sign of functional recovery in view of the fact that previous studies described an apomorphin-induced rotation to the contralateral (unlesioned) side after large unilateral lesioning with 6-hydroxydopamine (Hudson, et al; 1999, Da Cunha, et al; 2008). The observed ipsilateral rotation bias is most likely due to the increased fraction of TH$^+$ cells in L1 overexpressing versus control SENAs and not influenced by unspecific effects mediated by the increased graft size in L1 overexpressing SENAs since no apomorphine-induced rotation was observed in animals developing teratomas that exceeded the size of L1 overexpressing grafts (data not shown). Thus, L1 overexpressing SENAs enhanced functional recovery after transplantation into the MPTP-lesioned striatum. The serious movement disorder in Parkinson's disease results from the loss of dopaminergic neurons in the substantia nigra pars compacta with decreased levels of dopamine in the striatum (Samii, et al; 2004). Thus, the striatal dopamine level is an important parameter to measure the efficacy of cell replacement therapy in Parkinson's disease. L1 overexpressing SENAs increased dopamine level in the striatum ipsilateral to the grafted side when compared to the contralateral side after striatal engraftment, whereas control SENAs did not. This is probably due to the higher fraction of TH$^+$ neurons differentiated from transplantated cells. And this increased dopamine level is associated with improved locomotor function. In contrast, transplantation of SENAs did not alter striatal GABA levels,

As previously described (Dihné, et al; 2006), tumours were observed in a minor fraction of transplanted SENAs only. This is important as tumour formation remains a major issue in the transplantation of embryonic stem cells (Nishimura, et al; 2003, Brederlau, et al; 2006). Also, L1 overexpressing SENAs led to a decreased microglial activation indicating a decreased immune reaction of host tissues, which could prevent grafted cells from being attacked by the host immune system contributing to the enhanced survival observed in L1 overexpressing SENAS when compared to control SENAs.

In summary, the combination of the SENA differentiation protocol, which

provides enhanced neuronal differentiation, migration, and decreased tumor formation of embryonic stem cells and the overexpression of the neural cell adhesion molecule L1, which contributes enhanced neuronal differentiation and migration led to an increased survival of grafted cells. These grafted cells   showed an increased fraction of graft-derived TH$^+$ neurons that enhanced and sustained functional recovery after intrastriatal transplantation in the MPTP-model of PD. This is an important finding in view of the fact that human embryonic stem cell-derived TH$^+$ neurons in particular show poor survival after transplantation in rodent models of PD. Furthermore, it was shown for the first time, that a neural cell adhesion molecule enhanced the survival of endogenous dopaminergic neurons in the substantia nigra indicating that L1 might be a candidate to decrease the progressive loss of neurons in PD.

2. Transplantation of SENAs into the compression-lesioned murine spinal cord

In this study it was shown that the neural cell adhesion molecule L1 beneficially influences survival of grafted SENAs, migration of cells from grafted SENAs, the differentiation of embryonic stem cells into neurons, and the length of neurites of graft-derived neurons in SENAs after syngeneic transplantation into the compression-lesioned murine spinal cord. Furthermore, L1 overexpressing SENAs led to enhanced innervation and soma size of motor neurons distal to the lesion site leading to enhanced functional recovery. A previous study (Chen, et al; 2005) showed that transfection of embryonic stem cells with L1 had beneficial effects on the survival of stem cells after transplantation into the compression-lesioned adult mouse spinal cord. These results were confirmed and further corroborated in this study. In agreement with the previous study, this study found enhanced survival of transpanted L1 overexpressing SENAs when compared to control SENAs. In contrast to the previous study, where non-transfected control embryonic stem cells did not surviv one month after transplantation, control SENAs showed robust survival up to 6 weeks after transplantation indicating beneficial effects of the SENA differentiation protocol.

This may be due to the fact that SENAs that are transplanted as a compact structure create a beneficial microenvironment enhancing survival of grafted cells under the unfavorable conditions within the lesioned spinal cord while embryonic stem cells differentiated by the five stage protocol (Lee, et al; 2000) are transplanted as a single cell suspension with reduced capacity to create a beneficial microenvironment without the beneficial properties of L1. Interestingly, L1 showed a significant effect on graft survival caudal but not rostral to the lesion. It has been shown that in the injured spinal cord far more genes are differentially expressed caudal than rostral to the lesion-site, which includes apoptosis-related genes (App, Casp1, etc.), extracellular matrix-related genes (Col 1a 2, Ninj1, etc), growth factors (FGFr2, VEGF, etc), and inflammation/immune response related genes (Fcgr2, Fgg, Il6st, etc) (De Biase, et al; 2005). Nesic et al. (2005) also observed that genes which are involved in regulating inflammatory reactions show an increased upregulation in segments caudal than rostral to the lesion-site after spinal cord injury, for example STAT 3, MHC-II, TGFβ type I receptor and TGFβ type II receptor, etc. We hypothesize, that this leads to a more hostile caudal environment than that existing rostral to the lesion and thus the beneficial effects of L1 are more pronouncedly observed in an environment even more unfavorable to survival than the rostral area. Another beneficial property of L1, the enhanced migration of grafted cells into the host tissue is not affected by the location of the graft. The result is in agreement with previous studies showing enhanced migration of L1 overexpressing cells. (Bernreuther, et al; 2006). Furthermore, L1 overexpressing SENAs decreased the microglial reaction both rostral and caudal to the lesion-site, while control SENAs did not show an effect.

L1 beneficially influnced scar formation after engrafting L1 overexpressing SENAs into the compression-lesioned spinal cord in this study. Shortly after spinal cord injury, extracellular matrix molecules and glial cells form a scar surrounding the lesion site, which is thought to be the major factor limiting recovery (Fawcett and Asher, 1999; Grimpe and Silver, 2002). Apostolova et al (2006) discovered the correlation between scar volume and locomotor function after spinal cord injury. Therefore, scar volume is regarded as a useful parameter to judge the recovery after

spinal cord injury. In this study, the scar volume was significantly reduced in animals transplanted with L1 overexpressing SENAs when compared to control SENAs and sham-injected mice. This is in accordance with the finding of Chen et al. (2007) who observed that virus-mediated expression of L1 in the lesioned spinal cord decreased the expression of GFAP, thus modifying the micro-environment leading to a smaller scar volume at the lesion site. The mechanism by which L1 reduced the GFAP expression and decreased the scar volume at the lesion site has not yet been clarified, but it is probably not dependent on MAPK and FGFr3 signalling (Chen, et al; 2007). In this study it was shown, that L1 not only influenced the host environment with a reduction of the glial scar volume, but also dereased astrocytic differentiation of grafted SENAs. This phenomenon is probably due to an instructive role of L1 in the lineage decision. It was previously shown that L1 can enhance neuronal differentiation and decrease astrocytic differentiation of multipotent and neuron–astrocyte-restricted bipotential neural precursor cells (Dihné, et al; 2003).

Dopaminergic descending pathways, originating in the substantia nigra, brain stem tegmentum and reticular formation, are located in the ventral and lateral columns of the spinal cord (Barnes, et al; 1979). They mediate the excitability of spinal cord circuitries (Fouad and Pearson, 2004), which correlates with locomotor functional recovery in the injured spinal cord of mice (Jakovcevski, et al; 2007). L1 has been shown to enhance the regrowth of axons (Castellani, et al; 2002, Roonprapunt, et al; 2003, Xu, et al; 2004, Chen, et al; 2005, Zhang, et al; 2005) and to rescue fetal dopaminergic neurons (Hulley, et al; 1998). It's not surprising to find that L1 overexpressing SENAs enchanced dopaminergic reinnervation in the spinal cord caudal to the lesion after transplantation. These dopaminergic axons could reach their targets and reestitablish synaptic connections afterwards.

After spinal cord injury, motor neuron death, especially in the lumbar enlargements, can contribute to locomotor dysfunction (Pearse and Bunge, 2006). Therefore, an important aim of stem cell transplantation is to rescue endogenous motor neurons after spinal cord injury. In this study, L1 was shown to rescue host motor neurons as indicated by an enlarged soma size of motor neurons distal to the

lesion in mice grafted with L1 overexpressing SENAs when compared to control SENAs or PBS only. Furthermore, the density of cholinergic puncta on motor neurons was enhanced in mice transplanted with L1 overexpressing SENAs indicating enhanced numbers of cholinergic perisomatic synapses. Previous electrophisiologocal experiments showed that in the intact spinal cord, the cholinergic perisomatic synapses regulate motoneuron excitability during locomotion (Miles, et al; 2007). Thus, L1 exerts positive effects on recovery after spinal cord injury by rescuing motor neurons and enhancing the cholinergic perisomatic synapses.

Using a set of behavioral analyses to observe different motor abilities, this study showed that mice engrafted with L1 overexpressing SENAs had a significantly enhanced recovery compared to control SENAs or PBS. This is displayed in three parameters: the BBB score, the foot-stepping angle and the rump-height index. These parameters depict the plantar stepping ability of mice after spinal cord lesion. Previous studies showed that these parameters strongly correlate with the degree of monoaminergic innervation of the distal spinal cord and with cholinergic perisomatic innervation of motoneurons after spinal cord injury (Jakovcevski, et al; 2007). Thus, the enhanced dopaminergic reinnervation and cholinergic inputs to motor neurons in the caudal spinal cord observed in this study after transplantation of L1 overexpressing SENAs suggests a potential mechanism of the beneficial function of L1 overexpression in enhancing functional recovery.

The Hoffmann reflex (H-reflex) is an electrically elicited analog of the spinal stretch reflex providing information on the functional properties of Ia afferents and homonymous alpha-motoneurons under physiological and pathological conditions (Gozariu, et al; 1998; Pierrot-Deseilligny and Mazevet, 2000) Lee et al. (2009) demonstrated that the H-reflex is a useful tool for the assessment of motoneuron pool excitability in spinal cord-injured mice, and observed that the increase of H/M ratios under alternative stimulations is associated with locomotor functional recovery in mice after spinal cord injury. Thus, the H/M ratios were determined in the experimental groups 6 weeks after transplantation. The H/M ratios were increased at lower frequencies (0.1-0.5Hz) in mice engrafted with L1 overexpressing SENAs

when compared with mice grafted with control SENAs or sham-injected with PBS further supporting the positive effects of L1 overexpressing SENAs on functional recovery after spinal cord injury. The mechanism underlying the dependence of the increase of the H/M ration on the stimulation frequency is currently not understood.

The determination of an optimal timepoint for stem cell transplantation after spinal cord injury is important to ensure survival of transplanted ES cells. Due to the microenvironments of the acutely injuried spinal cord, 1-2 weeks after injury were previously regarded as the optimal time period for transplantation (Okano, 2002; Ogawa, et al; 2002, Kimura, et al; 2005, McDonald, et al; 1999, Howard, et al; 2005, Keirstead, et al; 2005, Harper, et al; 2004, Kerr, et al; 2003) since immediately after spinal cord injury, many inflammatory cytokines (e.g. IL-1, IL-6, and TNF) occur around the lesion site mediating neurotoxic or astrocyte-inducing effects that can lead to apoptosis of grafted cells or preferential differentiation into astrocytes. Recently, these immediate effects of trauma leading to spinal shock were considered to resolve within the first 72 hours after spinal cord injury (Atkinson and Atkinson, 1996; Ditunno, et al; 2004, Belegu, et al; 2007). Thus, three days after spinal cord injury was chosen as the time point for transplantation in this study, and for the first time it was shown that even at this early timepoint robust cell survival can be achieved at least when transplanting SENAs, especially L1 overexpressing SENAs and thereby to enhanced functional recovery.

In conclusion, the differentiation of mouse ES cells into SENAs combined with overexpression of the neural cell adhesion molecule L1 led to enhanced neuronal differentiation, migration, neurite outgrowth, and better survival after grafting into the compression-lesioned spinal cord when compared to control SENAs. L1 overexpressing SENAs enhanced monoaminergic reinnervation distal to the lesion-site, increased cholinergic synaptic innervation to endogenous motor neurons and rescued host motor neurons, this contributed to increased and sustained functional recovery. These findings corroborate the finding that L1 might be a candidate to ameliorate the progression of spinal cord injury (Chen, et al; 2005, Chen, et al; 2007) Moreover, it was shown for the first time, that SENAs allow successful

transplantation three days after spinal cord injury broadening the subacute therapeutic time window for ES cells transplantation in spinal cord injury.

VI Literature

"Parkinson's Disease Mechanism Discovered," HHMI Research News June 22,2006.

Akiyama Y, Honmou O, Kato T, Uede T, Hashi K, Kocsis JD (2001). Transplantation of clonal neural precursor cells derived from adult human brain establishes functional peripheral myelin in the rat spinal cord. Exp. Neurol. 167, 27–39.

Allen AR (1911). "Surgery of experimental lesions in the spinal cord equivalent to crush injury of fracture dislocation." Preliminary report. J Am Med Assoc. 57:878-880.

Apostolova I, Irintchev A, Schachner M (2006). Tenascin-R restricts posttraumatic remodeling ofmotoneuron innervation and functional recovery after spinal cord injury in adult mice. J Neurosci 26:7849–7859

Appel F, Holm J, Conscience JF, Schachner M (1993). Several extracellular domains of the neural cell adhesion molecule L1 are involved in neurite outgrowth and cell body adhesion. J Neurosci 13: 4764–75

Atkinson PP, Atkinson JL (1996). Spinal shock. Mayo Clin Proc. 71: 384–89.

Ausrubel, FM (1996) Current Protocols in Molecular Biology. Greene Publishing Associates, New York

Baldereschi M, Di Carlo A, Rocca WA, Vanni P, Maggi S, Perissinotto E, Grigoletto F, Amaducci L, Inzitari D (2000). Parkinson's disease and parkinsonism in a longitudinal study: two-fold higher incidence in men. Neurology. 55: 1358–63.

Ballard PA, Tetrud JW, Langston JW (1985). Permanent human parkinsonism due to 1-methyl-4-phenyl-1,2,3,6-tetrahydropyridine (MPTP): seven cases. Neurology 35: 949–956

Bambakidis NC, Miller RH (2004). Transplantation of oligodendrocyte precursors and sonic hedgehog results in improved function and white matter sparing in the spinal cords of adult rats after contusion. Spine J. 4, 16–26.

Barberi T, Klivenyi P, Calingasan NY, Lee H, Kawamata H, Loonam K, Perrier AL, Bruses J, Rubio ME, Topf N, Tabar V, Harrison NL, Beal MF, Moore MA, Studer L (2003). Neural subtype specification of fertilization and nuclear transfer embryonic stem cells and application in parkinsonian mice. Nat Biotechnol 21: 1200 – 1207.

Barres BA, Hart IK, Coles HS, Burne JF, Voyvodic JT, Richardson WD, Raff MC (1992). Cell

death and control of cell survival in the oligodendrocyte lineage. Cell 70, 31–46.

Bartsch U, Kirchhoff F, Schachner M (1989). Immunohistological localization of the adhesion molecules L1, N-CAM, and MAG in the developing and adult optic nerve of mice. J Comp Neurol *284*:451–62

Basso DM, Beattie MS, Bresnahan JC (1995). A sensitive and reliable locomotor rating scale for open field testing in rats. J Neurotrauma 12:1–21.

Becker JW, Erickson HP, Hoffman S, Cunningham BA, Edelman GM (1989). Topology of cell adhesion molecules. Proc Nat Acad Sci USA *86*:1088–92

Ben-Hur T, Einstein O, Mizrachi-Kol R, Ben-Menachem O, Reinhartz E, Karussis D, Abramsky O (2003). Transplanted multipotential neural precursor cells migrate into the inflamed white matter in response to experimental autoimmune encephalomyelitis. Glia 41, 73–80.

Bennett V, and Baines, AJ (2001). Spectrin and ankyrin-based pathways: metazoan inventions for integrating cells into tissues. Physiol. Rev. 81, 1353–1392

Benton RL, Woock JP, Gozal E, Hetman M, Whittemore SR (2005). Intraspinal application of endothelin results in focal ischemic injury of spinal gray matter and restricts the differentiation of engrafted neural stem cells. Neurochem. Res. 30, 809–823.

Beric A, Kelly PJ, Rezai A, Sterio D, Mogilner A, Zonenshayn M, Kopell B (2001). Complications of deep brain stimulation surgery. Stereotact Funct Neurosurg. 77: 73–78.

Bernreuther C, Dihné M, Johann V, Schiefer J, Cui Y, Hargus G, Schmid JS, Xu J, Kosinski CM, Schachner M (2006). Neural cell adhesion molecule L1-transfected embryonic stem cells promote functional recovery after excitotoxic lesion of the mouse striatum. J Neurosci. 26(45):11532-9.

Bernstine EG, Hooper ML, Grandchamp S, and Ephrussi B (1973). Alkaline phosphatase activity in mouse teratoma. Proc Natl Acad Sci USA 70: 3899–3903.

Bjorklund A (2000). Cell replacement strategies for neurodegenerative disorders. Novartis Found Symp 231:7-15.

Bjorklund LM, Sanchez-Pernaute R, Chung S, Andersson T, Chen IY, McNaught KS, Brownell AL, Jenkins BG, Wahlestedt C,Kim KS, Isacson O (2002). Embryonic stem cells develop into functional dopaminergic neurons after transplantation in a Parkinson rat model. Proc Natl Acad Sci USA 99: 2344－2349.

Blight, A.R (2002). Miracles and molecules - progress in spinal cord repair. Nat. Neurosci. 5, Suppl., 1051–1054.

Braak H, Del Tredici K, Rub U, de Vos RA, Jansen Steur EN, Braak E (2003). Staging of brain pathology related to sporadic Parkinson's disease. Neurobiol Aging. 24: 197–211.

Bradley A, Evans M, Kaufman MH, and Robertson E (1984). Formation of germ-line chimaeras from embryo-derived teratocarcinoma cell lines. Nature 309: 255–256.

Brederlau A, Correia AS, Anisimov SV, Elmi M, Paul G, Roybon L, Morizane A, Bergquist F, Riebe I, Nannmark U, Carta M, Hanse E, Takahashi J, Sasai Y, Funa K, Brundin P, Eriksson PS, Li JY (2006). Transplantation of human embryonic stem cell-derived cells to a rat model of Parkinson's disease: effect of in vitro differentiation on graft survival and teratoma formation. Stem Cells 24: 1433–1440.

Brümmendorf T, Kenwrick S, Rathjen FG (1998). Neural cell recognition molecule L1: from cell biology to human hereditary brain malformations. Curr Opin Neurobiol 8:87–97.

Brümmendorf T, Rathjen FG (1993). Axonal Glycoproteins with with immunoglobulin- and fibronectin type III-related domains in vertebrates: structural features, binding activities, and signal transduction. J Neurochem 61:1207–19

Brüstle O, Jones KN, Learish RD, Karram K, Choudhary K, Wiestler OD, Duncan ID, McKay RD (1999). Embryonic stem cell-derived glial precursors: a source of myelinating transplants. Science. 285, 754–756.

Bunge RP, Puckett WR, Becerra JL, Marcillo A, Quencer RM (1993). Observations on the pathology of human spinal cord injury. A review and classification of 22 new cases with details from a case of chronic cord compression with extensive focal demyelination. Adv. Neurol. 59, 75–89.

Burchiel KJ (1995). Thalamotomy for movement disorders. Neurosurg Clin N Am. 6: 55–71.

Burns RS, Chiueh DD, Markey SP, Ebert MH, Jacobowitz DM, Kopin IJ (1983). A primate model of parkinsonism: selective destruction of dopaminergic neurons in the pars compacta of the substantia nigra by N-methyl-4-phenyl-1,2,3,6- tetrahydropyridine. Proc Natl Acad Sci USA. 80: 4546–4550

Calne S, Schoenberg B, Martin W, Uitti RJ, Spencer P, Calne DB (1987). Familial Parkinson's disease: possible role of environmental factors. Can J Neurol Sci. 14: 303–05.

Cao Q, Xu XM, Devries WH, Enzmann GU, Ping P, Tsoulfas P, Wood PM, Bunge MB, Whittemore SR (2005b). Functional recovery in traumatic spinal cord injury after transplantation of multineurotrophin-expressing glial-restricted precursor cells. J. Neurosci. 25, 6947–6957.

Cao Q, Zhang YP, Iannotti C, DeVries WH, Xu XM, Shields CB, Whittemore SR (2005a). Functional and electrophysiological changes after graded traumatic spinal cord injury in adult rat. Exp. Neurol. 191, 3–16.

Cao QL, Howard RM, Dennison JB, Whittemore SR (2002b). Differentiation of engrafted neuronal-restricted precursor cells is inhibited in the traumatically injured spinal cord. Exp. Neurol. 177, 349–359.

Cao QL, Zhang YP, Howard RM, Walters WM, Tsoulfas P, Whittemore SR (2001). Pluripotent stem cells engrafted into the normal or lesioned adult rat spinal cord are restricted to a glial lineage. Exp. Neurol. 167, 48–58.

Castellani V, Chedotal A, Schachner M, Faivre-Sarrailh C, Rougon G (2000). Analysis of the L1-deficient mouse phenotype reveals cross-talk between Sema3A and L1 signaling pathways in axonal guiDA-ergicnce. Neuron *27*:237–249

Cazalets JR, Borde M, Clarac F (1995). Localization and organization of the central pattern generator for hindlimb locomotion in newborn rat. J. Neurosci. 15, 4943–4951.

Chen J, Bernreuther C, Dihné M, Schachner M (2005). Cell adhesion molecule l1-transfected embryonic stem cells with enhanced survival support regrowth of corticospinal tract axons in mice after spinal cord injury. J Neurotrauma. 22 (8):896-906.

Chen J, Wu J, Apostolova I, Skup M, Irintchev A, Kügler S, Schachner M (2007). Adeno-associated virus-mediated L1 expression promotes functional recovery after spinal cord injury. Brain. 130(Pt 4):954-69.

Chen S, Mantei N, Dong L, Schachner M (1999). Prevention of neuronal cell death by neural adhesion molecules L1 and CHL1. J Neurobiol *38*: 428–439.

Chow SY, Moul J, Tobias CA, Himes BT, Liu Y, Obrocka M, Hodge L, Tessler A, Fischer I (2000). Characterization and intraspinal grafting of EGF/bFGF-dependent neurospheres derived from embryonic rat spinal cord. Brain Res. 874, 87–106.

Chung S, Shin BS, Hedlund E, Pruszak J, Ferree A, Kang UJ, Isacson O, Kim KS (2006). Genetic selection of sox1GFP-expressing neural precursors removes residual tumorigenic

pluripotent stem cells and attenuates tumor formation after transplantation. J Neurochem 97: 1467 – 1480.

Cohen G, Pasik P, Cohen B, Leist A, Mytilineou C, Yahr MD (1984). Pargyline and deprenyl prevent the neurotoxicity of 1-methyl-4-phenyl-1,2,3,6-tetrahydropyridine (MPTP) in monkeys. Eur J Pharmacol. 106: 209–210.

Cohen NR, Taylor JS, Scott LB, Guillery RW, Soriano P, Furley AJ (1997). Errors in corticospinal axon guidance in mice lacking the neural cell adhesion molecule L1. Curr Biol. 8:26–33.

Cordes M, Snow BJ, Cooper S, Schulzer M, Pate BD, Ruth TJ, Calne DB (1994). Age-dependent decline of nigrostriatal dopaminergic function: a positron emission tomographic study of grandparents and their grandchildren. Ann Neurol. 36: 667–70.

Cummings BJ, Uchida N, Tamaki SJ, Salazar DL, Hooshmand M, Summers R, Gage FH, Anderson AJ (2005). Human neural stem cells differentiate and promote locomotor recovery in spinal cord–injured mice. Proc. Natl. Acad. Sci. USA 102, 14069–14074.

Curtis R, Green D, Lindsay RM, Wilkin GP (1993). Up-regulation of GAP-43 and growth of axons in rat spinal cord after compression injury. J Neurocytol 22:51–64.

Da Cunha C, Wietzikoski EC, Ferro MM, Martinez GR, Vital MA, Hipólide D, Tufik S, Canteras NS (2008). Hemiparkinsonian rats rotate toward the side with the weaker dopaminergic neurotransmission. Behav Brain Res. 3;189(2):364-72.

Dahme M, Bartsch U, Martini R, Anliker B, Schachner M, Mantei N (1997). Disruption of the mouse L1 gene leads to malformations of the nervous system. Nat Genet 17:346–9.

Davidoff MS, Irintchev AP (1986). Acetylcholinesterase activity and type C synapses in the hypoglossal, facial and spinal-cord motor nuclei of rats. An electron-microscope study. Histochemistry. 84:515–524.

Davis GC, William AC, Markey SP, Ebert MH, Caine ED, Reichert CM, Kopin IJ (1979). Chronic parkinsonism secondary to intravenous injection of meperidine analogues. Psychiatry Res 1: 249–254.

De Angelis E, Brummendorf T, Cheng L, Lemmon V, Kenwrick S (1991). Alternative use of a mini exon of the L1 gene affects L1 binding to neural ligands. J Biol Chem 276:32738–42.

De Biase A, Knoblach SM, Di Giovanni S, Fan C, Molon A, Hoffman EP, Faden AI (2005).

Gene expression profiling of experimental traumatic spinal cord injury as a function of distance from impact site and injury severity. Physiol Genomics. 22(3):368-81.

de Rijk MC, Launer LJ, Berger K, Breteler MM, Dartigues JF, Baldereschi M, Fratiglioni L, Lobo A, Martinez-Lage J, Trenkwalder C, Hofman A (2000). Prevalence of Parkinson's disease in Europe: a collaborative study of population-based cohorts. Neurology. 54 (11 suppl 5): S21–23.

Deep-Brain Stimulation for Parkinson's Disease Study Group (2001). Deep-brain stimulation of the subthalamic nucleus or the pars interna of the globus pallidus in Parkinson's disease. N Engl J Med345: 956–63.

Demyanenko GP, Tsai AY, Maness PF (1999). Abnormalities in neuronal process extension, hippocampal development, and the ventricular system of L1 knock-out mice. J Neurosci 19:4907–4920.

Dezawa M, Kanno H, Hoshino M, Cho H, Matsumoto N, Itokazu Y, Tajima N, Yamada H, Sawada H, Ishikawa H, Mimura T, Kitada M, Suzuki Y, Ide C (2004). Specific induction of neuronal cells from bone marrow stromal cells and application for autologous transplantation. J Clin Invest. 113(12):1701-10.

Dihné M, Bernreuther C, Hagel C, Wesche KO, Schachner M. (2006) Embryonic stem cell-derived neuronally committed precursor cells with reduced teratoma formation after transplantation into the lesioned adult mouse brain. Stem Cells. 24(6):1458-66.

Dihné M, Bernreuther C, Sibbe M, Paulus W, Schachner M (2003). A new role for the cell adhesion molecule L1 in neural precursor cell proliferation, differentiation, and transmitter-specific subtype generation. J Neurosci. 23(16):6638-50.

Doetschman TC, Eistetter H, Katz M, Schmidt W, and Kemler R (1985). The in vitro development of blastocyst-derived embryonic stem cell lines: formation of visceral yolk sac, blood islands and myocardium. J Embryol Exp Morphol 87: 27–45.

Dunnett SB, Bjorklund A, Lindvall O (2001). Cell therapy in Parkinson's disease - stop or go? Nat Rev Neurosci 2: 365–369.

Edelmann GM (1969). The covalent structure of an entire gamma G immunoglobulin module. Proc Nat Acad Sci USA 63:78–85.

Enzmann GU, Benton RL, Talbott JF, Cao Q, Whittemore SR (2006). Functional considerations of stem cell transplantation therapy for spinal cord repair. J Neurotrauma.

23(3-4):479-95.

Ericson C, Georgievska B, Lundberg C (2005). Ex vivo gene delivery of GDNF using primary astrocytes transduced with a lentiviral vector provides neuroprotection in a rat model of Parkinson's disease. Eur J Neurosci. 22(11):2755-64.

Eriksson PS, Perfilieva E, Björk-Eriksson T, Alborn AM, Nordborg C, Peterson DA, Gage FH (1998). Neurogenesis in the adult human hippocampus. Nat. Med. 4, 1313–1317.

Etminan M, Gill S, Samii A (2003). Comparison of the risk of adverse events with pramipexole and ropinirole in patients with Parkinson's disease: a meta-analysis. Drug Saf. 26: 439–44.

Etminan M, Samii A, Takkouche B, Rochon PA (2001). Increased risk of somnolence with the new dopamine agonists in patients with Parkinson's disease: a meta-analysis of randomised controlled trials. Drug Saf. 24: 863–8.

Fearnley JM, Lees AJ (1991). Ageing and Parkinson's disease: substantia nigra regional selectivity. Brain. 114: 2283–301.

Freed CR, Breeze RE, Rosenberg NL, Schneck SA, Kriek E, Qi JX, Lone T, Zhang YB, Snyder JA, Wells TH, et al (1992). Survival of implanted fetal dopamine cells and neurologic improvement 12 to 46 months after transplantation for Parkinson's disease. N Engl J Med. 327: 1549–55.

Freed CR, Greene PE, Breeze RE, Tsai WY, DuMouchel W, Kao R, Dillon S, Winfield H, Culver S, Trojanowski JQ, Eidelberg D, Fahn S (2001). Transplantation of embryonic dopamine neurons for severe Parkinson′s disease. N Engl J Med 344: 710–719.

Frielingsdorf H, Schwarz K, Brundin P, Mohapel P (2004). No evidence for new dopaminergic neurons in the adult mammalian substantia nigra. Proc Natl Acad Sci USA 101: 10177–10182.

Fu YS, Cheng YC, Lin MY, Cheng H, Chu PM, Chou SC, Shih YH, Ko MH, Sung MS (2006). Conversion of human umbilical cord mesenchymal stem cells in Wharton's jelly to dopaminergic neurons in vitro: potential therapeutic application for Parkinsonism. Stem Cells. 24(1):115-24.

Gage FH (2000). Mammalian neural stem cells. Science. 25;287(5457):1433-8.

Gao J, Coggeshall RE, Tarasenko YI, Wu P (2005). Human neural stem cell-derived cholinergic neurons innervate muscle in motoneuron deficient adult rats. Neuroscience 131, 257–262.

Gasser T (2001). Genetics of Parkinson's disease. J Neurol. 248: 833–40.

Gearhart JD and Mintz B (1974). Contact-mediated myogenesis and increased acetylcholinesterase activity in primary cultures of mouse teratocarcinoma cells. Proc Natl Acad Sci USA 71: 1734–1738.

Geijsen N, Horoschak M, Kim K, Gribnau J, Eggan K, and Daley GQ (2004). Derivation of embryonic germ cells and male gametes from embryonic stem cells. Nature 427(6970):148-54.

Gledhill RF, Harrison BM, McDonald WI (1973). Pattern of remyelination in the CNS. Nature. 244, 443–444.

Golbe LI (1991). Young-onset Parkinson's disease: a clinical review. Neurology. 41: 168–73.

Goodwin BL, Kite GC (1998). Environmental MPTP as a factor in the aetiology of Parkinson's disease? J Neural Transm 105: 1265–1269

Guest JD, Hiester ED, Bunge RP (2005). Demyelination and schwann cell responses adjacent to injury epicenter cavities following chronic human spinal cord injury. Exp. Neurol. 192, 384–393.

Guridi J, Lozano AM (1997). A brief history of pallidotomy. Neurosurgery. 41: 1169–80.

Hagell P, Piccini P, Bjorklund A, Brundin P, Rehncrona S, Widner H, Crabb L, Pavese N, Oertel WH, Quinn N, Brooks DJ, Lindvall O (2002). Dyskinesias following neural transplantation in Parkinson's disease. Nat Neurosci 5: 627–628.

Hall M (1841). On the diseases and derangements of the nervous system in their primary forms and in their modifications by age, sex, constitution, hereditary disposition, excesses, general disorder, and organic disease. London: Bailliere H. 256.

Hammang JP, Archer DR, Duncan ID (1997). Myelination following transplantation of EGF-responsive neural stem cells into a myelin-deficient environment. Exp. Neurol. 147, 84–95.

Han SS, Liu Y, Tyler-Polsz C, Rao MS, Fischer I (2004). Transplantation of glial-restricted precursor cells into the adult spinal cord: survival, glial-specific differentiation, and preferential migration in white matter. Glia. 45, 1–16.

Harper JM, Krishnan C, Darman JS, Deshpande DM, Peck S, Shats I, Backovic S, Rothstein JD, Kerr DA (2004). Axonal growth of embryonic stem cell-derived motoneurons in vitro and in motoneuron-injured adult rats. Proc. Natl. Acad. Sci. USA. 101, 7123–7128.

Hasegawa K, Chang YW, Li H, Berlin Y, Ikeda O, Kane-Goldsmith N, Grumet M (2005).

Embryonic radial glia bridge spinal cord lesions and promote functional recovery following spinal cord injury. Exp. Neurol. 193, 394–410.

Heikkila RE, Manzino L, Cabbat FS, Duvoisin RC (1984). Protection against the dopaminergic neurotoxicity of 1-methyl-4-phenyl-1,2,5,6-tetrahydropyridine by monoamine oxidase inhibitors. Nature. 311: 467–469

Hellstroem J, Oliveira AL, Meister B, Cullheim S (2003). Large cholinergic nerve terminals on subsets of motoneurons and their relation to muscarinic receptor type 2. J Comp Neurol. 460:476–486.

Hill CE, Proschel C, Noble M, Mayer-Proschel M, Gensel JC, Beattie MS, Bresnahan JC (2004). Acute transplantation of glial-restricted precursor cells into spinal cord contusion injuries: survival, differentiation, and effects on lesion environment and axonal regeneration. Exp. Neurol. 190, 289–310.

Hochedlinger K and Jaenisch R (2003). Nuclear transplantation, embryonic stem cells, and the potential for cell therapy. N Engl J Med 349: 275–286.

Hoffman S, Sorkin BC, White PC, Brackenbury R, Mailhammer R (1982). Chemical Characterization of a neural cell adhesion molecule purified from embryonic brain membranes. J Biol Chem 257:7720–29

Hofstetter CP, Holmström NA, Lilja JA, Schweinhardt P, Hao J, Spenger C, Wiesenfeld-Hallin Z, Kurpad SN, Frisén J, Olson L (2005). Allodynia limits the usefulness of intraspinal neural stem cell grafts; directed differentiation improves outcome. Nat. Neurosci. 8, 346–353.

Holm J, Hillenbrand R, Steuber V, Moos M, Lübbert H, Montag D, Schachner M (1996). Structural features of a close homolog of L1 (CHL1) in the mouse: a novel member of L1 family of neural recognition molecules. Eur J Neurosci 8:1613–29

Homann CN, Wenzel K, Suppan K, Ivanic G, Crevenna R, Ott E (2003). Sleep attacks: facts and fiction—a critical review. Adv Neurol. 91: 335–41.

Howard CV, Reed MG (1998). Unbiased Stereology. Three-dimensional Measurements in Microscopy. Oxford, Bios Scientific Publishers

Hudson JL, van Horne CG, Strömberg I, Brock S, Clayton J, Masserano J, Hoffer BJ, Gerhardt GA (1993). Correlation of apomorphine- and amphetamine-inducing turning with nigrostriatal dopamine content in unilateral 6-hydroxydopamine lesioned rats. Brain Res. 626, 167–174.

Huebner K, Fuhrmann G, Christenson LK, Kehler J, Reinbold R, De La FR, Wood J, Strauss IIIJF, Boiani M, and Schoeler HR (2003). Derivation of oocytes from mouse embryonic stem cells. Science 300: 1251–1256.

Hulley P, Schachner M, Lübbert H (1998). L1 neural cell adhesion molecule is a survival factor for fetal dopaminergic neurons. J Neurosci Res. 15;53(2):129-34.

Hynes M, Rosenthal A (2000). Embryonic stem cells go dopaminergic. Neuron. 28: 11 – 14.

Ikeda H, Markey CJ, Markey SP (1992). Search for neurotoxins structurally related to 1-methyl-4-phenylpyridine (MPP⁻) in the pathogenesis of Parkinson's disease. Brain Res. 575: 285–298

Irintchev A, Rollenhagen A, Troncoso E, Kiss JZ, Schachner M (2005a). Structural and functional aberrations in the cerebral cortex of tenascin-C deficient mice. Cereb Cortex. 15: 962

Iwanami A, Kaneko S, Nakamura M, Kanemura Y, Mori H, Kobayashi S, Yamasaki M, Momoshima S, Ishii H, Ando K, Tanioka Y, Tamaoki N, Nomura T, Toyama Y, Okano H (2005). Transplantation of human neural stem cells for spinal cord injury in primates. J. Neurosci. Res. 80, 182–190.

Jakob H, Boon T, Gaillard J, Nicolas JF, and Jacob F (1973). Teratocarcinoma of the mouse: isolation, culture and properties of pluripotential cells. Ann Microbiol. 124: 269–282.

Jakovcevski I, Wu J, Karl N, Leshchyns'ka I, Sytnyk V, Chen J, Irintchev A, Schachner M (2007). Glial scar expression of CHL1, the close homolog of the adhesion molecule L1, limits recovery after spinal cord injury. J Neurosci. 4;27(27):7222-33.

Jenner P (1998). Oxdative mechanisms in nigral cell death in Parkinson's disease. Mov Disord 13 Suppl 1: 24-34.

Jenner P, Rose SP, Nomoto M, Marsden CD (1986). MPTP-induced parkinsonism in the common marmoset: behavioral and biochemical effects. Adv Neurol 45: 183–186

Jones LL, Sajed D, Tuszynski MH (2003). Axonal regeneration through regions of chondroitin sulfate proteoglycan deposition after spinal cord injury: a balance of permissiveness and inhibition. J Neurosci 23:9276–88

Joshi M, FehlingsMG (2002). Development and characterization of a novel, gradedmodel of clip compressive spinal cord injury in themouse. Part 1. Clip design, behavioral outcomes, and histopathology. J Neurotrauma. 19:175–190

Kahan BW and Ephrussi B (1970). Developmental potentialities of clonal in vitro cultures of mouse testicular teratoma. J Natl Cancer Inst. 44: 1015–1036.

Kalus I, Schnegelsberg B, Seidah NG, Kleene R, Schachner M (2003). The proprotein convertase PC5A and a metalloprotease are involved in the proteolytic processing of the neural adhesion molecule L1. J Biol Chem 278:10381–8

Kamiguchi H, Long KE, Pendergast M, Schaefer AW, Rapoport I, Kirchhausen T, Lemmon V (1998). The neural cell adhesion molecule L1 interacts with the AP-2 adaptor and is endocytosed via the clathrin-mediated pathway. J. Neurosci. 18, 5311–5321.

Kaur D, Andersen J (2002). Ironing out Parkinson's disease: is therapeutic treatment with iron chelators a real possibility? Aging Cell. 1 (1): 17-21.

Kawasaki H, Mizuseki K, Nishikawa S, Kaneko S, Kuwana Y, Nakanishi S, Nishikawa SI, Sasai Y (2000). Induction of midbrain dopaminergic neurons from ES cells by stromal cell-derived inducing activity. Neuron 28: 31 – 40.

Keirstead HS, Ben-Hur T, Rogister B, O'Leary MT, Dubois-Dalcq M, Blakemore WF (1999). Polysialylated neural cell adhesion molecule-positive CNS precursors generate both oligodendrocytes and Schwann cells to remyelinate the CNS after transplantation. J. Neurosci. 19, 7529–7536.

Keirstead HS, Nistor G, Bernal G, Totoiu M, Cloutier F, Sharp K, Steward O (2005). Human embryonic stem cell-derived oligodendrocyte progenitor cell transplants remyelinate and restore locomotion after spinal cord injury. J. Neurosci. 25, 4694–4705.

Kenwrick S, Watkins A, De Angelis E (1999). Neural cell recognition molecule L1: relating biological complexity to human disease mutations. Hum Mol Genet. 9:879–86.

Kerr DA, Lladó J, Shamblott MJ, Maragakis NJ, Irani DN, Crawford TO, Krishnan C, Dike S, Gearhart JD, Rothstein JD (2003). Human embryonic germ cell derivatives facilitate motor recovery of rats with diffuse motor neuron injury. J. Neurosci. 23, 5131–5140.

Keshet GI, Tolwani RJ, Trejo A, Kraft P, Doyonnas R, Clayberger C, Weimann JM, Blau HM (2007). Increased host neuronal survival and motor function in BMT Parkinsonian mice: involvement of immunosuppression. J Comp Neurol. 20;504(6):690-701.

Kim JH, Auerbach JM, Rodriguez-Gomez JA, Velasco I, Gavin D, Lumelsky N, Lee SH, Nguyen J, Sanchez-Pernaute R, Bankiewicz K, McKay R (2002). Dopamine neurons derived from

embryonic stem cells function in an animal model of Parkinson's disease. Nature 418: 50–56.

Kitada T, Asakawa S, Hattori N, Matsumine H, Yamamura Y, Minoshima S, Yokochi M, Mizuno Y, Shimizu N (1998). Mutations in the parkin gene cause autosomal recessive juvenile parkinsonism. Nature 392: 605–08.

Kordower JH, Freeman TB, Snow BJ, Vingerhoets FJ, Mufson EJ, Sanberg PR, Hauser RA, Smith DA, Nauert GM, Perl DP, et al (1995). Neuropathological evidence of graft survival and striatal reinnervation after the transplantation of fetal mesencephalic tissue in a patient with Parkinson's disease. N Engl J Med. 332: 1118–24.

Lai BC, Schulzer M, Marion S, Teschke K, Tsui JK (2003). The prevalence of Parkinson's disease in British Columbia, Canada, estimated by using drug tracer methodology. Parkinsonism Relat Disord. 9: 233–38.

Langston JW, Ballard PA, Tetrud JW, Irwin I (1983). Chronic parkinsonism in humans due to a product of meperidine-analog synthesis. Science. 219: 979–980.

Langston JW, Forno LS, Tetrud J, Reeves AG, Kaplan JA, Karluk D (1999). Evidence of active nerve cell degeneration in the substantia nigra of humans years after 1-methyl-4-phenyl-1,2,3,6-tetrahydropyridine exposure. Ann Neurol. 46: 598–605.

Lee HJ, Jakovcevski I, Radonjic N, Hoelters L, Schachner M, Irintchev A (2008). Better functional outcome of compression spinal cord injury in mice is associated with enhanced H-reflex responses. Exp Neurol. [Epub ahead of print]

Lee SH, Lumelsky N, Studer L, Auerbach JM, McKay RD (2000). Efficient generation of midbrain and hindbrain neurons from mouse embryonic stem cells. Nat Biotechnol 18:675–9.

Leroy E, Boyer R, Auburger G, Leube B, Ulm G, Mezey E, Harta G, Brownstein MJ, Jonnalagada S, Chernova T, Dehejia A, Lavedan C, Gasser T, Steinbach PJ, Wilkinson KD, Polymeropoulos MH (1998). The ubiquitin pathway in Parkinson's disease. Nature 395: 451–52.

Lie DC, Dziewczapolski G, Willhoite AR, Kaspar BK, Shults CW, Gage FH (2002). The adult substantia nigra contains progenitor cells with neurogenic potential. J Neurosci. 22: 6639–6649.

Lindvall O, Hagell P (2000). Clinical observations after neural transplantation in Parkinson's disease. Prog Brain Res. 127: 299–320.

Liu S, Qu Y, Stewart TJ, Howard MJ, Chakrabortty S, Holekamp TF, McDonald JW (2000). Embryonic stem cells differentiate into oligodendrocytes and myelinate in culture and after spinal

cord transplantation. Proc. Natl. Acad. Sci. USA. 97, 6126–6131.

Lladó J, Haenggeli C, Maragakis NJ, Snyder EY, Rothstein JD (2004). Neural stem cells protect against glutamate-induced excitotoxicity and promote survival of injured motor neurons through the secretion of neurotrophic factors. Mol. Cell. Neurosci. 27, 322–331.

Lois C, Alvarez-Buylla A (1993). Proliferating subventricular zone cells in the adult mammalian forebrain can differentiate into neurons and glia. Proc. Natl. Acad. Sci. USA. 90, 2074–2077.

Lozano AM (2003). Surgery for Parkinson's disease, the five W's: why, who, what, where, and when. Adv Neurol. 91: 303–07.

Lu P, Jones LL, Snyder EY, Tuszynski MH (2003). Neural stem cells constitutively secrete neurotrophic factors and promote extensive host axonal growth after spinal cord injury. Exp. Neurol. 181, 115–129.

Lucidi-Phillipi CA, Gage FH, Shults CW, Jones KR, Reichardt LF, Kang UJ (1995). Brain-derived neurotrophic factor-transduced fibroblasts: production of BDNF and effects of grafting to the adult rat brain. J Comp Neurol. 10; 354(3):361-76.

Luthi A, Mohajeri H, Schachner M, Laurent JP (1996). Reduction of hippocampal long-term potentiation in transgenic mice ectopically expressing the neural cell adhesion molecule L1 in astrocytes. J Neurosci Res 46:1−6.

Magnuson DS, Trinder TC, Zhang YP, Burke D, Morassutti DJ, Shields CB (1999). Comparing deficits following excitotoxic and contusion injuries in the thoracic and lumbar spinal cord of the adult rat. Exp. Neurol. 156, 191–204.

Main AL, Harvey TS, Baron M, Boyd J, Campbell ID (1992). The three dimensional structure of the tenth type III module of fibronectin: an insight into RGD-mediated interactions. Cell 71:671−78.

Maness PF, Schachner M (2007). Neural recognition molecules of the immunoglobulin superfamily: signaling transducers of axon guidance and neuronal migration. Nat Neurosci. 10(1):19-26.

Manyam BV, Sánchez-Ramos JR (1999). Traditional and complementary therapies in Parkinson's disease. Advances in neurology. 80: 565-74.

Martinat C, Bacci JJ, Leete T, Kim J, Vanti WB, Newman AH, Cha JH, Gether U, Wang H,

Abeliovich A (2006). Cooperative transcription activation by Nurr1 and Pitx3 induces embryonic stem cell maturation to the midbrain dopamine neuron phenotype. Proc Natl Acad Sci U S A. 21; 103(8):2874-9.

Martini R, Schachner M (1988). Immunoelectron microscopic localization of neural cell adhesion molecules (l1, NCAM, and MAG) in regenerating adult mouse sciatic nerve. J Cell Biol 106:1735–46.

Masliah E, Rockenstein E, Veinbergs I, et al (2000). Dopaminergic loss and inclusion body formation in alpha-synuclein mice: implications for neurodegenerative disorders. Science 287 (5456): 1265-9.

Matute C, Sanchez-Gomez MV, Martinez-Millan L, Miledi R (1997). Glutamate receptor-mediated toxicity in optic nerve oligodendrocytes. Proc Natl Acad Sci USA . 94: 8830–35.

McBurney MW, Jones-Villeneuve EM, Edwards MK, and Anderson PJ (1982). Control of muscle and neuronal differentiation in a cultured embryonal carcinoma cell line. Nature 299: 165–167.

McDonald JW, Althomsons SP, Hyrc KL, Choi DW, Goldberg MP (1998). Oligodendrocytes are highly vulnerable to AMPA/kainate receptor-mediated excitotoxicity. Nat Med. 4: 291–97.

McDonald JW, Liu XZ, Qu Y, Liu S, Mickey SK, Turetsky D, Gottlieb DI, Choi DW (1999). Transplanted embryonic stem cells survive, differentiate and promote recovery in injured rat spinal cord. Nat. Med. 5, 1410–1412.

McDonald JW, Sadowsky C (2002). Spinal-cord injury. Lancet. 2; 359(9304): 417-25.

McDonald WM, Richard IH, DeLong MR (2003). Prevalence, etiology, and treatment of depression in Parkinson's disease. Biol Psychiatry. 54: 363–75.

McGeer PL, McGeer EG, Suzuki JS. Aging and extrapyramidal function (1977). Arch Neurol. 34: 33–35.

McGinness J, Corry P, Proctor P (1974). Amorphous semiconductor switching in melanins. (Reprint). Science. 183 (127): 853-5.

McNaught KS, Olanow CW, Halliwell B, Isacson O, Jenner P (2001). Failure of the ubiquitin-proteasome system in Parkinson's disease. Nat Rev Neurosci. 2: 589–94.

Mendez I, Viñuela A, Astradsson A, Mukhida K, Hallett P, Robertson H, Tierney T, Holness R,

Dagher A, Trojanowski JQ, Isacson O (2008). Dopamine neurons implanted into people with Parkinson's disease survive without pathology for 14 years. Nat Med. 14(5):483-5.

Mintz B and Illmensee K (1975). Normal genetically mosaic mice produced from malignant teratocarcinoma cells. Proc Natl Acad Sci USA. 72: 3585–3589.

Mohajeri MH, Bartsch U, van der Putten H, Sansig G, Mucke L, Schachner M. (1996). Neurite outgrowth on non-permissive substrates in vitro is enhanced by ectopic expression of the neural adhesion molecule L1 by mouse astrocytes. Eur J Neurosci. 8:1085−1085.

Moos M, Tacke R, Scherer H, Teplow D, Früh K, Schachner M (1988). Neural adhesion molecule L1 as a member of the immunoglobulin superfamily with binding domains similar to firbonectin. Nature. 334: 701−703.

Morens DM, Grandinetti A, Reed D, White LR, Ross GW (1995). Cigarette smoking and protection from Parkinson's disease: false association or etiologic clue? Neurology. 45: 1041–51.

Moscoso LM, Sanes JR (1995) Expression of four immunoglobulin superfamily adhesion molecules (L1, NrCAM/Bravo, Neurofascin/ABGP, and NCAM) in the developing mouse spinal cord. J Comp Neurol. 352:321−334.

Mujtaba T, Piper DR, Kalyani A, Groves AK, Lucero MT, Rao MS (1999). Lineage-restricted neural precursors can be isolated from both the mouse neural tube and cultured ES cells. Dev. Biol. 214, 113–127.

Muthane UB, Swamy HS, Satishchandra P, Subhash MN, Rao S, Subbakrishna D (1994). Early onset Parkinson's disease: are juvenile- and young-onset different? Mov Disord. 9: 539–44.

Nayeem N, Silletti S, Yang X, Lemmon VP, Reisfeld RA, Stallcup WB, Montgomery AM (1999) A potential role for the plasmin(ogen) system in the posttranslational cleavage of the neural cell adhesion molecule L1. J Cell Sci. 112:4739−49.

Nesic O, Lee J, Johnson KM, Ye Z, Xu GY, Unabia GC, Wood TG, McAdoo DJ, Westlund KN, Hulsebosch CE, Regino Perez-Polo J (2005). Transcriptional profiling of spinal cord injury-induced central neuropathic pain. J Neurochem. 95(4):998-1014.

Nicolas JF, Dubois P, Jakob H, Gaillard J, and Jacob F (1975). Mouse teratocarcinoma: differentiation in cultures of a multipotential primitive cell line. Ann Microbiol. 126: 3–22.

Nishimura F, Yoshikawa M, Kanda S, Nonaka M, Yokota H, Shiroi A, Nakase H, Hirabayashi H, Ouji Y, Birumachi J, Ishizaka S, Sakaki T (2003). Potential use of embryonic stem cells for the

treatment of mouse parkinsonian models: improved behavior by transplantation of in vitro differentiated dopaminergic neurons from embryonic stem cells. Stem Cells. 21(2):171-80.

Nistor GI, Totoiu MO, Haque N, Carpenter MK, Keirstead HS (2005). Human embryonic stem cells differentiate into oligodendrocytes in high purity and myelinate after spinal cord transplantation. Glia. 49, 385–396.

Nutt JG. Motor fluctuations and dyskinesia in Parkinson's disease (2001). Parkinsonism Relat Disord. 8: 101–08.

Ogawa Y, Sawamoto K, Miyata T, Miyao S, Watanabe M, Nakamura M, Bregman BS, Koike M, Uchiyama Y, Toyama Y, Okano H (2002). Transplantation of in vitro–expanded fetal neural progenitor cells results in neurogenesis and functional recovery after spinal cord contusion injury in adult rats. J. Neurosci. Res. 69, 925–933.

Okabe S, Forsberg-Nilsson K, Spiro AC, Segal M, McKay RD (1996). Development of neuronal precursor cells and functional postmitotic neurons from embryonic stem cells in vitro. Mech Dev. 59:89−102.

Olanow CW, Goetz CG, Kordower JH, Stoessl AJ, Sossi V, Brin MF, Shannon KM, Nauert GM, Perl DP, Godbold J, Freeman TB (2003). A double-blind controlled trial of bilateral fetal nigral transplantation in Parkinson's disease. Ann Neurol. 54: 403-414.

Olanow CW, Kordower JH, Freeman TB (1996). Fetal nigral transplantation as a therapy for Parkinson's disease. Trends Neurosci. 19: 102−109.

Ostenfeld T, Caldwell MA, Prowse KR, Linskens MH, Jauniaux E, Svendsen CN (2000). Human neural precursor cells express low levels of telomerase in vitro and show diminishing cell proliferation with extensive axonal outgrowth following transplantation. Exp Neurol. 164(1):215-26.

Ourednik J, Ourednik V, Bastmeyer M, Schachner M (2001). Ectopic expression of the neural cell adhesion molecule L1 in astrocytes leads to changes in the development of the corticospinal tract. Eur J Neurosci 14:1464−1474.

Ourednik J, Ourednik V, Lynch WP, Schachner M, Snyder EY (2002). Neural stem cells display an inherent mechanism for rescuing dysfunctional neurons. Nat Biotechnol. 20(11):1103-10.

Papaioannou VE, McBurney MW, Gardner RL, and Evans MJ (1975). Fate of teratocarcinoma

cells injected into early mouse embryos. Nature. 258: 70–73.

Parish CL, Parisi S, Persico MG, Arenas E, Minchiotti G (2005). Cripto as a target for improving embryonic stem cell-based therapy in Parkinson's disease. Stem Cells. 3: 71–476.

Park CH, Minn YK, Lee JY, Choi DH, Chang MY, Shim JW, Ko JY, Koh HC, Kang MJ, Kang JS, Rhie DJ, Lee YS, Son H, Moon SY, Kim KS, Lee SH (2005). In vitro and in vivo analyses of human embryonic stem cell-derived dopamine neurons. J Neurochem. 92(5):1265-76.

Park HJ, Lee PH, Bang OY, Lee G, Ahn YH (2008). Mesenchymal stem cells therapy exerts neuroprotection in a progressive animal model of Parkinson's disease. J Neurochem. 107(1):141-51.

Parkinson J (2002). An essay on the shaking palsy. 1817. (Reproduced). J Neuropsychiatry Clin Neurosci 14 (2): 223-36; discussion 222.

Parkinson Study Group (2000). Pramipexole vs levodopa as initial treatment for Parkinson disease: a randomized controlled trial. JAMA. 284: 1931–38.

Payami H, Larsen K, Bernard S, Nutt J (1994). Increased risk of Parkinson's disease in parents and siblings of patients. Ann Neurol. 36: 659–61.

Pearse DD, Bunge MB (2006). Designing cell- and gene-based regeneration strategies to repair the injured spinal cord. J Neurotrauma. 23(3-4):438-52.

Pearson, KG (2001). Could enhanced reflex function contribute to improving locomotion after spinal cord repair? J. Physiol. (Lond.) 533, 75–81.

Perrier AL, Tabar V, Barberi T, Rubio ME, Bruses J, Topf N, Harrison NL, Studer L (2004). Derivation of midbrain dopamine neurons from human embryonic stem cells. Proc Natl Acad Sci USA 101: 12543–12548.

Persohn E and Schachner M (1987). Immunoelectron microscopic localization of the neural cell adhesion molecules L1 and N–CAM during postnatal development of the mouse cerebellum. J Cell Biol. 105:569–576.

Piccini P, Brooks DJ, Bjorklund A, Gunn RN, Grasby PM, Rimoldi O, Brundin P, Hagell P, Rehncrona S, Widner H, Lindvall O (1999). Dopamine release from nigral transplants visualized in vivo in a Parkinson's patient. Nat Neurosci. 2: 1137–1140.

Pitt D, Werner P, Raine CS (2000). Glutamate excitotoxicity in a model of multiple sclerosis. Nat Med. 6: 67–70.

Pluchino S, Quattrini A, Brambilla E, Gritti A, Salani G, Dina G, Galli R, Del Carro U, Amadio S, Bergami A, Furlan R, Comi G, Vescovi AL, Martino G (2003). Injection of adult neurospheres induces recovery in a chronic model of multiple sclerosis. Nature. 422, 688–694.

Polymeropoulos MH, Lavedan C, Leroy E, Ide SE, Dehejia A, Dutra A, Pike B, Root H, Rubenstein J, Boyer R, Stenroos ES, Chandrasekharappa S, Athanassiadou A, Papapetropoulos T, Johnson WG, Lazzarini AM, Duvoisin RC, Di Iorio G, Golbe LI, Nussbaum RL. (1997). Mutation in the alpha-synuclein gene identified in families with Parkinson's disease. Science. 276: 2045–47.

Pradhan S, Pandey N, Shashank S, Gupta RK, Mathur A (1999). Parkinsonism due to predominant involvement of substantia nigra in Japanese encephalitis. Neurology. 53: 1781–86.

Priyadarshi A, Khuder SA, Schaub EA, Priyadarshi SS (2001). Environmental risk factors and Parkinson's disease: a metaanalysis. Environ Res. 86: 122–27.

Przedborski S, Jackson-Lewis V (1998). Mechanisms of MPTP toxicity. Mov Disord 13 [Suppl 1]: 35–38.

Rajput AH. Frequency and cause of Parkinson's disease (1992). Can J Neurol Sci. 19 (1 suppl): 103–07.

Ramon Y Cajal, S. (1928). Degeneration and Regeneration of the Nerve System. Hafner: New York.

Rao MS, and Mayer-ProscheL M (1997). Glial-restricted precursors are derived from multipotent neuroepithelial stem cells. Dev. Biol. 188, 48–63.

Rascol O, Brooks DJ, Korczyn AD, De Deyn PP, Clarke CE, Lang AE (2000). A five-year study of the incidence of dyskinesia in patients with early Parkinson's disease who were treated with ropinirole or levodopa. N Engl J Med. 342: 1484–91.

Redmond DE Jr, Bjugstad KB, Teng YD, Ourednik V, Ourednik J, Wakeman DR, Parsons XH, Gonzalez R, Blanchard BC, Kim SU, Gu Z, Lipton SA, Markakis EA, Roth RH, Elsworth JD, Sladek JR Jr, Sidman RL, Snyder EY (2007). Behavioral improvement in a primate Parkinson's model is associated with multiple homeostatic effects of human neural stem cells. Proc Natl Acad Sci USA. 17; 104(29):12175-80.

Renoncourt Y, Carroll P, Filippi P, Arce V, Alonso S (1998). Neurons derived in vitro from ES cells express homeoproteins characteristic of motoneurons and interneurons. Mech. Dev. 79, 185–197.

Reubinoff BE, Pera MF, Fong CY, Trounson A, Bongso A (2000). Embryonic stem cell lines from human blastocysts: somatic differentiation in vitro. Nat. Biotechnol. 18, 399–404.

Ribotta MG, Orsal D, Feraboli-Lohnherr D, Privat A, Provencher J, Rossignol S. (1998). Kinematic analysis of recovered locomotor movements of the hindlimbs in paraplegic rats transplanted with monoaminergic embryonic neurons. Ann. N. Y. Acad. Sci. 860, 521–523.

Ribotta MG, Provencher J, Feraboli-Lohnherr D, Rossignol S, Privat A, Orsal D (2000). Activation of locomotion in adult chronic spinal rats is achieved by transplantation of embryonic raphe cells reinnervating a precise lumbar level. J. Neurosci. 20, 5144–5152.

Roonprapunt C, Huang W, Grill R, Friedlander D, Grumet M, Chen S, Schachner M, Young W (2003). Soluble cell adhesion molecule L1-Fc promotes locomotor recovery in rats after spinal cord injury. J Neurotrauma. 20:871−82.

Ross GW, Abbott RD, Petrovitch H, Morens DM, Grandinetti A, Tung KH, Tanner CM, Masaki KH, Blanchette PL, Curb JD, Popper JS, White LR. (2000). Association of coffee and caffeine intake with the risk of Parkinson disease. JAMA. 283: 2674–79.

Roy NS, Cleren C, Singh SK, Yang L, Beal MF, Goldman SA (2006). Functional engraftment of human ES cell-derived dopaminergic neurons enriched by coculture with telomerase-immortalized midbrain astrocytes. Nat Med. 12: 1259–1268.

Ruoslathi E, Pierschbacher MD (1987). New perspectives in cell adhesion: RGD and integrins. Science. 238:491−97.

Saghatelyan AK, Nikonenko AG, Sun M, Rolf B, Putthoff P, Kutsche M, Bartsch U, Dityatev A, Schachner M (2004). Reduced GABAergic transmission and number of hippocampal perisomatic inhibitory synapses in juvenile mice deficient in the neural cell adhesion molecule L1. Mol Cell Neurosci. 26:191−203.

Sambrook J, Fritsch EF, Maniatis T (1989). Molecular cloning: A Laboratory Manual. (Cold Spring Habor: Cold Spring Habor Laboratory)

Samii A, Calne DB (1999). Research into the etiology of Parkinson's disease. In: Oertel W, LeWitt PA, eds. Parkinson's disease: the treatment options. London: Martin Dunitz Publishers. 229–43.

Samii A, Nutt JG, Ransom BR. (2004). Parkinson's disease. Lancet. 29; 363(9423):1783-93.

Sánchez-Pernaute R, Studer L, Ferrari D, Perrier A, Lee H, Viñuela A, Isacson O (2005).

Long-term survival of dopamine neurons derived from parthenogenetic primate embryonic stem cells (cyno-1) after transplantation. Stem Cells. 23(7):914-22.

Sasai Y (2002). Generation of dopaminergic neurons from embryonic stem cells. J Neurol. 249(suppl 2): II41 – II44.

Schachner M (1989). Families of neural adhesion molecules. Ciba Found Symp 145:156–69.

Schmidt N, Ferger B (2001). Neuroprotective effects of (_)-kavain in the MPTP mouse model of Parkinson's disease. Synapse. 40: 47–54

Schrag A, Ben-Shlomo Y, Brown R, Marsden CD, Quinn N (1998). Young-onset Parkinson's disease revisited—clinical features, natural history, and mortality. Mov Disord. 13: 885–94.

Schuldiner M, Eiges R, Eden A, Yanuka O, Itskovitz-Eldor J, Goldstein RS, and Benvenisty N (2001). Induced neuronal differentiation of human embryonic stem cells. Brain Res 913: 201–205.

Schulz TC, Noggle SA, Palmarini GM, Weiler DA, Lyons IG, Pensa KA, Meedeniya AC, Davidson BP, Lambert NA, Condie BG (2004). Differentiation of human embryonic stem cells to dopaminergic neurons in serum-free suspension culture. Stem Cells. 22(7):1218-38.

Shen MM (2003). Decrypting the role of Cripto in tumorigenesis. J Clin Invest. 112: 500 – 502.

Silletti S, Mei F, Sheppard D, Montgomery AM (2000). Plasmin-sensitive dibasic sequences in the third fibronectin-like domain of L1-cell adhesion molecule (CAM) facilitate homomultimerization and concomitant integrin recruitment. J Cell Biol. 149:1485–502.

Singer TP, Ramsay RR (1990). Mechanism of the neurotoxicity of MPTP: an update. FEBS Lett. 274: 1–8.

Smith PM, and Blakemore WF (2000). Porcine neural progenitors require commitment to the oligodendrocyte lineage prior to transplantation in order to achieve significant remyelination of demyelinated lesions in the adult CNS. Eur. J. Neurosci. 7, 2424.

Smith T, Groom A, Zhu B, Turski L (2000). Autoimmune encephalomyelitis ameliorated by AMPA antagonists. Nat Med. 6: 62–66.

Sonntag KC, Pruszak J, Yoshizaki T, van Arensbergen J, Sanchez-Pernaute R, Isacson O (2006). Enhanced yield of neuroepithelial precursors and midbrain-like dopaminergic neurons from human embryonic stem cells using the BMP antagonist noggin. Stem Cells. 25: 411 – 418.

Steece-Collier K, Maries E, Kordower JH (2002). Etiology of Parkinson's disease: Genetics

and environment revisited. Proc Natl Acad Sci USA. 99: 13972–74.

Stevens LC (1967). Origin of testicular teratomas from primordial germ cells in mice. J Natl Cancer Inst. 38: 549–552.

Suda Y, Suzuki M, Ikawa Y, Aizawa S (1987). Mouse embryonic stem cells exhibit indefinite proliferative potential. J Cell Physiol. 133(1):197-201.

Tan EK, Chua E, Fook-Chong SM, Teo YY, Yuen Y, Tan L, Zhao Y (2007). Association between caffeine intake and risk of Parkinson's disease among fast and slow metabolizers. Pharmacogenet Genomics. 17(11):1001-5.

Tanner CM, Ottman R, Goldman SM, Ellenberg J, Chan P, Mayeux R, Langston JW (1999). Parkinson disease in twins: an etiologic study. JAMA. 281: 341–46.

Tator CH, Koyanagi I (1997). Vascular mechanism in pathophysiology of human spinal cord injury. J Neurosurg. 86: 483–92.

Teismann P, Ferger B (2001). Inhibition of the cyclooxygenase isoenzymes COX-1 and COX-2 provide neuroprotection in the MPTP-mouse model of Parkinson's disease. Synapse. 39: 167–174.

The National SCI Statistical Center (1999). Facts and figures at a glance. Birmingham: University of Alabama.

Thompson LH, Andersson E, Jensen JB, Barraud P, Guillemot F, Parmar M, Bjorklund A (2006). Neurogenin2 identifies a transplantable dopamine neuron precursor in the developing ventral mesencephalon. Exp Neurol. 198: 183–198.

Thomson JA, Itskovitz-Eldor J, Shapiro SS, Waknitz MA, Swiergiel JJ, Marshall VS, and Jones JM (1998). Embryonic stem cell lines derived from human blastocysts. Science. 282: 1145–1147.

Thor G, Probstmeier R, Schachner M (1987). Characterization of the cell adhesion molecules L1, NCAM and J1 in the mouse intestine. EMBO. 6:2581–86.

Tipton KF, Singer TP (1993). Advances in our understanding of the mechanisms of the neurotoxicity of MPTP and related compounds. J Neurochem. 61: 1191–1206.

Totoiu MO, Nistor GI, Lane TE, Keirstead HS (2004). Remyelination, axonal sparing, and locomotor recovery following transplantation of glial-committed progenitor cells into the MHV model of multiple sclerosis. Exp. Neurol. 187, 254–265.

Towbin H, Staehelin T, and Gordon J (1979). Electrophoretic transfer of proteins from polyacrylamide gels to nitrocellulose sheets: procedure and some applications. Proc Natl Acad Sci USA. 76:4350–4354.

Toyooka Y, Tsunekawa N, Akasu R, and Noce T (2003). Embryonic stem cells can form germ cells in vitro. Proc Natl Acad Sci USA. 100: 11457–11462.

Tropepe V, Hitoshi S, Sirard C, Mak TW, Rossant J, van der Kooy D (2001). Direct neural fate specification from embryonic stem cells: a primitive mammalian neural stem cell stage acquired through a default mechanism. Neuron. 30: 65–78.

Tsui JK, Calne DB, Wang Y, Schulzer M, Marion SA (1999). Occupational risk factors in Parkinson's disease. Can J Public Health. 90: 334–37.

Umemura A, Jaggi JL, Hurtig HI, Siderowf AD, Colcher A, Stern MB, Baltuch GH (2003). Deep brain stimulation for movement disorders: morbidity and mortality in 109 patients. J Neurosurg. 98: 779–84.

van Dyck CH, Seibyl JP, Malison RT, Laruelle M, Zoghbi SS, Baldwin RM, Innis RB (2002). Age-related decline in dopamine transporters: analysis of striatal subregions, nonlinear effects, and hemispheric asymmetries. Am J Geriatr Psychiatry. 10: 36–43.

Van Kampen JM, Eckman CB (2006). Dopamine D3 receptor agonist delivery to a model of Parkinson's disease restores the nigrostriatal pathway and improves locomotor behavior. J Neurosci. 26: 7272–7280.

Vroemen M, Aigner L, Winkler J, Weidner N (2003). Adult neural progenitor cell grafts survive after acute spinal cord injury and integrate along axonal pathways. Eur. J. Neurosci. 18, 743–751.

Wakabayashi K, Takahashi H (1997). Neuropathology of autonomic nervous system in Parkinson's disease. Eur Neurol. 38 (suppl 2): 2–7.

Webb K, Budko E, Neuberger TJ, Chen S, Schachner M, Tresco PA (2001). Substrate-bound human recombinant L1 selectively promotes neuronal attachment and outgrowth in the presence of astrocytes and fibroblasts. Biomaterials. 22:1017–28.

Wichterle H, Lieberam I, Porter JA, Jessell TM (2002). Directed differentiation of embryonic stem cells into motor neurons. Cell. 110, 385–397.

Wiencken-Barger AE, Mavity-Hudson J, Bartsch U, Schachner M, Casagrande VA (2004). The

role of L1 in axon pathfinding and fasciculation. Cereb Cortex. 14:121–31.

Williams AF, Barclay AN (1988). This immunoglobulin superfamily – domains for cell surface recognition. Annu Rev Immunol. 6:381–405.

Winkler C, Kirik D, Bjorklund A (2005). Cell transplantation in Parkinson's disease: how can we make it work? Trends Neurosci. 28: 86‑92.

Wobus AM, Holzhausen H, Jakel P, and Schoneich J (1984). Characterization of a pluripotent stem cell line derived from a mouse embryo. Exp Cell Res. 152: 212–219.

Wu P, Ye Y, Svendsen CN (2002). Transduction of human neural progenitor cells using recombinant adeno-associated viral vectors. Gene Ther. 9, 245–255.

Yamada T, Yamanaka I, Takahashi H, Nakajima K (1996). Invasion of brain by neurovirulent influenza A virus after intranasal inoculation. Parkinsonism Relat Disord. 2: 187–93.

Ying QL, Stavridis M, Griffiths D, Li M, Smith A (2003). Conversion of embryonic stem cells into neuroectodermal precursors in adherent monoculture. Nat Biotechnol. 21: 183‑186.

Zeng X, Cai J, Chen J, Luo Y, You ZB, Fotter E, Wang Y, Harvey B, Miura T, Backman C, Chen GJ, Rao MS, Freed WJ (2004). Dopaminergic differentiation of human embryonic stem cells. Stem Cells. 22(6):925-40.

Zhang SC, Ge B, Duncan ID (1999). Adult brain retains the potential to generate oligodendroglial progenitors with extensive myelination capacity. Proc. Natl. Acad. Sci. USA. 96, 4089–4094.

Zhang Y, Roslan R, Lang D, Schachner M, Lieberman AR, Anderson PN (2000). Expression of CHL1 and L1 by neurons and glia following sciatic nerve and dorsal root injury. Mol Cell Neurosci. 16:71–86.

Zhao M, Momma S, Delfani K, Carlen M, Cassidy RM, Johansson CB, Brismar H, Shupliakov O, Frisen J, Janson AM (2003). Evidence for neurogenesis in the adult mammalian substantia nigra. Proc Natl Acad Sci USA. 100: 7925‑7930.

VII   Appendix

1. Abbreviation

∅	without
AMPA	α-amino-3-hydroxy-5-methyl-4-isoxazole propionic acid
ANSC	adult neural stem cells
APP	amyloid beta (A4) precursor protein
BDNF	brain-derived neurotrophic factor
bFGF	basic fibroblast growth factor, fibroblast growth factor 2
BrdU	bromodeoxyuridine
BSA	bovine serum albumine
Casp 1	caspase 1
ChAT	choline acetyltransferase
CNPase	2', 3'-cyclic nucleotide 3'-phosphodiesterase
CNS	central nervous system
Col 1a 2	procollagen, type I, alpha 2
DAPI	4',6'-diamidino-2-phenylindole
DMSO	dimethylsulfoxide
DNA	deoxyribonucleic acid
dNTP	2'-desoxyribonucleotide-5'-triphosphate
EB	embryoid body
EC	embryonic carcinoma
EG	embryonic germ
ELISA	enzyme-linked immuno sorbent assay
ES	embryonic stem
FCS	fetal calf serum
Fcgr2	low affinity immunoglobulin gamma FC region receptor II precursor
Fgfr2	fibroblast growth factor receptor 2b, keratinocyte growth factor receptor
Fgg	Fibrinogen, gamma polypeptide
FNIII	Fibronectin type III

GABA	gamma-amino-N-butyric acid
GAD	glutamic acid decarboxylase
GDNF	glia-derived neurotrophic factor
GFAP	glial fibrillary acidic protein
GFP	green fluorescent protein
HBSS$^-$	Hank's balanced salts solution without Ca^{2+} and Mg^{2+}
Iba 1	ionized binding calciumadaptermolecule 1
ICM	inner cell mass
Ig	immunoglobulin
IH	immunohistochemistry
IL6st	interleukin-6 signal transducing molecule gp130 - rat
ITSFn	insulin-transferrin-selenium-fibronectin
kb	kilo base pairs
LIF	leukaemia inhibitory factor
MAPK	mitogen activated protein kinase
MEF	mouse embryonic fibroblasts
MHC II	major histocompatibility complex II
MPP$^+$	1-methyl-4-phenylpyridinium
MPTP	1-methyl-4-phenyl-1,2,3,6-tetrahydropyridine
mRNA	messenger ribonucleic acid
NCAM	neural cell adhesion molecule
NeuN	neuronal nuclei
NF	neurofilament
NGF	nerve growth factor
Ninj 1	ninjurin 1
NSC	neural stem cell
OPC	oligodendrocytes precursor cell
PAGE	polyacrylamide gel electrophoresis
PBS	phosphate-buffered saline

PD	Parkinson's disease
PET	positron emission tomography
PGK	3-phospho-glycerokinase I
PLO	poly-L-ornithine
PNS	peripheral nervous system
RIA	radioimmunoassay
RIPA buffer	radioimmunoprecipitation buffer
RT	room temperature
SCI	spinal cord injury
s.e.m.	standard error of the mean
SENA	substrate-adherent embryonic stem cell-derived neural aggregate
Shh	sonic hedgehog homolog
SNpc	Substantia nigra, pars compacta
SPECT	Single photon emission computed tomography
STAT-3	Signal Transducer and Activator of Transcription 3
TAE	tris-acetate-EDTA
TBS	Tris-buffered saline
TE	tris-EDTA
TGF β	transforming growth factor-β
TH	tyrosin hydroxylase
TN	terminal nerve
v/v	volume per volume
Vegf	vascular endothelial growth factor
w/v	weight per volume
XLSP	X-linked spastic paraplegia
ZMNH	Zentrum für Molekulare Neurobiologie Hamburg

2. Publications

1. Neural cell adhesion molecule L1-transfected embryonic stem cells promote functional recovery after excitotoxic lesion of the mouse striatum. J Neurosci. 2006 Nov 8;26(45):11532-9.

Bernreuther C, Dihné M, Johann V, Schiefer J, **Cui Y**, Hargus G, Schmid JS, Xu J, Kosinski CM, Schachner M.

2. Tenascin-R promotes neuronal differentiation of embryonic stem cells and recruitment of host-derived neural precursor cells after excitotoxic lesion of the mouse striatum. Stem Cells. 2008 Aug;26(8):1973-84

Hargus G, **Cui Y**, Schmid JS, Xu J, Glatzel M, Schachner M, Bernreuther C.

3. Stress-resistant neural stem cells positively influence regional energy metabolism after spinal cord injury in the adult mouse. In submitting.

Schwerdtfeger K, Mautes A E.M., Bernreuther C, **Cui Y**, Manville J, Dihné M, Schachner M.

4. Embryonic stem cell-derived neural aggregates overexpressing the neural cell adhesion molecule L1 promote functional recovery after transplantation in the murine MPTP model of Parkinson's disease. 2008 FENS poster

Cui Y, Hargus G, Schachner M, Bernreuther C.

3. Acknowledgements

This project has been done in the Institute for Biosynthesis of Neuronal Structures of the Centre for Molecular Neurobiology (ZMNH) at the University of Hamburg under the supervision of Prof. Melitta Schachner. I am especially grateful to Prof. Melitta Schachner for providing facilities for this research, fruitful discussions and for support and guidance during these years.

I would like to thank Dr. Christian Bernreuther for his excellent supervision, great ideas, constant help with experiments, helpful discussions, proofreading of this manuscript and patience, and also for introducing me into SENAs culture and transplantation. I wish to thank Privatdozent Dr. Andrey Irintchev and Dr. Igor Jakovcevski for their kindly help in morphologic analysis. I also wish to thank Dr. Fabio Morellini for his help in bahavioral and statistical analysis. And, I would like to thank Hyun Joon Lee for electrophysiological experiments. Last but not least, I would like to thank Elizabeth D. Marlow for her help in correcting my thesis.

I also wish to thank the present and former colleagues in the lab for their constant support during this work. Everybody contributed either actively or passively by keeping up the good spirit and there was always an answer to every question. Especially, I would like to thank my friends Gunnar Hargus, Ali Mehanna, Jinchong Xu, Shan Bian, Hyun Joon Lee, Daria Guseva and all my stem cell group members, thank for the happy moments you brought to me.

Finally, I wish to thank my family who always supported me and allowed me to work as much as I wanted.